Mathematisches Forschungsinstitut Oberwolfach

Report No. 15/2017

DOI: 10.4171/OWR/2017/15

Space-time Methods for Time-dependent Partial Differential Equations

Organised by
Ricardo Nochetto, College Park
Stefan Sauter, Zürich
Christian Wieners, Karlsruhe

March 12–18, 2017

Abstract. Modern discretizations of time-dependent PDEs consider the full problem in the space-time cylinder and aim to overcome limitations of classical approaches such as the method of lines (first discretize in space and then solve the resulting ODE) and the Rothe method (first discretize in time and then solve the PDE). A main advantage of a holistic space-time method is the direct access to space-time adaptivity and to the backward problem (required for the dual problem in optimization or error control). Moreover, this allows for parallel solution strategies simultaneously in time and space.

Several space-time concepts where proposed (different conforming and nonconforming space-time finite elements, the parareal method, wavefront relaxation etc.) but this topic has become a rapidly growing field in numerical analysis and scientific computing. In this workshop the focus is the development of adaptive and flexible *space-time discretization methods* for solving parabolic and hyperbolic space-time partial differential equations.

Mathematics Subject Classification (2010): 65N30, 65N38, 65N12.

Introduction by the Organisers

The main motivation for developing new space-time discretization and solution methods are the severe limitations of methods with separate constructions of space and time approximations. The goal of this research is to develop novel methods with respect to the following paradigms:

- Discretization: Develop and analyze discretization methods for parabolic and hyperbolic partial differential equations on the Cartesian product of the spatial domain with the time interval which are not necessarily of

tensor-product form but can be flexibly adapted to the local space-time behavior of the solution.
- Complexity: Develop and analyze fast algorithms for solving the arising sparse systems which have less algebraic structure than those which arise for the conventional approaches which lead often, e.g., to block-triangular, block-circulant, or block-Toeplitz matrices.
- Adaptivity: Develop and analyze algorithms for full space-time adaptivity on general space-time meshes.
- Regularity: Develop a detailed local space-time regularity theory for the solution of parabolic and hyperbolic PDEs which allows to enrich the ansatz spaces within an adaptive refinement process in a most efficient way.

All these questions are well investigated for elliptic problems, but they are far from being matured in the general time-dependent case. The research in space-time methods is driven by recent developments of discretizations specially designed for fully coupled approximation schemes, e.g., adaptive discontinuous Galerkin methods, Petrov-Galerkin methods, boundary elements with collocation in time, and hybrid methods.

The programme of this workshop was structured by themed days with contributions to one aspect of space-time methods:

A) Discretization methods for space-time problems
(new schemes, convergence in space and time, regularity in space and time)
B) A posteriori error control
(adaptivity in space and time)
C) Integral equations for time-dependent problems
(convolution quadrature, retarded potentials)
D) Solution methods for space-time problems
(multigrid in space and time, parareal method)
E) Geometric PDEs and methods
(numerical methods for PDEs on time-dependent manifolds)

For these topics the construction of new methods, the numerical analysis of convergence properties, and the application to large-scale applications where presented.

In summary, the workshop presentations yield a representative overview of the state-of-the-art and recent progress of space-time methods and its analysis, and the fruitful discussions will initiate further research in this area.

Acknowledgement: The MFO and the workshop organizers would like to thank the National Science Foundation for supporting the participation of junior researchers in the workshop by the grant DMS-1049268, "US Junior Oberwolfach Fellows".

Space-time Methods for Time-dependent Partial Differential Equations

Table of Contents

Georgios Akrivis
Multistep methods for nonlinear parabolic equations in Hilbert spaces ... 869

Marek Behr (joint with Violeta Karyofylli)
Simplex space-time meshes in mold filling simulations 872

Andrea Bonito (joint with Irene Kyza, Ricardo H. Nochetto)
Higher Order Estimates in Time for the Arbitrary Lagrangian Eulerian Formulation in Moving Domains 875

Willy Dörfler (joint with Stefan Findeisen, Christian Wieners, Daniel Ziegler)
Discontinuous Petrov-Galerkin discretizations in space and time for linear acoustic waves 877

Silvia Falletta
Space-time FEM-BEM coupling methods for wave propagation problems in unbounded domains 879

Martin J. Gander
Three Different Multigrid Interpretations of the Parareal Algorithm and an Adaptive Variant 882

Marcus J. Grote (joint with Michaela Mehlin, Stefan Sauter)
High-order Explicit Local Time-stepping Methods for Wave Propagation 885

Marlis Hochbruck (joint with Andreas Sturm)
On the error analysis of full discretizations of linear Maxwell's equations 888

Patrick Joly (joint with Maryna Kachanovska, Adrien Semin)
Propagation of acoustic waves in fractal networks 891

Maryna Kachanovska (joint with Eliane Bécache)
Stable Perfectly Matched Layers for a Class of Anisotropic Dispersive Models 894

Uwe Köcher
Space-Time Discretisation and Solver Technology for Biot's Model of Poroelasticity 897

Omar Lakkis (joint with E.H. Georgoulis and C.G. Makridakis and J.M. Virtanen)
Aposteriori analysis of fully discretized wave equation via leap-frog type schemes 899

Ulrich Langer (joint with S. Moore, M. Neumüller, I. Toulopoulos)
Space-Time Isogeometric Analysis of Parabolic Diffusion Problems 902

Stig Larsson (joint with Christoph Schwab)
Compressive space-time Galerkin discretizations of parabolic partial differential equations 905

Dmitriy Leykekhman (joint with Boris Vexler)
Discrete maximal parabolic regularity for Galerkin finite element methods and the fully discrete best approximation results 907

María López-Fernández
Time or space adaptivity for exterior wave problems with gCQ 910

Andrea Moiola (joint with Ilaria Perugia)
Space–time Trefftz discontinuous Galerkin methods for wave problems .. 913

Martin Neumüller
Space-time multigrid methods for parabolic optimal control problems 915

Enrique Otárola
A PDE approach to space–time fractional parabolic problems 920

Arnold Reusken (joint with Jörg Grande, Sven Groß, Christoph Lehrenfeld, Maxim Olshanskii, Igor Voulis)
Space-time Trace Finite Element Methods 923

Abner J. Salgado
Nonlinear evolution problems involving fractional operators 924

Francisco-Javier Sayas (joint with Thomas S Brown, Shukai Du, Hasan Eruslu)
Discrete waves in viscoelastic media 927

Martin Schanz (joint with Stefan A. Sauter)
Boundary Element formulation with variable time steps in Acoustics and Thermoelasticity 930

Iain Smears (joint with Alexandre Ern and Martin Vohralík)
Guaranteed energy norm a posteriori error estimates for high-order discretizations of parabolic problems 933

Andreas Veeser (joint with Francesca Tantardini and, partially, Christian Kreuzer and Rüdiger Verfürth)
Quasi-optimality in parabolic spatial semidiscretizations 934

Martin Vohralík (joint with Vít Dolejší, Alexandre Ern)
A posteriori error estimates for linear and nonlinear evolution problems using space-time dual norms 937

Thomas P. Wihler (joint with Mario Amrein)
Iterative Galerkin Methods for Semilinear Parabolic PDE 937

Mohammad Zakerzadeh (joint with Georg May)
Analysis of Space-Time Discontinuous Galerkin Methods for Hyperbolic Conservation Laws 939

Abstracts

Multistep methods for nonlinear parabolic equations in Hilbert spaces

Georgios Akrivis

Let $T > 0$ and $u^0 \in H$, and consider the initial value problem, for a possibly nonlinear abstract parabolic equation,

$$\begin{cases} u'(t) + A(t)u(t) = B(t, u(t)), \quad 0 < t < T, \\ u(0) = u^0, \end{cases} \tag{1}$$

in a usual triple of separable complex Hilbert spaces $V \subset H = H' \subset V'$, with V densely and continuously imbedded in H. Here $A(t) : V \to V', t \in [0, T]$, is a linear operator, whereas the operator $B(t, \cdot) : V \to V', t \in [0, T]$, may be nonlinear. We assume that (1) possesses a unique, smooth solution.

Let (α, β) and (α, γ) be implicit and explicit q-step methods, respectively, generated by three polynomials α, β and γ,

$$\alpha(\zeta) = \sum_{i=0}^{q} \alpha_i \zeta^i, \quad \beta(\zeta) = \sum_{i=0}^{q} \beta_i \zeta^i, \quad \gamma(\zeta) = \sum_{i=0}^{q-1} \gamma_i \zeta^i,$$

with real coefficients α_i, β_i and γ_i.

Let $N \in \mathbb{N}, k := T/N$ be the constant time step, and $t^n := nk, n = 0, \dots, N$, be a uniform partition of the interval $[0, T]$. For given starting approximations $U^0, \dots, U^{q-1} \in V$, we recursively define a sequence of approximations $U^m \in V$ to the nodal values $u^m := u(t^m)$ of the solution u of the initial value problem (1) by discretizing the differential equation in (1) either by the implicit scheme (α, β),

$$\sum_{i=0}^{q} \big(\alpha_i I + k\beta_i A(t^{n+i})\big) U^{n+i} = k \sum_{i=0}^{q} \beta_i B(t^{n+i}, U^{n+i}), \tag{2}$$

$n = 0, \dots, N - q$, or by the implicit–explicit scheme (α, β, γ),

$$\sum_{i=0}^{q} \big(\alpha_i I + k\beta_i A(t^{n+i})\big) U^{n+i} = k \sum_{i=0}^{q-1} \gamma_i B(t^{n+i}, U^{n+i}), \tag{3}$$

$n = 0, \dots, N - q$. The implicit–explicit scheme (α, β, γ) results by employing the implicit scheme (α, β) for the discretization of the linear part and the explicit scheme (α, γ) for the discretization of the nonlinear part of the differential equation. The implicit scheme (2) has in general more advantageous stability properties than its implicit–explicit counterpart (3); however, if $B(t, \cdot)$ is nonlinear, (2) is a nonlinear equation in the unknown U^{n+q}. In contrast to (2), the unknown U^{n+q} appears in (3) only linearly, since $\gamma_q = 0$; therefore, to advance with the implicit–explicit scheme (3) in time, we need to solve, at each time level, just one linear equation.

We assume that the implicit method (α, β) is strongly A(0)-stable and denote by $\vartheta, 0 < \vartheta \le 90°$, the largest angle for which the method (α, β) is A(ϑ)-stable.

We denote by $(\cdot,\cdot)$ both the inner product on H and the antiduality pairing between V' and V, and by $|\cdot|, \|\cdot\|$ and $\|\cdot\|_\star$ the norms on H, V and V', respectively. We assume that the operator $A(t) : V \to V'$ is uniformly coercive and bounded.

Quantification of the non-self-adjointness of $A(t)$. To take advantage of the A(ϑ)-stability of the implicit scheme (α,β), in case $\vartheta < 90°$, we need to quantify the non-self-adjointness of the operator $A(t)$. We decompose $A(t)$ in its self-adjoint and anti-self-adjoint parts $A_s(t) := \big(A(t)+A(t)^\star\big)/2$ and $A_a(t) := \big(A(t)-A(t)^\star\big)/2$, respectively,

$$A(t) = A_s(t) + A_a(t), \quad t \in [0,T].$$

Then, with the bounded anti-self-adjoint operator $\mathscr{A}_a(t) := A_s^{-1/2}(t)A_a(t)A_s^{-1/2}(t) : H \to H$, we have

$$\forall v \in V \;\; (A(t)v, v) \in S_\varphi \iff |\mathscr{A}_a(t)| \le \tan\varphi,$$

for any angle $\varphi < 90°$ and S_φ the sector $S_\varphi := \{z \in \mathbb{C} : z = \rho e^{i\psi}, \rho \ge 0, |\psi| \le \varphi\}$; therefore, $|\mathscr{A}_a(t)|$ is an *exact measure* of the non-self-adjointness of $A(t)$.

Assumptions. Our key assumption on the linear operator $A(t)$ is

$$|\mathscr{A}_a(t)v| \le \lambda_1(t)|v| \quad \forall v \in H \;\; \forall t \in [0,T], \tag{4}$$

with a non-negative continuous *stability function* λ_1. Our main assumption on the nonlinear operator $B(t,\cdot) : V \to V'$ is that it satisfies the local Lipschitz condition

$$|A_s^{-1/2}(t)\big(B(t,v)-B(t,\tilde v)\big)| \le \lambda_2(t)|A_s^{1/2}(t)(v-\tilde v)| + \mu_2(t)|v-\tilde v| \;\; \forall t \in [0,T], \tag{5}$$

for all $v, \tilde v$ in a tube $T_u, T_u := \{v \in V : \min_t \|v - u(t)\| \le 1\}$, around the solution u, defined in terms of the norm $\|\cdot\|$ on V, with a non-negative continuous *stability function* λ_2 and a bounded function μ_2.

Furthermore, we assume that the operators $A(t), B(t,\cdot) : V \to V', t \in [0,T]$, satisfy a Lipschitz condition in t,

$$\|\big(A(t) - A(s)\big)v\|_\star \le L_A|t-s|\,\|v\| \quad \forall s,t \in [0,T] \;\; \forall v \in V, \tag{6}$$

and a local Lipschitz-like condition, namely

$$\|[B(t,v) - B(t,\tilde v)] - [B(s,v) - B(s,\tilde v)]\|_\star \le L_B|t-s|\,\|v-\tilde v\| \quad \forall s,t \in [0,T], \tag{7}$$

for $v, \tilde v \in T_u$, respectively. Actually, the Lipschitz conditions (6) and (7) can be relaxed to bounded variation conditions.

With $\mathscr{K}$ the unit circle in the complex plane, $\mathscr{K} := \{z \in \mathbb{C} : |z| = 1\}$, let

$$K_{(\alpha,\beta)} := \sup_{x>0} \max_{\zeta\in\mathscr{K}} \frac{|x\beta(\zeta)|}{|(\alpha+x\beta)(\zeta)|}, \quad K_{(\alpha,\beta,\gamma)} := \sup_{x>0} \max_{\zeta\in\mathscr{K}} \frac{|x\gamma(\zeta)|}{|(\alpha+x\beta)(\zeta)|}.$$

The stability result. Combining spectral and Fourier stability techniques, and using a discrete perturbation argument, we obtain the following stability result:

Theorem ([1]) *Let λ_1 and λ_2 be the stability functions of the boundedness condition* (4) *and of the local Lipschitz condition* (5)*, respectively. Then, under the linear conditions*

$$(\cot\vartheta)\lambda_1(t) + K_{(\alpha,\beta)}\lambda_2(t) < 1 \quad \forall t \in [0,T] \tag{8}$$

and

$$(\cot\vartheta)\lambda_1(t) + K_{(\alpha,\beta,\gamma)}\lambda_2(t) < 1 \quad \forall t \in [0,T], \tag{9}$$

respectively, on the stability functions λ_1 *and* λ_2, *the implicit multistep scheme* (2) *and the implicit–explicit multistep scheme* (3) *are locally stable in the following sense*: *If* $U^0,\dots,U^N \in T_u$ *satisfy* (2) *and* (3), *respectively, and* $V^0,\dots,V^N \in T_u$ *satisfy the corresponding perturbed equations*

$$\sum_{i=0}^{q} \big(\alpha_i I + k\beta_i A(t^{n+i})\big)V^{n+i} = k\sum_{i=0}^{q} \beta_i B(t^{n+i}, V^{n+i}) + kE^n \tag{10}$$

and

$$\sum_{i=0}^{q} \big(\alpha_i I + k\beta_i A(t^{n+i})\big)V^{n+i} = k\sum_{i=0}^{q-1} \gamma_i B(t^{n+i}, V^{n+i}) + kE^n, \tag{11}$$

$n = 0,\dots,N-q$, *respectively, then, with* $\vartheta^m := V^m - U^m$, *for sufficiently small time step* k, *we have*

$$|\vartheta^n|^2 + k\sum_{\ell=0}^{n} \|\vartheta^\ell\|^2 \le C\Big\{ \sum_{j=0}^{q-1} \big(|\vartheta^j|^2 + k\|\vartheta^j\|^2\big) + k\sum_{\ell=0}^{n-q} \|E^\ell\|_\star^2 \Big\}, \tag{12}$$

$n = q,\dots,N$, *with a constant* C *independent of the time step* k, *the approximations* U^n, V^n, *and the perturbations* E^n. □

On the stability conditions (8) *and* (9). A necessary stability condition for the implicit scheme (2) is $(\cot\vartheta)\lambda_1(t) + K_{(\alpha,\beta)}\lambda_2(t) \le 1$, for $t \in [0,T]$, i.e., the stability condition (8) is *sharp*. None of the coefficients $\cot\vartheta$ and $K_{(\alpha,\beta,\gamma)}$ in (9) can be replaced by a smaller coefficient; in other words, (9) is a best possible *linear* sufficient stability condition for the implicit–explicit scheme (3).

References

[1] G. Akrivis, *Stability of implicit and implicit–explicit multistep methods for nonlinear parabolic equations*, Submitted for publication.

[2] G. Akrivis, *Implicit–explicit multistep methods for nonlinear parabolic equations*, Math. Comp. **82** (2013), 45–68.

[3] G. Akrivis, *Stability of implicit–explicit backward difference formulas for nonlinear parabolic equations*, SIAM J. Numer. Anal. **53** (2015), 464–484.

[4] G. Akrivis, *Stability properties of implicit–explicit multistep methods for a class of nonlinear parabolic equations*, Math. Comp. **85** (2016), 2217–2229.

[5] G. Akrivis, M. Crouzeix, and Ch. Makridakis, *Implicit–explicit multistep methods for quasi-linear parabolic equations*, Numer. Math. **82** (1999), 521–541.

[6] G. Akrivis and E. Katsoprinakis, *Backward difference formulae*: *new multipliers and stability properties for parabolic equations*, Math. Comp. **85** (2016), 2195–2216.

[7] G. Akrivis and C. Lubich, *Fully implicit, linearly implicit and implicit–explicit backward difference formulae for quasi-linear parabolic equations*, Numer. Math. **131** (2015), 713–735.

[8] M. Crouzeix, *Une méthode multipas implicite–explicite pour l'approximation des équations d'évolution paraboliques*, Numer. Math. **35** (1980), 257–276.

[9] C. Lubich, *On the convergence of multistep methods for nonlinear stiff differential equations*, Numer. Math. **58** (1991), 839–853.
[10] G. Savaré, *$A(\Theta)$-stable approximations of abstract Cauchy problems*, Numer. Math. **65** (1993), 319–335.

Simplex space-time meshes in mold filling simulations

Marek Behr
(joint work with Violeta Karyofylli)

Abstract

We present the use of fully unstructured space-time meshes in two-phase flow problems including surface tension effects. Our basis for constructing simplex-type space-time meshes is the method presented in [1]. The whole approach is based on the discontinuous-Galerkin method in time (space-time elements), details of which can be found in [2, 3]. The interface is approximated by the level-set method [4], which describes implicitly the interface and is able to cope with extreme topological changes of the propagating front between the two phases. The numerical examples, used for validating the unstructured space-time mesh solver, involve the benchmark cases of a rising bubble in a rectangular domain, a rising droplet in a cuboid tank and the filling of mold cavities.

Filling of a coat hanger distributer and a rectanglular cavity

Here, we demonstrate only a complicated example for verifying our numerical approach and our implementation of Navier's slip condition, which is not trivial for simplex-type space-time elements. If the slip boundary does not coincide with

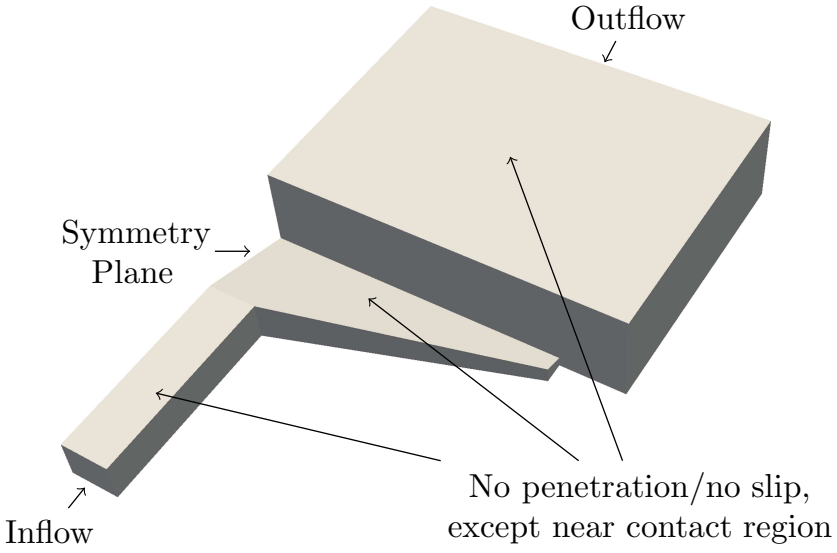

Figure 1. Coat hanger distributer and rectangular cavity: Computational domain.

a Cartesian co-ordinate plane, the equations corresponding to the velocity components at the boundary are locally aligned with the normal-tangent-bi-tangent co-ordinate system. This procedure is described by Engelman et al. [5].

We simulate the filling stage of a coat hanger distributer and a rectanglular cavity, considered by Rao et al. [6]. The molten material enters the mold with a uniform velocity and displaces the air, which is initially quiescent.

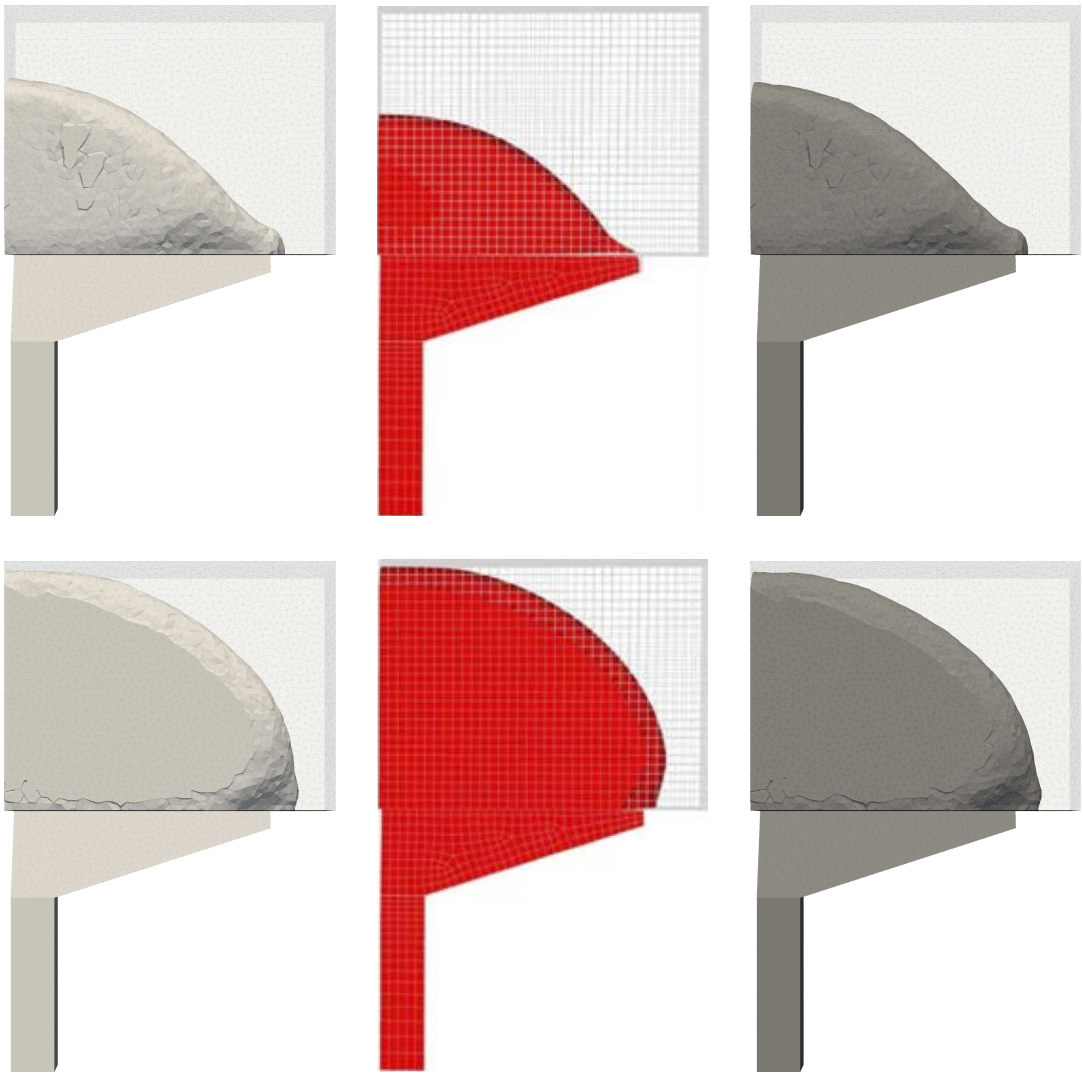

FIGURE 2. Molten material position at $t = 0.5\,\mathrm{s}$ (top row) and $t = 0.9\,\mathrm{s}$ (bottom row), obtained with a **prism-type** space-time discretization (left column) and a **simplex-type** space-time discretization (right column) and compared with reference data (middle column) [6].

The computational domain is illustrated in Figure 1. The spatial discretization of the domain consists of 98561 triangular elements. The time-slab size is $\Delta t = 0.0005\,\mathrm{s}$. Navier's slip boundary condition is assumed on the walls, except for those

of the inflow, outflow and symmetry plane. The Blake wetting condition is not taken into consideration, though. A uniform velocity of size 190 cm/s is imposed at the inflow boundary, whereas traction-free boundary conditions are used at the outflow boundary. Slip boundary condition is used for the symmetry plane. We consider isothermal condition, so natural convection and phase-change effects are disregarded. The material properties correspond to those of [6] and are as follows: $\rho_{\text{air}} = 0.0045\,\text{g/cm}^3$, $\rho_{\text{liquid}} = 4.5\,\text{g/cm}^3$, $\mu_{\text{air}} = 4\,\text{g/(s cm)}$, $\mu_{\text{liquid}} = 4000\,\text{g/(s cm)}$. The gravitational acceleration is equal to $f_y = -g = -981\,\text{cm/s}^2$. The surface tension effects are not neglected, so the surface tension coefficient γ is equal to $42.4\,\text{g/s}^2$.

The molten material filled the mold first for $t = 0.2\,\text{s}$ using the usual (prismatic space-time elements. These standard results were then compared with the filling results obtained with a pentatope-based space-time mesh discretization of the slab without any temporal refinement. This pentatope-based space-time mesh was generated using the technique presented in [1]. Figure 2 illustrates the front position of the molten material at various time instances. The results obtained with the usual prismatic space-time discretization and with the simplex-type space-time mesh are also compared with those reported in Reference [6]. As we can see from Figure 2, the results show a good agreement with the reference data [6]. This benchmark case also reveals that the simulation results obtained with the fully unstructured space-time discretization are equivalent to those obtained with the standard discretization.

Acknowledgements

The authors gratefully acknowledge the support of the German Research Foundation (DFG) under the program SFB 1120 “Precision Melt Engineering”. The computations were conducted on computing clusters provided by the RWTH Aachen University IT Center and by the Jülich Aachen Research Alliance (JARA). Furthermore, we would like to thank the student Niklas Bauer for his contribution by simulating different benchmark cases.

References

[1] M. Behr, *Simplex space–time meshes in finite element simulations*, International journal for numerical methods in fluids **57**(9):1421–1434 (2008).

[2] T. Hughes, L. Franca, G. Hulbert, *A new finite element formulation for computational fluid dynamics: VIII. The Galerkin/least-squares method for advective-diffusive equations*, Computer Methods in Applied Mechanics and Engineering **73**(2):173–189 (1989).

[3] T. Hughes, L. Franca, M. Mallet, *A new finite element formulation for computational fluid dynamics: VI. Convergence analysis of the generalized SUPG formulation for linear time-dependent multidimensional advective-diffusive systems*, Computer Methods in Applied Mechanics and Engineering **63**(1):97–112 (1987).

[4] S. Osher, J. Sethian, *Fronts propagating with curvature-dependent speed: Algorithms based on Hamilton-Jacobi formulations*, Journal of computational physics **79**(1):12–49 (1988).

[5] M. Engelman, R. Sani, P. Gresho, *The implementation of normal and/or tangential boundary conditions in finite element codes for incompressible fluid flow*, International Journal for Numerical Methods in Fluids **2**:225–238 (1982).

[6] R. Rao, L. Mondy, D. Noble, M. Hopkins, P. Notz, Th. Baer, L. Halbleib, P. Yang, G. Burns, A. Grillet, C. Brooks, R. Cote, and J. Castañeda, *Modeling Injection Molding of Net- Shape Active Ceramic Components*, SAND2006-6786, Sandia National Laboratories, Albuquerque, NM (2006).

Higher Order Estimates in Time for the Arbitrary Lagrangian Eulerian Formulation in Moving Domains

Andrea Bonito

(joint work with Irene Kyza, Ricardo H. Nochetto)

Arbitrary Lagrangian Eulerian (ALE) formulations arise naturally in the context of parametric representations of deformable domains. We motivate this study by describing an ALE formulations tailored to the prediction of red blood cells evolutions, where the Navier-Stokes systems is coupled with the Canham-Helfrich boundary force [5]. We argue the need of ALE methods in view of the complex streamlines generated during the relaxation of a $5 \times 5 \times 1$ ellipsoid towards a red-blood cell type equilibrium shape. Furthermore, higher order methods and a-posteriori error control are of paramount importance due to presence of different time scales.

ALE formulations on deformable domains are based on an extension of the domain velocity from the boundary. This somewhat arbitrary extension, is selected with the purpose of keeping mesh regularity and has no effect on the stability of the system. However, time discrete schemes may not be able to capture the inherent interplay between space and time, thereby exhibiting stability properties influenced by the extended velocity. We examine this critical issue for higher order time stepping without space discretization on time-dependent advection-diffusion model problems in moving domains.

We advocate time-discrete discontinuous Galerkin (dG) numerical schemes because of their natural ability to couple space and time. In fact, their stability properties hinge on the validity of the Reynolds' identity

$$\frac{d}{dt}\int_{\Omega_t} v(t)\ dt = \int_{\Omega_t} \nabla\cdot\mathbf{w}(t)\ v(t)\ dt + \int_{\Omega_t} \frac{D}{Dt}v(t)\ dt,$$

where $\Omega_t \subset \mathbb{R}^d$ is the deformable domain, $\mathbf{w}$ is the ALE (extended) velocity and $\frac{D}{Dt}$ is the ALE (material) derivative. Exploiting the variational structure and assuming exact integration, we prove that, as in the continuous case, conservative and non-conservative dG(q) schemes, $q \geq 0$, are equivalent and unconditionally stable. The same results remain true for piecewise polynomial ALE maps of any degree as long as the quadrature guarantees the validity of the Reynolds' identity, i.e. exact for polynomial degree $2q + d(q+1) - 1$. We call these quadratures *Reynold's quadratures*, which generalizes the concept of geometric conservation law (GCL) [6, 7] to higher order methods. We refer to [1] for more details.

Worth mentioning, Reynold's quadratures require more than what is strictly sufficient to preserve the convergence order of the dG methods. However, we also

prove that simpler Runge-Kutta-Radau (RKR) methods based on $q+1$ Radau points are conditionally stable, that is subject to a mild ALE constraint on the time steps. Numerical experiments are provided to corroborate and complement our theoretical results.

We then present the optimal a priori error estimates derived in [2]. These estimates are valid without any restrictions on the time steps when exact integration or Reynolds' quadratures are used but require a mild restriction on the time steps for RKR methods. The key ingredients are the stability results discussed previously along with a novel ALE projection of the exact solutions on the discrete piecewise polynomial spaces. Again, our theoretical findings are supplemented by numerical experiments.

In the last part of the talk, we derive optimal order a posteriori error bounds for the dG, Reynolds', and RKR methods. These estimates generalize to moving domain the dG reconstruction technique of [8]. The proposed ALE time reconstruction accounts for the domain deformation and relies, once again, on the Reynolds' identity. The provided a posteriori error control gives important information on the behavior of the error with respect to the movement of the domain. In particular, our analysis allows variable time-steps and suggests that time adaptivity is essential for oscillatory ALE maps. This is also seen numerically with a series of numerical experiments. We refer to [3] and [4] for more details.

References

[1] A. Bonito, I. Kyza, and R.H. Nochetto. Time-discrete higher order ALE formulations: Stability. To appear in SIAM J. Numer. Anal.

[2] A. Bonito, I. Kyza, and R.H. Nochetto. Time-discrete higher order ALE formulations: A priori error analysis. To appear in Numer. Math.

[3] A. Bonito, I. Kyza, and R.H. Nochetto. *A dG approach to higher order ALE formulations in time*, volume 157 of *2012 Barrett Lectures, The IMA Volume in Mathematics and its Applications*. Springer, 2013.

[4] A. Bonito, I. Kyza, and R.H. Nochetto. *Time-discrete higher order ALE formulations: A posteriori error analysis*, in preparation.

[5] A. Bonito, R.H. Nochetto, and M.S. Pauletti. Dynamics of biomembranes: Effect of the bulk fluid. *Math. Model. Nat. Phenom.*, 6(5):25–43, 2011.

[6] L. Formaggia and F. Nobile. Stability analysis of second-order time accurate schemes for ALE-FEM. *Comput. Methods Appl. Mech. Engrg.*, 193(39-41):4097–4116, 2004.

[7] L. Formaggia and F. Nobile. A stability analysis for the arbitrary Lagrangian Eulerian formulation with finite elements. *East-West J. Numer. Math.*, 7(2):105–131, 1999.

[8] Ch. Makridakis and R.H. Nochetto. A posteriori error analysis for higher order dissipative methods for evolution problems. *Numer. Math.*, 104(4):489–514, 2006.

Discontinuous Petrov-Galerkin discretizations in space and time for linear acoustic waves

Willy Dörfler
(joint work with Stefan Findeisen, Christian Wieners, Daniel Ziegler)

A space-time setting for acoustic waves. We consider linear acoustic waves in the form of a first-order hyperbolic systems of conservation laws on a bounded domain $\Omega \subset \mathbb{R}^D$ and for some time $T > 0$,

$$Lu = f \quad \text{on } Q := \Omega \times (0,T)\,, \qquad u(\cdot,0) = u_0\,,$$

where $u = (p,v)\colon Q \to \mathbb{R}^{1+D}$, $M(p,v) = (\kappa^{-1}, \rho)$ and $A(p,v) = (\nabla \cdot v, \nabla p)$.

Following [4, 3] this can be analyzed in a Petrov-Galerkin setting defining the Hilbert spaces $W := \mathrm{L}_2(Q)^{1+D}$ with norm

$$\|w\|_W := (Mw, w)_{0,Q}^{1/2} = \|M^{1/2} w\|_{0,Q}$$

and $V \subset W$ as closure of

$$\mathscr{D}(L) = \Big\{ (p,v) \in \mathrm{C}^1\big([0,T], \mathrm{L}_2(\Omega; \mathbb{R} \times \mathbb{R}^D)\big) \cap \mathrm{C}^0\big([0,T], \mathrm{H}^1_0(\Omega) \times \mathrm{H}(\mathrm{div}, \Omega)\big) : p(0) = 0\,,\ v(0) = 0 \Big\}$$

with respect to the weighted graph norm $\|u\|_V := \Big(\|u\|_W^2 + \|M^{-1} L u\|_W^2 \Big)^{1/2}$. Stability in this setting is achieved by the estimate $\|u\|_W \le 2T \, \|M^{-1} L u\|_W$ for $u \in V$. For given $f \in \mathrm{L}_2(Q)^{1+D}$ a unique solution $u \in V$ of the variational problem

$$(Lu, w)_{0,Q} = (f, w)_{0,Q} \qquad \text{for all } w \in W$$

exists [4, Thm. 2].

A space-time discontinuous Galerkin discretization. Let $Q = \Omega \times (0,T)$ be decomposed into space-time cells $\mathscr{R} = \bigcup R$ with $R = K \times I$ composed from cells K and intervals I. Choosing local degrees p_R, q_R we define the discontinuous test space W_h with local spaces $W_{R,h} = \big(\mathbb{P}_{p_R}(K) \otimes \mathbb{P}_{q_R - 1}(I) \big)^{1+D}$. This determines $V_h \subset \mathrm{H}^1\big((0,T), \mathrm{L}_2(\Omega)^{1-D}\big)$ with $u_h(x,t) = \frac{t_+ - t}{t_+ - t_-} u_h(x,t_-) + \frac{t - t_-}{t_+ - t_-} w_{h,R}(x,t)$ for $(x,t) \in R = K \times (t_-, t_+)$, where $w_{h,R} \in W_{R,h}$ and $u_h(x,0) = 0$.

The operator A is approximated in space by the nodal discontinuous Galerkin method [5]. For acoustic waves we obtain $A_h(p_h, v_h) \in W_h$ for $(p_h, v_h) \in V_h$ by

$$\big(A_h(p_h, v_h), (\varphi_{K,h}, \psi_{K,h})\big)_{0,Q} = \sum_{R = K \times I} -\big(\mathrm{div}\, v_{K,h}, \varphi_{K,h}\big)_{0,R} - \big(\nabla p_{K,h}, \psi_{K,h}\big)_{0,R}$$
$$- \frac{1}{2\rho c} \sum_{F \subset \partial K} \big([p_h]_{K,F} + \rho c n_K \cdot [v_h]_{K,F}, \varphi_{K,h} + \rho c n_K \cdot \psi_{K,h} \big)_{0,F \times I}$$

for all $w_h \in W_h$, where $c = \sqrt{\kappa/\rho}$ is the wave speed. The Petrov-Galerkin approximation $u_h \in V_h$ is uniquely defined by

$$\big(M\partial_t u_h + A_h u_h, w_h\big)_{0,Q} = (f, w_h)_{0,Q} \qquad \text{for all } w_h \in W_h\,.$$

Stability and convergence is analyzed in [4, Thm. 3 and 4].

A numerical test for space-time adaptivity. The method is realized in the parallel finite element system M++ [6]. The linear systems are solved with a preconditioned multigrid methods in space and time, and the adaptivity is controlled by a duality based goal-oriented error estimator.

The example is motivated by an application in tunnel exploration, see the 2D geometry in Fig. 1. A smooth pulse at the tunnel boundary propagates and is reflected at the boundary, and the reflected wave front is measured by a goal functional E. We compare the results for uniform and adaptive refinement in Tab. 1.

ref-step	(p,q)	#DoFs (effort)	GMRES steps (rate)	$E(u_h)$	$\triangle E_{\text{ex}}$
		uniform refinement			
$r=0$	$(0,1)$	267 264	7 (5.64e-2)	3.4808e-4	5.6091e-3
...		...	...	...	
$r=3$	$(3,3)$	8 017 920	19 (4.15e-1)	5.9523e-3	4.8958e-6
$r=4$	$(4,4)$	16 035 840	26 (5.68e-1)	5.9568e-3	3.9528e-7
		adaptive refinement			
$r=0$		267 264	7 (5.64e-2)	3.4808e-4	5.6091e-3
...		...	...	...	
$r=3$		2 518 482 (31%)	19 (4.21e-1)	5.9524e-3	4.8069e-6
$r=4$		4 642 725 (29%)	31 (6.22e-1)	5.9568e-3	3.9599e-7

TABLE 1. Uniform vs. adaptive refinement on 89 088 space-time cells on 64 procs (extrapolated value of the goal functional $E_{\text{ex}} \approx 5.9572\text{e-}3$).

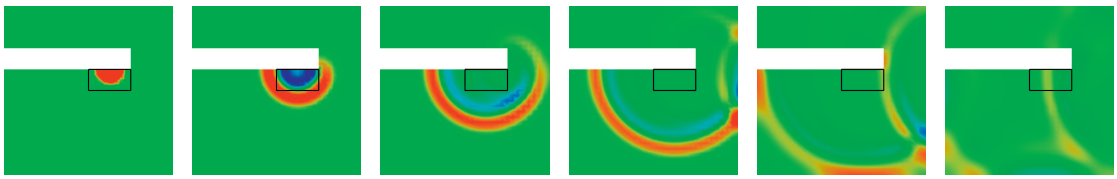

(A) $t = 0.0$ (B) $t = 0.6$ (C) $t = 1.2$ (D) $t = 1.8$ (E) $t = 2.4$ (F) $t = 3.0$

FIGURE 1. Propagation of the acoustic wave. The region of interest $S \subset \Omega$ defines $E_q(u) = \int_{S\times\{T\}} u^2 \,\mathrm{d}x$.

REFERENCES

[1] Bangerth, W. and Rannacher, R. Finite element approximation of the acoustic wave equation: Error control and mesh adaptation. *East-West J. Numer. Math.*, **7** (1999), 263–282.

[2] Braess, D. *Finite Elements. Theory, fast solvers, and applications in solid mechanics. 3th ed.* Cambridge University Press, Cambridge, 2007.

[3] Dörfler, W., *An adaptive space-time discontinuous Galerkin method for linear hyperbolic systems*, Oberwolfach Report 1636 (2016).
[4] Dörfler, W. and Findeisen, S. and Wieners, C., *Space-time discontinuous Galerkin discretizations for linear first-order hyperbolic evolution systems*, Computational Methods in Applied Mathematics **16** (2016), 409–428.
[5] Hesthaven, J. S. and Warburton, T. *Nodal Discontinuous Galerkin Methods*. Springer, 2008.
[6] Wieners, C. *A geometric data structure for parallel finite elements and the application to multigrid methods with block smoothing*, Comput. Visual. Sci. **13** (2010) 161–175.

Space-time FEM-BEM coupling methods for wave propagation problems in unbounded domains

Silvia Falletta

Let $\mathscr{O}(t) \subset \mathbb{R}^2$ be an open bounded domain, subject to a rigid motion, with a sufficiently smooth boundary $\Gamma(t)$. We consider the wave propagation problem in $\mathbb{R}^2 \setminus \bar{\mathscr{O}}(t)$ and, for its solution by a finite element method, we introduce a fix artificial boundary $\mathscr{B}$ where we impose the transparent conditions $\frac{1}{2}u(\mathbf{x},t) - \mathscr{V}\partial_n u(\mathbf{x},t) + \mathscr{K}u(\mathbf{x},t) = 0$, being

$$\mathscr{V}\psi(\mathbf{x},t) = \int_0^t \int_{\mathscr{B}} G(\mathbf{x}-\mathbf{y}, t-\tau)\psi(\mathbf{y},\tau) d\mathscr{B}_{\mathbf{y}} d\tau,$$

and

$$\mathscr{K}\varphi(\mathbf{x},t) = \int_0^t \int_{\mathscr{B}} \partial_n G(\mathbf{x}-\mathbf{y}, t-\tau)\varphi(\mathbf{y},\tau) d\mathscr{B}_{\mathbf{y}} d\tau,$$

the single and double layer integral operators, and $G(\mathbf{x},t) = \frac{H(t-\|\mathbf{x}\|)}{2\pi\sqrt{t^2-\|\mathbf{x}\|^2}}$ the fundamental solution of the wave equation ($H(\cdot)$ denotes the Heaviside function).

1. The fictitious domain approach

We introduce the larger and simpler time-independent domain $\widetilde{\Omega}$ that includes $\mathscr{O}(t)$ and is bounded by the artificial boundary $\mathscr{B}$. The main idea of the fictitious domain method (or domain embedding method) consists in extending artificially the solution of the exterior problem inside the obstacle, and to solve the new problem in the whole extended domain $\widetilde{\Omega}$. The main advantage of this approach is the possibility of solving the problem in a simpler domain by treating the Dirichlet boundary conditions on $\Gamma(t)$ by Lagrange multipliers. Moreover, the mesh of the enlarged domain can be chosen independent of the geometry of the obstacle, thus allowing to use structured, regular meshes over the extended domain. For a generic function w, we set $w(t)(\mathbf{x}) := w(\mathbf{x},t)$. Then, the problem defined in the domain of interest $\widetilde{\Omega}$ is stated as follows:

find the unknown functions $u(t) \in H^1(\widetilde{\Omega})$, $\lambda_\Gamma(t) \in H^{-1/2}(\Gamma(t))$, $\lambda_{\mathscr{B}}(t) \in H^{-1/2}(\mathscr{B})$ such that the following generalized saddle-point evolution problem

$$
(1)\qquad \begin{cases} (\ddot{u}(t),v)_{\widetilde{\Omega}} + a(u(t),v) + \langle \lambda_\Gamma(t), v\rangle_{\Gamma(t)} + \langle \lambda_{\mathscr{B}}(t), v\rangle_{\mathscr{B}} = (f(t),v)_{\widetilde{\Omega}} \\ \langle \varphi, u(t)\rangle_{\Gamma(t)} = 0 \\ 2\langle \mu, \mathscr{V}\lambda_{\mathscr{B}}(t)\rangle_{\mathscr{B}} - \langle \mu, u(t)\rangle_{\mathscr{B}} - 2\langle \mu, \mathscr{K}u(t)\rangle_{\mathscr{B}} = 0 \\ u(0) = u_0 \\ \dot{u}(0) = v_0 \end{cases}
$$

holds in the distributional sense in $(0,T)$, where $a : H^1(\widetilde{\Omega}) \times H^1(\widetilde{\Omega}) \to \mathbb{R}$ is the bilinear form $a(v,w) = \int_{\widetilde{\Omega}} \nabla v \cdot \nabla w$, and $(v,w)_S = \int_S vw$, with $S = \widetilde{\Omega}$ or $\mathscr{B}$. The bilinear forms $\langle \lambda_\Gamma(t), v\rangle_{\Gamma(t)}$ and $\langle \lambda_{\mathscr{B}}(t), v\rangle_{\mathscr{B}}$ denote the duality pairing between $H^{-1/2}(\Gamma(t))$ and $H^{1/2}(\Gamma(t))$, and $H^{-1/2}(\mathscr{B})$ and $H^{1/2}(\mathscr{B})$, respectively.

We discretize the space-time integral equation on $\mathscr{B}$ by combining a second order (in time) BDF convolution quadrature and a Galerkin (or a collocation) method in space. Such a discretization is then coupled with an uncoditionally stable ODE integrator in time and a FEM in space. The finite element mesh for the solution in the enlarged domain $\widetilde{\Omega}$ is chosen independently of the geometry of the obstacle, and the constraint on $\Gamma(t)$ is imposed by a matrix $B_h(t)$ that represents a discrete trace operator. A particularly useful application of this approach is the study of waves scattered by moving rigid bodies. In this case the method avoids the complexity of constructing at each time step a new finite element computational mesh and requires only the construction of the discrete trace operator $B_h(t)$. We have applied the proposed approach to problems of waves generated by non trivial data and scattered by rotating bodies.

Example 1. In Figure 1 we show the snapshots of a wave that, starting from a initial value u_0 with initial null velocity v_0, impinges upon two scatterers, both having helicoidal shape, that rotate around their own center with constant angular velocity and in opposite directions. The two obstacles are surrounded by an artificial circular boundary of radius 10.

2. A mortar approach

We have tested the roboustness of the NRBC defined by the BIE as well as its accuracy, which turns out to be superior to that of the corresponding FEM. Such properties justify the choice of its discretization in space on a numerical grid of the artificial boundary coarser than the one inherited by the spatial discretization of the finite computational domain. In this context, a mortar like coupling strategy turns out to be an approach more feasible than the conforming one, allowing to relax the pointwise continuity of the solution and of the flux to a weak one, by using suitable Lagrange multipliers. The main advantage of this approach is that non matching grids can be used at the interface $\mathscr{B}$ of the interior and exterior domains. In what follows, we denote by u^W the solution obtained by imposing weakly the NRBC obtained by using M^W boundary points for the partition of the artificial boundary $\mathscr{B}$. To test the accuracy of u^W, we compare it with u^S, the approximate solution obtained by the FEM method where the NRBC is imposed strongly, and in this case the coupling relation is defined at the M^S boundary

FIGURE 1. Example 1. Snapshots of the solution at different times (in seconds).

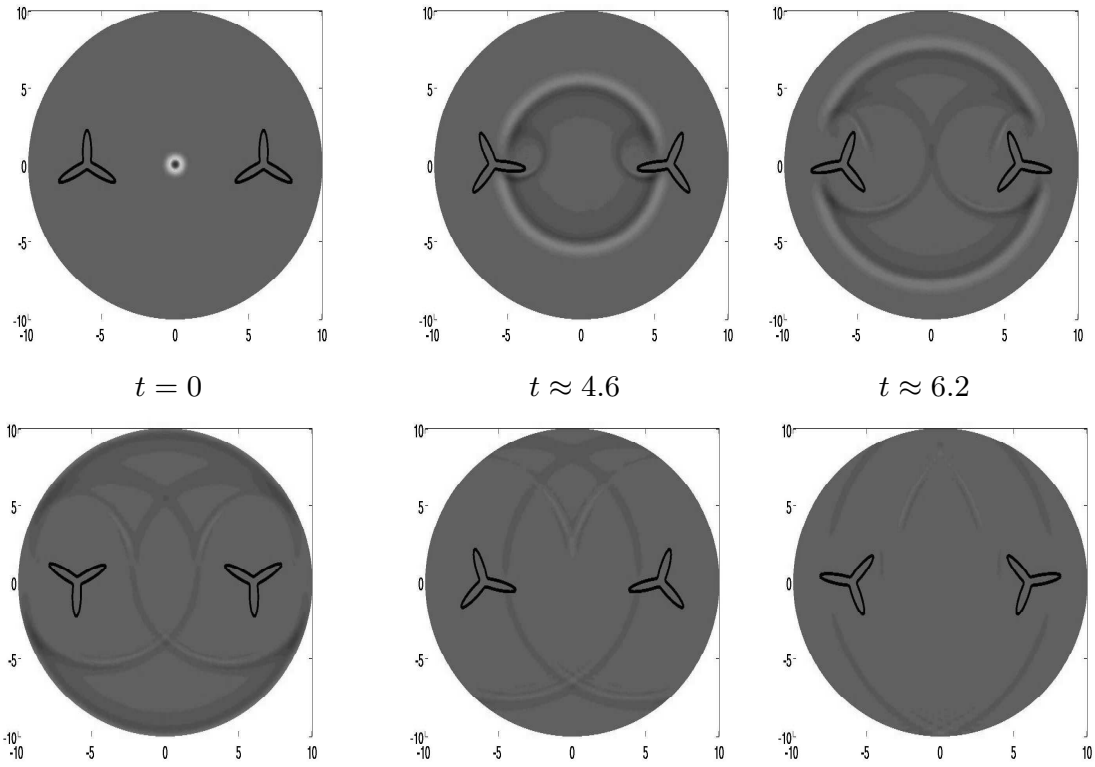

points of $\mathscr{B}$ inherited by the triangulation of the finite computational domain (see [2]). In Figure 2 we show the behavior of the solutions u^S ($M^S = 506$) and u^W($M^W = 128$) of Example 1 at a point $P \approx (0, 4)$ (left plot) and the corresponding behavior of the energies E^S and E^W of system with respect to time (right plot).

FIGURE 2. Example 1. Behavior of u^S and u^W at $P \approx (0, 4)$ (left) and energy dissipations (right).

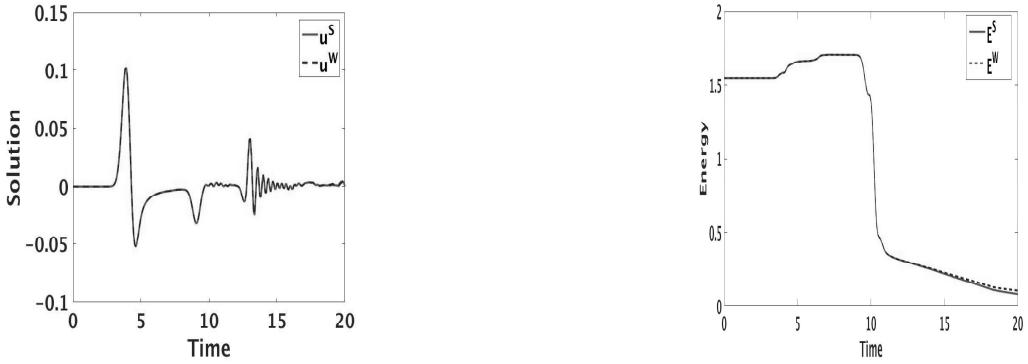

For details on the argument see [1, 2, 3, 4, 5].

References

[1] S. Falletta, G. Monegato, L. Scuderi, *A space-time BIE method for nonhomogeneous exterior wave equation problems. The Dirichlet case*, IMA J. Numer. Anal. **32(1)** (2012), 202–226.

[2] S. Falletta, G. Monegato, *An exact non reflecting boundary condition for 2D time-dependent wave equation problems*, Wave Motion, **51(1)** (2014), 168–192.

[3] S. Falletta, G. Monegato, *Exact nonreflecting boundary conditions for exterior wave equation problems*, Publ. Inst. Math. (Beograd) (N.S.) **96(110)** (2014), 103–123.

[4] S. Falletta, G. Monegato, *Exact non-reflecting boundary condition for 3D time-dependent multiple scattering-multiple source problems*, Wave Motion, **58** (2015), 281–302.

[5] S. Falletta, *BEM coupling with the FEM-fictitious domain approach for the solution of the exterior Poisson problem and of the wave scattering by rotating rigid bodies*, IMA J. Num. Anal., to appear.

Three Different Multigrid Interpretations of the Parareal Algorithm and an Adaptive Variant

Martin J. Gander

Time parallel time integration methods have a long history [1], and the parareal algorithm [2] sparked renewed interest in such methods. To define the parareal algorithm for the ordinary differential equation

$$\frac{du}{dt} = f(u), \quad \text{in } (0,T) \text{ with } u(0) = u_0, \tag{1}$$

one needs a coarse solver $G(t_2, t_1, u_1)$ which solves the differential equation in (1) starting with initial value u_1 at t_1 and gives an approximate solution at time t_2, and a fine solver $F(t_2, t_1, u_1)$ which does the same with much more accuracy. The parareal algorithm is then defined for a partition of the time interval $(0, T)$ into subintervals $0 = T_0 < T_1 < T_2 < \ldots < T_N = T$ by the iteration

$$U_{n+1}^{k+1} = F(T_{n+1}, T_n, U_n^k) + G(T_{n+1}, T_n, U_n^{k+1}) - G(T_{n+1}, T_n, U_n^k), \tag{2}$$

where k is the iteration index, $U_0^{k+1} = u_0$, and the initial approximation can be obtained for example using the coarse solver,

$$U_{n+1}^0 = G(T_{n+1}, T_n, U_n^0), \quad U_0^0 = u_0. \tag{3}$$

The values U_n^k approximate the solution $u(T_n)$ of (1). The most natural interpretation of the parareal algorithm is that it is a multiple shooting method with approximate Jacobian on a coarse grid, and its convergence properties are well understood, see [3] for linear partial differential equations, and [4] for the non-linear case.

Because of the two grids that are often used, a fine one for F and a coarse one for G, the parareal algorithm is also a two-grid method, and it is interesting to consider multigrid variants. There are three ways to obtain these, see [5]:

(1) In the linear case, one can write the parareal iteration (2) as a preconditioned Richardson iteration, where the preconditioner is given by the coarse solve, see also [6]. One can then easily apply again (2) to approximately invert the coarse solver and get a multilevel parareal method.
(2) The parareal iteration (2) can also be interpreted in the geometric multigrid setting as a two level method using one presmoothing step with block Jacobi, but not updating the coarse nodes (sometimes called an F-smoother), and using injection for the restriction R, with prolongation $P := R^T$, and for the coarse matrix a coarse time stepper. This holds also in the non-linear setting using the full approximation scheme, see for example [3]. Again then applying the algorithm recursively for the coarse time stepper leads to a multilevel version.
(3) Finally, one can consider the parareal algorithm (2) in the framework of algebraic multigrid, where the nodes are first partitioned into fine, so called F-nodes, and coarse, so called C-nodes. It can then be shown that the parareal algorithm in fact uses optimal restriction and prolongation operators, and only approximates the optimal coarse correction by a simple coarse solve. This interpretation, together with a modification from the F-smoother to a so called FCF-smoother led to the MGRIT algorithm in [7], which corresponds to a parareal algorithm with overlap, see [5].

A new idea is to use the parareal algorithm adaptively as follows: one first determines the time intervals T_n using an adaptive coarse solver G in the initialization step (3). On this time grid, one then runs the correction iteration (2), also using adaptive fine solvers F and coarse solvers G, without changing the time partition T_n any more. To illustrate this, we now solve an Arenstorf orbit problem. Arenstorf orbits are non-trivial closed orbits of a light object moving in the gravity field of two heavy objects, following the equations of motion

$$\ddot{x} = x + 2\dot{y} - b\frac{x+a}{D_1} - a\frac{x-b}{D_2}, \quad \ddot{y} = y - 2\dot{x} - b\frac{y}{D_1} - a\frac{y}{D_2},$$

where D_j, $j = 1, 2$ are functions of x and y,

$$D_1 = ((x+a)^2 + y^2)^{\frac{3}{2}}, \; D_2 = ((x-b)^2 + y^2)^{\frac{3}{2}}.$$

If the parameters are $a = 0.012277471$ and $b = 1-a$, with initial conditions $x(0) = 0.994$, $\dot{x}(0) = 0$, $y(0) = 0$, $\dot{y}(0) = -2.00158510637908$, then the solution is a nice closed orbit with period $T = 17.06521656015796$, see [8], which can be interpreted as a space craft that tries to return from moon to earth and unfortunately lands again back at the moon, as illustrated by the converged trajectory on top right in Figure 1.

The top row in this figure represents the initial approximation and the first four iterations of the parareal algorithm when using `ode45` in Matlab with tolerance $1e-2$ for the coarse integration[1], determining in the first iteration also the adaptive

[1]A small modification was needed to reduce the minimum number of time steps Matlab takes from 10 to 1 to avoid over-resolution

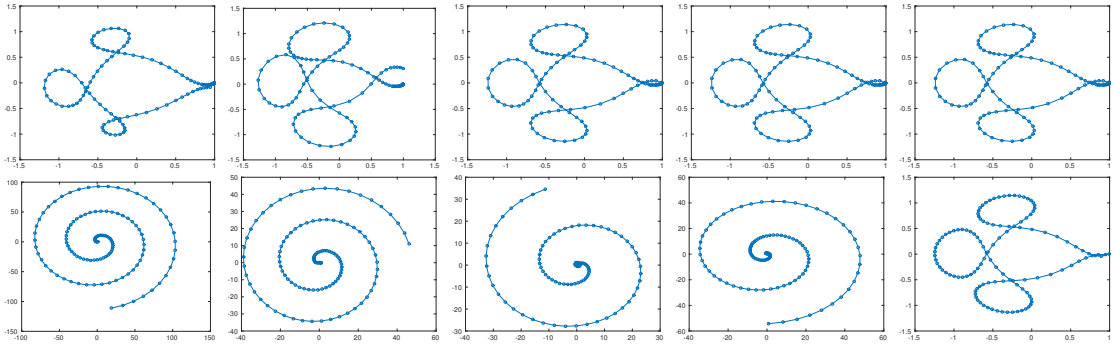

FIGURE 1. Initial approximation and first four iterations of the parareal algorithm applied to the Arenstorf problem. Top row: adaptive variant. Bottom row: fixed step size variant.

time partition, and tolerance $1e-10$ for the fine integration. Convergence to an error tolerance of $1e-6$ is achieved in four iterations, as one can see in Figure 2.

The accuracy in this converged solution is also $1e-6$, and the adaptive parareal algorithm needed a total of $36'458$ function evaluations, using 121 coarse time steps. We next use 121 equidistant coarse time steps and one time step of the classical 4th order Runge-Kutta method for the coarse integrator, and found that 4133 equidistant 4th order Runge-Kutta steps are needed in each coarse time interval for the fine integrator to reach the same error of size $1e-6$. Running the parareal algorithm with these fixed step sizes leads to the result shown in Figure 1 in the bottom row. We see that the initial guess and the first three iterations are very far away from the solution, and only the fourth iteration brings the trajectory closer to the recognizable shape of the Arenstorf orbit. It takes then almost twice the number of iterations to converge, see Figure 2, using a total of $20'011'948$ function evaluations! This is about 550 times more than the adaptive parareal algorithm, for the same accuracy. The adaptive parareal algorithm has the same potential for parallelism and multilevel extension.

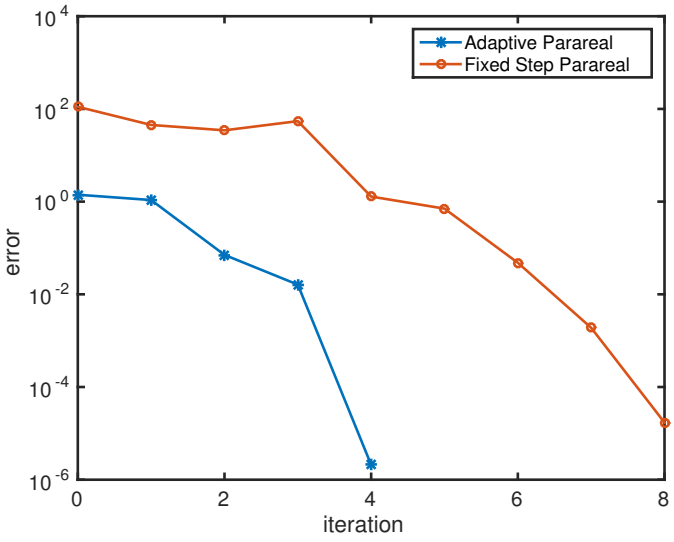

FIGURE 2. Decay of the error as a function of the iteration.

References

[1] Martin J. Gander. 50 years of time parallel time integration. In *Multiple Shooting and Time Domain Decomposition Methods*, pages 69–113. Springer, 2015.

[2] Jacques-Louis Lions, Yvon Maday, and Gabriel Turinici. A parareal in time discretization of PDEs. *C.R. Acad. Sci. Paris, Serie I*, 332:661–668, 2001.

[3] Martin J. Gander and Stefan Vandewalle. Analysis of the parareal time-parallel time-integration method. *SIAM Journal on Scientific Computing*, 29(2):556–578, 2007.

[4] Martin J. Gander and Ernst Hairer. Nonlinear convergence analysis for the parareal algorithm. In Olof B. Widlund and David E. Keyes, editors, *Domain Decomposition Methods in Science and Engineering XVII*, volume 60 of *Lecture Notes in Computational Science and Engineering*, pages 45–56. Springer, 2008.

[5] Martin J. Gander, Felix Kwok and Hui Zhang. Multigrid Interpretations of the Parareal Algorithm Leading to an Overlapping Variant. In preparation, 2017.

[6] Daniel Ruprecht, Robert Speck, and Rolf Krause. Parareal for diffusion problems with space- and time-dependent coefficients. In *Domain Decomposition Methods in Science and Engineering XXII*, pages 371–378. Springer, 2016.

[7] Robert D. Falgout, Stephanie Friedhoff, T.V. Kolev, Scott P. MacLachlan, and Jacob B. Schroder. Parallel time integration with multigrid. *SIAM Journal on Scientific Computing*, 36(6):C635–C661, 2014.

[8] Ernst Hairer, Syvert P. Nørsett and Gerhard Wanner. Solving Ordinary Differential Equations I: Nonstiff Problems. Springer-Verlag, Second Revised Edition, 1993.

High-order Explicit Local Time-stepping Methods for Wave Propagation

Marcus J. Grote

(joint work with Michaela Mehlin, Stefan Sauter)

Local adaptivity and mesh refinement are key to the efficient simulation of wave phenomena in heterogeneous media or complex geometry. Locally refined meshes, however, dictate a small time-step everywhere with a crippling effect on any explicit time-marching method. In [4] a leap-frog (LF) based explicit local time-stepping (LTS) method was proposed, which overcomes the severe bottleneck due to a few small elements by taking small time-steps in the locally refined region and larger steps elsewhere. Here convergence of the LTS-LF method is proved when combined with a standard conforming finite element method (FEM) in space. Numerical results further illustrate the usefulness of the LTS-LF Galerkin FEM in the presence of corner singularities.

1. Introduction

We consider the classical wave equation

$$u_{tt} - \nabla \cdot (c^2 \nabla u) = f \qquad \text{in } \Omega \times (0,T) \tag{1}$$

$$u|_{t=0} = u_0 \quad u_t|_{t=0} = v_0 \qquad \text{in } \Omega, \tag{2}$$

where Ω denotes a bounded domain in $\mathbb{R}^d$, f a (known) source and u_0, v_0 prescribed initial conditions. The speed of propagation, $c = c(x)$, is assumed piecewise

smooth and strictly positive. At the boundary, we impose appropriate boundary conditions for well-posedness.

For the spatial discretization of (1), we consider a conforming finite element (FE) method with mass-lumping. For the time discretization, we opt for the leap-frog based local time-stepping (LTS-LF) method to circumvent the bottleneck caused by the overly stringent CFL condition in the presence of local refinement [4, 5, 6]. Hence we split the mesh into a "coarse" and a "fine" sub-region with mesh size h and h_{f}, respectively. During each time-step Δt inside the "coarse" region, we use p time-steps of smaller size $\Delta\tau = \Delta t/p$ inside the "fine" region, where $p \simeq h/h_{\mathrm{f}}$ — see [4] for details.

Despite the many different explicit LTS methods that were proposed and successfully used for wave propagation in recent years – see [7] and references therein –, a rigorous space-time convergence theory (in the PDE sense) is still lacking. In fact, convergence has been proved only for the method of Collino et al. [1, 2] and very recently for the locally implicit method for Maxwell's equations by Verwer [10, 3, 9], which combines the explicit Verlet scheme with the implicit Crank–Nicolson, neither fully explicit. Indeed, the difficulty in proving convergence of fully explicit LTS methods is twofold. On the one hand, classical proofs of convergence for FE discretizations of the wave equation always assume standard time discretizations, while proofs for explicit multirate schemes (in the ODE literature) are always restricted to the finite-dimensional case. On the other hand, when explicit LTS schemes are reformulated as perturbed one-step schemes, they involve products of differential and restriction operators, which do not commute and seem to inevitably lead to a loss of regularity.

2. Convergence theory

To develop a general convergence theory for explicit LTS methods, we first define finite-dimensional restriction operators to the "fine" grid and formulate the leap-frog (LF) based LTS method from [4] in a Galerkin conforming finite element setting. Next, we prove continuity and coercivity estimates for the LTS operator that are robust with respect to the number of local time-steps p, provided a genuine CFL condition is satisfied. Here, new estimates on the coefficients that appear when rewriting the LTS-LF scheme in "leap-frog manner" play a key role. Those estimates pave the way for the stability estimate of the time iteration operator, for which we then prove a stability bound independently of p.

Due to the local restriction, however, a judicious splitting of the iteration operator and its inverse is required to avoid negative powers of h via inverse inequalities. By combining our analysis of the semi-discrete formulation, which takes into account the effect of local time-stepping, with classical error estimates, we eventually obtain optimal space-time convergence rates.

Let u_h denote the fully discrete Galerkin solution with continuous piecewise polynomial finite elements of order ℓ. Under standard smoothness assumptions on the solution u of (1)–(2), we rigorously prove that for $\Delta t, h \to 0$:

$$\|u - u_h\|_{L^\infty([0,T];L^2(\Omega))} \leq C(1+T)(h^{\ell+1} + \Delta t^2),$$

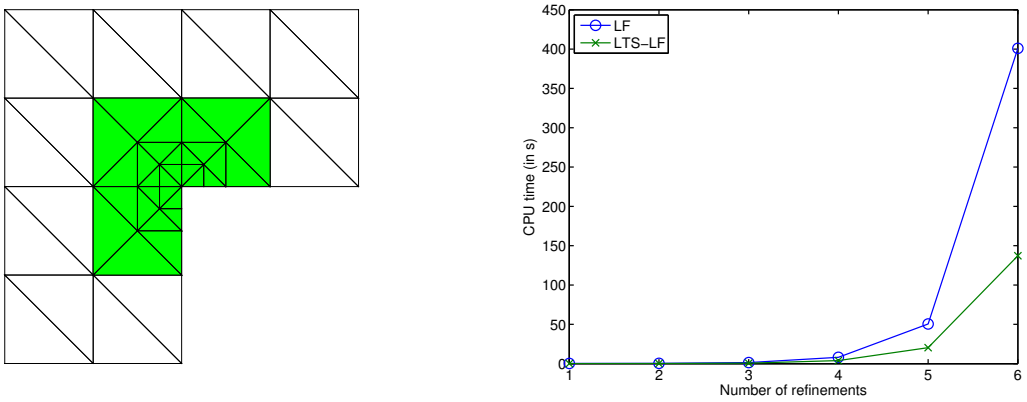

FIGURE 1. Left: Computational mesh with two levels of local refinement. The "fine" region (in green) always corresponds to the innermost 30 elements; right: Comparison of run times between LTS-LF and standard LF vs. number of global refinements, with constant coarse/fine mesh size ratio $p = 4$.

where the constant C depends only on u, but not on h, Δt, p or T.

3. Numerical experiment

We consider (1)–(2) in an L-shaped domain Ω, shown in Fig. 1, and set $c = 1$, $f = 0$ and the final time $T = 1$. Next, we impose homogeneous Neumann conditions on the boundary. For the spatial discretization we opt for $\mathscr{P}^2$ continuous finite elements with mass lumping.

First, we partition Ω into equal triangles of size h_{init}. Towards the re-entrant corner, we then locally refine the mesh by subdividing twice the three elements nearest to the corner – see Fig. 1. Hence the mesh refinement ratio, that is the ratio between smallest elements in the "coarse" and the "fine" regions, in the resulting mesh is 4:1. We therefore choose a four times smaller time-step $\Delta\tau = \Delta t/p$ with $p = 4$ inside the "fine" region.

Clearly, this time-stepping strategy, albeit local, is not optimal as the region of local mesh refinement itself contains a sub-region of even smaller elements. Thus, any local time-step will again be overly restricted due to even smaller elements inside the "fine" region. To remedy the repeated bottleneck caused by hierarchical mesh refinement, multi-level local time-stepping methods were proposed in [5, 6], which permit the use of the appropriate time-step at every level of mesh refinement. For simplicity, however, we restrict ourselves here to the original (two-level) LTS-LF scheme from [4].

In Fig. 1 we compare the runtime of the LTS-LF method on a sequence of meshes with the runtime of a standard LF scheme with a time-step $\Delta t/4$ throughout the entire domain. As expected, the LTS-LF method is faster than the standard LF scheme, in fact increasingly so, as the number of refinement levels increases.

References

[1] F. Collino, T. Fouquet and P. Joly, *A conservative space-time mesh refinement method for the 1-D wave equation. II. Analysis*, Numer. Math. **95** (2003), 223–251.

[2] P. Joly and J. Rodriguez, *An error analysis of conservative space-time mesh refinement methods for the one-dimensional wave equation*, SIAM J. Numer. Anal. **43** (2005), 825–859.

[3] S. Descombes, S. Lanteri and L. Moya, *Locally implicit time integration strategies in a discontinuous Galerkin method*, J. Sci. Comput. **56** (2013), 190–218.

[4] J. Diaz and M.J. Grote, *Energy Conserving Explicit Local Time-stepping for Second-order Wave Equations*, SIAM J. Sci. Comp. **31** (2009), 1985–2014.

[5] J. Diaz and M.J. Grote, *Multilevel Explicit Local Time-stepping For Second-order Wave Equations*, Comp. Meth. Appl. Mech. Engin. **291** (2015), 240–265.

[6] M. Rietmann, M.J. Grote, D. Peter and O. Schenk, *Newmark Local Time Stepping on High-Performance Computing Architectures*, J. Comp. Phys. **334** (2017) 308–326.

[7] M.J. Grote, M. Mehlin and T. Mitkova, *Runge-Kutta Based Explicit Local Time-Stepping Methods for Wave Propagation*, *SIAM J. Sc. Comp.* **37** (2015), A747–A775.

[8] M.J. Grote, M. Mehlin, and S. Sauter, *Convergence Analysis of Energy Conserving Explicit Local Time-stepping Methods for the Wave Equation*, submitted for publication.

[9] M. Hochbruck and A. Sturm, *Error analysis of a second-order locally implicit method for linear Maxwell's equations*, SIAM J. Numer. Anal. **54** (2016), 3167–3191.

[10] J.G. Verwer, *Component splitting for semi-discrete Maxwell equations*, BIT Numer. Math. **51** (2010), 427–445.

On the error analysis of full discretizations of linear Maxwell's equations

Marlis Hochbruck

(joint work with Andreas Sturm)

1. Introduction

In this paper we sketch the key ingredients of an error analysis of the full discretization of linear Maxwell's equations. Our analysis covers space discretization with the discontinuous Galerkin (dG) method and time integration with the Verlet, the Crank–Nicolson, and the implicit midpoint method. We show that the Verlet and the implicit midpoint method can be analyzed by interpreting them as perturbations of the Crank–Nicolson scheme. The same holds true for locally implicit variants, for which detailed results can be found in [2, 3, 4].

2. Maxwell's equations and their spatial discretization

Let $\Omega \subset \mathbb{R}^3$ be a bounded domain and T be a finite time. We consider Maxwell's equations in a linear, isotropic material with a perfectly conducting boundary

$$
\begin{aligned}
\mu \partial_t \mathbf{H} &= -\operatorname{curl} \mathbf{E}, && (0,T)\times\Omega,\\
\varepsilon \partial_t \mathbf{E} &= \operatorname{curl} \mathbf{H} - \mathbf{J}, && (0,T)\times\Omega,\\
\mathbf{H}(0) &= \mathbf{H}^0, \quad \mathbf{E}(0) = \mathbf{E}^0, && \Omega,\\
n \times \mathbf{E} &= 0, && (0,T)\times\partial\Omega.
\end{aligned}
\tag{1}
$$

Here, $\mathbf{H}$ and $\mathbf{E}$ denote the magnetic and electric field, respectively, $\mathbf{J}$ is a given external current density, and ε and μ are piecewise constant material parameters. We discretize Maxwell's equations in space with a central fluxes discontinuous Galerkin (dG) method [1] resulting in the semidiscrete problem

$$\begin{aligned} \partial_t \mathbf{H}_h(t) &= -\boldsymbol{\mathcal{C}}_{\mathbf{E}} \mathbf{E}_h(t), \\ \partial_t \mathbf{E}_h(t) &= \boldsymbol{\mathcal{C}}_{\mathbf{H}} \mathbf{H}_h(t) - \mathbf{J}_h(t), \\ \mathbf{H}_h(0) &= \pi_h \mathbf{H}^0, \quad \mathbf{E}_h(0) = \pi_h \mathbf{E}^0, \end{aligned} \tag{2}$$

where π_h denotes the L^2-orthogonal projection onto the approximation space of the dG method, and where $\mathbf{J}_h = \pi_h(\varepsilon^{-1}\mathbf{J})$. Here, $\boldsymbol{\mathcal{C}}_{\mathbf{E}}$ and $\boldsymbol{\mathcal{C}}_{\mathbf{H}}$ denote the spatially discretized curl-operators, whereby $\boldsymbol{\mathcal{C}}_{\mathbf{E}}$ includes the boundary condition on $\mathbf{E}_h$. In the following, we use

$$\mathbf{u}_h = \begin{pmatrix} \mathbf{H}_h \\ \mathbf{E}_h \end{pmatrix}, \qquad \mathbf{j}_h = \begin{pmatrix} 0 \\ -\mathbf{J}_h \end{pmatrix}, \qquad \boldsymbol{\mathcal{C}} = \begin{pmatrix} 0 & -\boldsymbol{\mathcal{C}}_{\mathbf{E}} \\ \boldsymbol{\mathcal{C}}_{\mathbf{H}} & 0 \end{pmatrix},$$

to keep a short notation.

3. Time integration

Given a time stepsize τ we approximate the solution at times $t_n = n\tau$, i.e., $u_h^n \approx \mathbf{u}_h(t_n)$. Suitable implicit time integrators for the semidiscrete Maxwell's equations (2) are e.g. the Crank–Nicolson method

$$u_h^{n+1} - u_h^n = \frac{\tau}{2}\boldsymbol{\mathcal{C}}(u_h^{n+1} + u_h^n) + \frac{\tau}{2}(\mathbf{j}_h^{n+1} + \mathbf{j}_h^n), \tag{3a}$$

where $\mathbf{j}_h^n = \mathbf{j}_h(t_n)$, or the implicit midpoint method

$$u_h^{n+1} - u_h^n = \frac{\tau}{2}\boldsymbol{\mathcal{C}}(u_h^{n+1} + u_h^n) + \tau \mathbf{j}_h^{n+1/2}. \tag{3b}$$

A popular explicit time integration scheme for (2) is the Verlet (or leap frog) method

$$\begin{aligned} \mathbf{H}_h^{n+1/2} - \mathbf{H}_h^n &= -\frac{\tau}{2}\boldsymbol{\mathcal{C}}_{\mathbf{E}} \mathbf{E}_h^n, \\ \mathbf{E}_h^{n+1} - \mathbf{E}_h^n &= \tau \boldsymbol{\mathcal{C}}_{\mathbf{H}} \mathbf{H}_h^{n+1/2} - \frac{\tau}{2}(\mathbf{J}_h^{n+1} + \mathbf{J}_h^n), \\ \mathbf{H}_h^{n+1} - \mathbf{H}_h^{n+1/2} &= -\frac{\tau}{2}\boldsymbol{\mathcal{C}}_{\mathbf{E}} \mathbf{E}_h^{n+1}. \end{aligned} \tag{3c}$$

Introducing the operators

$$\boldsymbol{\mathcal{R}}_\pm = \boldsymbol{\mathcal{I}} \pm \frac{\tau}{2}\boldsymbol{\mathcal{C}}, \qquad \widehat{\boldsymbol{\mathcal{R}}}_\pm = \boldsymbol{\mathcal{R}}_\pm - \frac{\tau^2}{4}\begin{pmatrix} 0 & 0 \\ 0 & \boldsymbol{\mathcal{C}}_{\mathbf{H}}\boldsymbol{\mathcal{C}}_{\mathbf{E}} \end{pmatrix},$$

we can rewrite the schemes (3) as

$$\boldsymbol{\mathcal{R}}_- u_h^{n+1} = \boldsymbol{\mathcal{R}}_+ u_h^n + \frac{\tau}{2}(\mathbf{j}_h^{n+1} + \mathbf{j}_h^n), \tag{4a}$$

$$\boldsymbol{\mathcal{R}}_- u_h^{n+1} = \boldsymbol{\mathcal{R}}_+ u_h^n + \tau \mathbf{j}_h^{n+1/2}, \tag{4b}$$

$$\widehat{\boldsymbol{\mathcal{R}}}_- u_h^{n+1} = \widehat{\boldsymbol{\mathcal{R}}}_+ u_h^n + \frac{\tau}{2}(\mathbf{j}_h^{n+1} + \mathbf{j}_h^n), \tag{4c}$$

respectively. We have the following bounds [2, Lemmas 3.2, 4.1, 4.2]: The operators $\boldsymbol{\mathcal{R}}_-$ and $\boldsymbol{\mathcal{R}}_+$ satisfy

$$\|\boldsymbol{\mathcal{R}}_-^{-1}\|_{\mu\times\varepsilon} \le 1, \qquad \|\boldsymbol{\mathcal{R}}^m\|_{\mu\times\varepsilon} = 1, \quad \text{where } \boldsymbol{\mathcal{R}} = \boldsymbol{\mathcal{R}}_-^{-1}\boldsymbol{\mathcal{R}}_+,$$

where $\|\cdot\|_{\mu\times\varepsilon}$ is a weighted L^2-norm. For the bounds on the operators $\widehat{\boldsymbol{\mathcal{R}}}_-$ and $\widehat{\boldsymbol{\mathcal{R}}}_+$ we assume the following CFL condition

$$\tau \le C\theta h_{\min}, \qquad \theta \in (0,1), \tag{5}$$

where $h_{\min}$ is the smallest mesh width of the spatial grid and C depends on the regularity of the mesh, the polynomial degree employed in the dG method and on the material parameters. Then, we have that

$$\|\widehat{\boldsymbol{\mathcal{R}}}_-^{-1}\|_{\mu\times\varepsilon} \le (1-\theta^2)^{-1}, \qquad \|\widehat{\boldsymbol{\mathcal{R}}}^m\|_{\mu\times\varepsilon} \le (1-\theta^2)^{-1/2}, \quad \text{where } \widehat{\boldsymbol{\mathcal{R}}} = \widehat{\boldsymbol{\mathcal{R}}}_-^{-1}\widehat{\boldsymbol{\mathcal{R}}}_+.$$

These bounds imply the stability of the Crank–Nicolson and the implicit midpoint method and, under assumption of the CFL condition, of the Verlet method.

4. Error analysis

Let $\mathbf{u} = (\mathbf{H}, \mathbf{E})$ be the exact solution of Maxwell's equations (1) and assume that $\mathbf{u}$ is sufficiently smooth. We consider the full discretization error

$$\mathbf{e}^n = \mathbf{e}_\pi^n - \mathbf{e}_h^n, \qquad \mathbf{e}_\pi^n = \mathbf{u}(t_n) - \pi_h\mathbf{u}(t_n), \qquad \mathbf{e}_h^n = u_h^n - \pi_h\mathbf{u}(t_n).$$

For the methods (3) we obtain the error recursions

$$\boldsymbol{\mathcal{R}}_-\mathbf{e}_h^{n+1} = \boldsymbol{\mathcal{R}}_+\mathbf{e}_h^n + \tau\mathbf{d}_\pi^n + \delta^n, \tag{6a}$$

$$\boldsymbol{\mathcal{R}}_-\mathbf{e}_h^{n+1} = \boldsymbol{\mathcal{R}}_+\mathbf{e}_h^n + \tau\bar{\mathbf{d}}_\pi^n + \bar{\delta}^n + (\boldsymbol{\mathcal{R}}_- - \boldsymbol{\mathcal{R}}_+)\pi_h\bar{\boldsymbol{\xi}}^n, \tag{6b}$$

$$\widehat{\boldsymbol{\mathcal{R}}}_-\mathbf{e}_h^{n+1} = \widehat{\boldsymbol{\mathcal{R}}}_+\mathbf{e}_h^n + \tau\widehat{\mathbf{d}}_\pi^n + \delta^n + (\widehat{\boldsymbol{\mathcal{R}}}_- - \widehat{\boldsymbol{\mathcal{R}}}_+)\pi_h\widehat{\boldsymbol{\xi}}^n, \tag{6c}$$

respectively. Here, $\mathbf{d}_\pi^n$, $\bar{\mathbf{d}}_\pi^n$, and $\widehat{\mathbf{d}}_\pi^n$ are projection errors, which are of order h^k when using polynomials of degree k in the space discretization, while δ^n and $\bar{\delta}^n$ correspond to quadrature errors of order τ^3. The remaining defects

$$\bar{\boldsymbol{\xi}}^n = -\frac{1}{2}(\mathbf{u}(t_{n+1}) - 2\mathbf{u}(t_{n+1/2}) + \mathbf{u}(t_n)), \qquad \widehat{\boldsymbol{\xi}}^n = \frac{\tau}{4}\begin{pmatrix}\partial_t(\mathbf{H}(t_{n+1}) - \mathbf{H}(t_n))\\ 0\end{pmatrix}$$

are of lower order and have to be investigated further. The key idea to prove full order is to split the defect into $\boldsymbol{\eta}^n + (\boldsymbol{\mathcal{R}}_- - \boldsymbol{\mathcal{R}}_+)\boldsymbol{\xi}^n$, where, e.g., for the implicit midpoint method we have

$$\boldsymbol{\eta}^n = \tau\bar{\mathbf{d}}_\pi^n + \bar{\delta}^n, \qquad \boldsymbol{\xi}^n = \pi_h\bar{\boldsymbol{\xi}}^n.$$

This results in an error recursion of the form

$$\begin{aligned}\mathbf{e}_h^{n+1} &= \sum_{m=0}^{n}\boldsymbol{\mathcal{R}}^{n-m}\boldsymbol{\mathcal{R}}_-^{-1}\boldsymbol{\eta}^m + \sum_{m=0}^{n}\boldsymbol{\mathcal{R}}^{n-m}(\boldsymbol{\mathcal{I}} - \boldsymbol{\mathcal{R}})\boldsymbol{\xi}^m\\ &= \boldsymbol{\xi}^n - \boldsymbol{\mathcal{R}}^{n+1}\boldsymbol{\xi}^0 + \sum_{m=0}^{n}\boldsymbol{\mathcal{R}}^{n-m}\boldsymbol{\mathcal{R}}_-^{-1}\boldsymbol{\eta}^m - \sum_{m=0}^{n-1}\boldsymbol{\mathcal{R}}^{n-m}(\boldsymbol{\xi}^{m+1} - \boldsymbol{\xi}^m).\end{aligned}$$

The same representation holds with the operators $\widehat{\boldsymbol{\mathcal{R}}}_-$ and $\widehat{\boldsymbol{\mathcal{R}}}_+$ if the CFL condition (5) is satisfied. Because both $\bar{\boldsymbol{\xi}}^{m+1} - \bar{\boldsymbol{\xi}}^m$ and $\widehat{\boldsymbol{\xi}}^{m+1} - \widehat{\boldsymbol{\xi}}^m$ are of order τ^3 we obtain for all methods the error bound

$$\|\mathbf{e}^n\|_{\mu\times\varepsilon} \le C(h_{\max}^k + \tau^2), \qquad n\tau \le T,$$

where the constant C is independent of the mesh width h and the time step τ.

References

[1] D. A. Di Pietro, A. Ern, *Mathematical aspects of discontinuous Galerkin methods*, Springer **69** (2012).

[2] M. Hochbruck, A. Sturm, *Error analysis of a second-order locally implicit method for linear Maxwell's equations*, SIAM J. Numer. Anal. **54** (2016), 3167–3191.

[3] M. Hochbruck, A. Sturm, *Upwind discontinuous Galerkin space discretization and locally implicit time integration for linear Maxwell's equations*, CRC 1173-Preprint **4** (2017), Karlsruhe Institute for Technology (KIT).

[4] A. Sturm, *Locally implicit time integration for Maxwell's equations*, PhD Thesis (2017), Karlsruhe Institute for Technology (KIT).

Propagation of acoustic waves in fractal networks

Patrick Joly

(joint work with Maryna Kachanovska, Adrien Semin)

Sound propagation in lungs is a useful tool for diagnostics of lung diseases. It is modelled by the wave equation in a network of thin slots, the latter being asymptotically reduced to a self-similar fractal one-dimensional tree. Efficient resolution of this problem constitutes the subject of the present work.

Given a compact self-similar p-adic tree $\mathscr{T}$ consisting of a countable set of edges and vertices, we study the wave equation defined on its edges

$$\mu\partial_t^2 u - \partial_x(\mu\partial_x u) = 0, \tag{1}$$

with the condition $u(M^*, t) = f(t)$ at the root vertex M^* of $\mathscr{T}$. The weight μ is constant along every edge Σ. Provided the length ℓ of an edge Σ at a generation $k \ge 0$, the length of each of its p children Σ_j, $j = 0, \dots, p-1$, located at the generation $(k+1)$, is $\alpha_j \ell$ with $0 < \alpha_j < 1$. Moreover, the value of μ along Σ_j is μ_j times its value along Σ, with $\mu_j > 0$. The tree $\mathscr{T}$ has infinitely many such generations, defined inductively. The problem (1) is completed with the

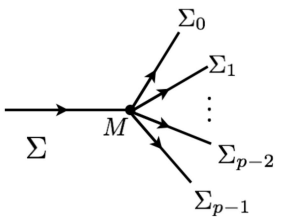

$$u|_{\Sigma}(M,t) = u|_{\Sigma_k}(M,t), \quad k = 0, \dots, p-1,$$

$$\partial_x u|_{\Sigma}(M,t) = \sum_{k=0}^{p-1} \mu_k \, \partial_x u|_{\Sigma_k}(M,t),$$

Figure 1. Transmission conditions on the non-root vertices.

transmission conditions on non-root vertices, cf. Figure 1. One of its difficulties and originalities of this problem is the treatment of the 'infinity' (notice however that the tree is compact). Particularly, (1) is equipped with Neumann/Dirichlet BCs, incorporated into the variational formulation. E.g., for the Neumann BCs:

$$\frac{d^2}{dt^2}(\mu u, v)_{\mathscr{T}} + (\mu \partial_x u, \partial_x v)_{\mathscr{T}} = 0,\ v \in H^1_\mu,\ u \in C^1(0,T;L^2_\mu) \cup C^0(0,T;H^1_\mu), \tag{2}$$

and for the Dirichlet BCs H^1_μ is substituted by $H^1_{\mu,0}$. For the definition of spaces L^2_μ, H^1_μ, $H^1_{\mu,0}$ and scalar products, see [1]. We consider the case when Dirichlet and Neumann problems differ and the embedding $H^1_\mu \subset L^2_\mu$ is compact, or, cf. [1],

$$\sum_i \mu_i\, \alpha_i < 1, \quad \sum_i \mu_i/\alpha_i > 1. \tag{3}$$

In order to perform the computation, we truncate the tree at a certain level using a transparent boundary condition at each end point M:

$$\partial_x u(M,\cdot) = \sum_{i=0}^{p-1} \mu_i \Lambda_i(\partial_t) u(M,\cdot)$$

where $\Lambda_i(\partial_t) = \ell_i^{-1}\Lambda(\ell_i\,\partial_t)$, $\Lambda(\partial_t)$ is the DtN operator associated with a reference tree (whose root edge has length 1) and ℓ_i are the lengths of the p edges of the truncated subtree terminating at M. $\Lambda(\partial_t)$ is a convolution operator whose symbol $\Lambda(\omega)$ (through $\partial_t \leftrightarrow -i\omega$) is not known explicitly, but satisfies the equation

$$\Lambda(\omega)\cos(\omega) + \omega \sin\omega = \Big(\cos\omega - \Lambda(\omega)\frac{\sin\omega}{\omega}\Big)\Big(\sum_{i=0}^{p-1} \frac{\mu_i}{\alpha_i}\Lambda(\alpha_i\omega)\Big). \tag{4}$$

We look for an even meromorphic solution [1] to the above problem, whose uniqueness is ensured provided the value $\Lambda(0)$ (which is 0 for the Neumann problem and $\big(1 - \big(\sum_i \mu_i/\alpha_i\big)^{-1}\big)$ for the Dirichlet problem). In [1] the authors proposed transparent BCs based on the Laurent expansion of $\Lambda(\omega)$ near $\omega = 0$. Such BCs require truncating the tree at the level where $|\ell\omega| \ll 1$. In this work we relax this condition using two methods: a) construction of transparent BCs for the discretized problem (convolution quadrature (CQ)); b) approximation of $\Lambda(\omega)$ by rational functions.

Approach 1: Convolution Quadrature (CQ). We apply a trapezoid CQ [2] for the approximation of $\Lambda(\partial_t)$, coupled with an explicit leap-frog scheme for the discretization of the volumetric terms. Given $\mathscr{T}_i$ the subtree for which the computation is done using FEM (w.l.o.g. we assume that all the end edges have the same length ℓ), and by $\mathscr{T}_e = \mathscr{T} \setminus \mathscr{T}_i$, we rewrite (2):

$$\frac{d^2}{dt^2}(\mu u, v)_{\mathscr{T}_i} + (\mu\,\partial_x u, \partial_x v)_{\mathscr{T}_i} + \frac{d^2}{dt^2}(\mu u, v)_{\mathscr{T}_e} + (\mu \partial_x u, \partial_x v)_{\mathscr{T}_e} = 0,\ v \in H^1_\mu. \tag{5}$$

After the space discretization along $\mathscr{T}_i$ (not along $\mathscr{T}_e$) we discretize in time, with constant Δt, $u|_{\mathscr{T}_i}$ with leapfrog and $u|_{\mathscr{T}_e}$ with the trapezoidal rule:

$$\left(\mu\frac{u_{n+1}-2u_n+u_{n-1}}{\Delta t^2},v\right)_{\mathscr{T}}+(\mu\,\partial_x u_n,\partial_x v)_{\mathscr{T}_i}+\left(\mu\,\partial_x u_{n,\frac14},\partial_x v\right)_{\mathscr{T}_e}=0,$$

where $u_{n,\frac14}=(u_{n+1}+2u_n+u_{n-1})/4$. Denoting $u_{\Delta t}=(u_n)_{n=1}^N$ the semi-discrete solution, this can be rewritten as, provided $\{M_k\}$ the set of the end nodes of $\mathscr{T}_e$,

$$\left(\mu\frac{u_{n+1}-2u_n+u_{n-1}}{\Delta t^2},v\right)_{\mathscr{T}_i}+(\mu\,\partial_x u_n,\partial_x v)_{\mathscr{T}_i}$$
$$+\sum_k\sum_{j=0}^{p-1}\mu_j\left(\Lambda_j^{\Delta t}u_{\Delta t}(M_k)\right)_{n,\frac14}v(M_k)=0.$$

Here $\Lambda_j^{\Delta t}$ are the discrete DtN operators with the symbols (with abuse of notation)

$$\Lambda_j^{\Delta t}(\omega)=\ell_j^{-1}\Lambda\big(\ell_j\;\Omega_{\Delta t}(\omega)\big),\qquad \Omega_{\Delta t}(\omega)=\frac{2i}{\Delta t}\frac{1-\mathrm{e}^{i\omega\Delta t}}{1+\mathrm{e}^{i\omega\Delta t}}.$$

Defining the convolution weights λ_j^n by $\Lambda_j^{\Delta t}(\omega)=\sum\limits_{n=0}^{+\infty}\lambda_j^n(\Delta t)\;e^{in\omega\Delta t}$, we obtain

$$\left(\Lambda_j^{\Delta t}u_{\Delta t}\right)_n=\sum_{q=0}^{n}\lambda_j^{n-q}(\Delta t)\,u_q(M_k).$$

The computation of $\lambda_i^n(\Delta t), n\geq 0$, requires a procedure of the evaluation of $\Lambda(\omega)$ in the complex plane; one way to do so is described in [3]. The stability of the scheme can be shown by energy techniques.

Approach 2: Rational Approximations. From coercivity properties of the DtN, it follows that $-\omega^{-1}\Lambda(\omega)$ is a Herglotz function (i. e. an analytic map from the upper complex half-space into itself). Moreover, $\Lambda(\omega)$ is of the form

$$\Lambda(\omega)=\Lambda(0)-\sum_{j=0}^{\infty}\frac{a_j\omega^2}{\Omega_j^2-\omega^2},\qquad \Omega_j\neq 0,\;a_j>0,\;\Lambda(0)\geq 0. \tag{6}$$

We will look for rational approximations of $\Lambda(\omega)$ in a class of rational Herglotz functions (obtained, for example, by truncating at the order N the above sum). In this case (5) becomes: for all $v\in H_\mu(\mathscr{T})$,

$$\frac{d^2}{dt^2}(\mu u,v)_{\mathscr{T}_i}+(\mu\partial_x u,\partial_x v)_{\mathscr{T}_i}+\sum_k\sum_{j=0}^{p-1}\mu_j\,\Lambda_j^N(\partial_t)u(M_k,\cdot)\,v(M_k)=0, \tag{7}$$

where the operators $\Lambda_j^N(\partial_t)$ are given by

$$\begin{aligned}&\Lambda_j^N(\partial_t)\,u(M_k,.)=\ell_j^{-1}\big(\Lambda(0)u(M_k,.)+\sum_{i=0}^{N-1}a_i\,\partial_t\psi_{j,i}^k\big),\\&\partial_{tt}\psi_{j,i}^k+\ell_j^{-2}\,\Omega_i^2\;\psi_{j,i}^k=\partial_t u(M_k,.),\qquad 0\leq i\leq N-1.\end{aligned} \tag{8}$$

The stability of (7) coupled with (8) follows from the energy conservation:

$$\frac{d}{dt}(\mathscr{E}_i + \mathscr{E}_b) = 0, \qquad \mathscr{E}_i = \frac{1}{2}\left((\mu u, u)_{\mathscr{T}_i} + (\mu \partial_x u, \partial_x u)_{\mathscr{T}_i}\right),$$
$$\mathscr{E}_b = \sum_k \sum_{j=0}^{p-1} \mu_j \ell_j^{-1} \left(\Lambda(0)|u(M_k)|^2 + \sum_{i=0}^{N-1} a_i \left(|\partial_t \psi_{j,i}^k|^2 + \ell_j^{-2} \Omega_i^2 |\psi_{j,i}^k|^2 \right) \right).$$

The volumetric terms in (7) can be semidiscretized in time using the leapfrog scheme, and the boundary terms with the help of the implicit trapezoid rule, similarly to how it is done for the Maxwell equations in dispersive media. The resulting scheme can be reformulated in an explicit manner.

References

[1] P. Joly and A. Semin, *Wave Propagation in Fractal Trees. Mathematical and Numerical Issues*. Submitted.

[2] C. Lubich, *Convolution Quadrature and Discretized Operational Calculus. I.* Numer. Math. 52, 129-145 (1988).

[3] C. Lubich, *Convolution Quadrature and Discretized Operational Calculus. II.* Numer. Math. 52, 413-425 (1988).

Stable Perfectly Matched Layers for a Class of Anisotropic Dispersive Models

Maryna Kachanovska

(joint work with Eliane Bécache)

For many applications in physics (modelling of plasmas in tokamaks, or superlenses made of metamaterials), it is required to model the wave propagation in unbounded anisotropic dispersive media. There exist numerous techniques to deal with the unboundedness of the domain in practical computations, e.g. boundary integral equations, absorbing/transparent boundary conditions, pole conditions etc., but, to our knowledge, none of them can be applied as is in this context. Here we concentrate on the method of perfectly matched layers (PMLs), proposed by Bérenger [1, 2]. The advantages of PMLs include the ease of implementation and effortless treatment of corners, however, PMLs are known to exhibit instabilities when applied to problems with anisotropy and/or dispersion [3, 4]. In this talk we show how to construct stable PMLs for a particular class of 2D Maxwell anisotropic dispersive problems. All the presented results can be found in [5].

1. Problem Setting

We consider the wave propagation in 2D dispersive anisotropic media modelled by the Maxwell's equations

$$\partial_t \mathbf{D} - \mathbf{curl} H_z = 0, \qquad \partial_t B_z + \operatorname{curl} \mathbf{E} = 0, \tag{1}$$

complemented with constitutive relations, which we write in the Laplace domain. Denoting by $\hat{u}(s,x),\ s \in \mathbb{C}_+ = \{z \in \mathbb{C} :\ \Re z > 0\}$, the Laplace transform of a causal tempered $u(t,x)$, we assume that

$$\hat{\mathbf{D}} = \varepsilon(s)\hat{\mathbf{E}}, \qquad \hat{B}_z = \mu(s)\hat{H}_z, \qquad \varepsilon(s) = \begin{pmatrix} \varepsilon_x(s) & 0 \\ 0 & \varepsilon_y(s) \end{pmatrix}. \tag{2}$$

In the time domain the above corresponds to convolutions.

Assumption 1. *The dielectric permittivity $\varepsilon_x(s)$, $\varepsilon_y(s)$ and the magnetic permeability $\mu(s)$ satisfy the following assumptions, see* [5, 6] *for the justification:*

(1) $\varepsilon_x(s)$, $\varepsilon_y(s)$, $\mu(s)$ are analytic in $\mathbb{C}_+$, and $\Re\left(s\varepsilon_x(s)\right) > 0$, $\Re\left(s\varepsilon_y(s)\right) > 0$, $\Re(s\mu(s)) > 0$ for all $s \in \mathbb{C}_+$. We will call this property of the analyticity and the sign condition in $\mathbb{C}_+$ passivity.
(2) they are even rational functions with real coefficients;
(3) $\varepsilon_x(s),\ \varepsilon_y(s),\ \mu(s) \to 1$ as $|s| \to +\infty$.

It is known [7, 8] that the only generalized Lorentz materials satisfy the above.

Theorem 1. *Assume $c(s) = 1 + \frac{p(s^2)}{q(s^2)}$, where p, q are polynomials with real coefficients, and $\deg p < \deg q$. Then $c(s)$ is passive if and only if*

$$c(s) = 1 + \sum_{\ell=0}^{n} \frac{c_\ell}{s^2 + \omega_\ell^2}, \qquad c_\ell > 0,\ \omega_\ell \in \mathbb{R}.$$

In the time domain, (1-2) can be written as the Maxwell's equations with currents, coupled with the ordinary differential equations for currents [4, 5].

To (1-2) we associate the following sesquilinear form

$$\mathscr{A}(\hat{H}_z, v) = \varepsilon_y(s)^{-1}(\partial_x \hat{H}_z, \partial_x v) + \varepsilon_x(s)^{-1}(\partial_y \hat{H}_z, \partial_y v) + s^2\mu(s)(\hat{H}_z, v),\ \hat{H}_z,\ v \in H^1(\mathbb{R}^2).$$

Here $(u,v) = \int\limits_{\mathbb{R}^2} u\bar{v}dx$. It can be shown [5] that

$$\text{Passivity of } \varepsilon_x,\ \varepsilon_y,\ \mu \implies \text{Stability of (1-2) in the time domain} \tag{3}$$

Definition 1. *A sesquilinear form $A(u,v) = a(s)(\partial_x u, \partial_x v) + b(s)(\partial_y u, \partial_y v) + s^2 c(s)(u,v),\ u, v \in H^1(\mathbb{R}^2)$, is called passive if $a(s)^{-1}$, $b(s)^{-1}$, $c(s)$ are passive.*

2. Perfectly Matched Layers for Dispersive Models

The main idea of the PML method is to surround the computational domain by an absorbing layer, inside which the solution would decay fast, so that this layer can be truncated by vanishing boundary conditions. Importantly, it is constructed so that no reflection on the boundary between the computational domain and the absorbing layer is produced.

Let us assume that the PML is constructed in the half-space $x > 0$. Then it amounts to performing the change of variables, cf. [4]

$$x \to x + \frac{\psi(s)}{s} \int_{0y}^{x} \sigma(x')dx', \qquad x > 0, \tag{4}$$

where $\sigma(x') \geq 0$ for $x \geq 0$ and $\sigma(x') \equiv 0$ for $x < 0$. In the traditional Bérenger's PMLs $\psi(s) \equiv 1$, however, for many dispersive models it is necessary to choose $\psi(s) \neq 1$ in order to ensure the stability of the resulting PML model [4].

Performing the PML change of variables results in the following form

$$\tilde{\mathscr{A}_\sigma}(\hat{H}_z, v) = \varepsilon_y(s)^{-1} \left(\frac{1}{1 + s^{-1}\psi(s)\sigma(x)} \partial_x \hat{H}_z, \partial_x \left(\frac{v}{1 + \overline{s^{-1}\psi(s)}\sigma(x)} \right) \right)$$
$$+ \varepsilon_x(s)^{-1}(\partial_y \hat{H}_z, \partial_y v) + s^2 \mu(s)(\hat{H}_z, v),\ \hat{H}_z,\ v \in H^1(\mathbb{R}^2).$$

The first step of the PML analysis consists in taking in the above $\sigma(x) \equiv \sigma \equiv$ const ≥ 0, and studying the well-posedness and stability of the resulting time-domain problem [5]. The corresponding sesquilinear form then reads

$$\mathscr{A}_\sigma(\hat{H}_z, v) = \frac{\varepsilon_y(s)^{-1}}{\left(1 + s^{-1}\psi(s)\sigma\right)^2} \left(\partial_x \hat{H}_z, \partial_x v \right) + \varepsilon_x(s)^{-1}(\partial_y \hat{H}_z, \partial_y v)$$
$$+ s^2 \mu(s)(\hat{H}_z, v), \qquad \hat{H}_z,\ v \in H^1(\mathbb{R}^2),\ \sigma \geq 0.$$

This amounts in substituting (4) by

$$x \to x(1 + s^{-1}\psi(s)\sigma), \qquad \sigma \geq 0, \qquad x \in \mathbb{R}. \tag{5}$$

In view of (3), for the stability of the PMLs it suffices to study the passivity properties of the above sesquilinear form. Before doing this, let us limit the class of the functions $\psi(s)$. We suggest to choose $\psi(s)$ that satisfy the same hypothesis as $\varepsilon_y(s)^{-1}$. Such functions are characterized in the following result.

Theorem 2. *Assume $\psi(s) = 1 + \frac{p(s^2)}{q(s^2)}$, where p, q are polynomials with real coefficients, and $\deg p < \deg q$. Then $\psi(s)^{-1}$ is passive if and only if*

$$\psi(s) = 1 - \sum_{\ell=0}^{n} \frac{\psi_\ell}{s^2 + \omega_\ell^2}, \qquad \psi_\ell > 0,\ \omega_\ell \in \mathbb{R} \setminus \{0\}, \qquad \psi(0) \geq 0.$$

Given a (meromorphic) function $r : \mathbb{C} \to \mathbb{C}$, let us denote $\tilde{r}(\omega) = r(-i\omega)$, $\omega \in \mathbb{R}$. The following result provides an easy characterization of the functions $\psi(s)$ leading to stable PMLs, where the stability is ensured by passivity (3).

Theorem 3. *Let $\psi(s) = 1 + \frac{p(s^2)}{q(s^2)}$, where p, q are polynomials with real coefficients, and $\deg p < \deg q$. Let also $\psi(s)^{-1}$ be passive. Additionally, we assume that ε_x, ε_y, μ satisfy Assumption 1. Then the following two conditions are equivalent:*

(1) the sesquilinear form $\psi(s)\varepsilon_y(s)\mathscr{A}_\sigma(\hat{H}_z, v)$ is passive;
(2) for all $\omega \in \mathbb{R}$, s.t. $\tilde{\varepsilon}_x(\omega)\tilde{\varepsilon}_y(\omega) < 0$ or $\tilde{\varepsilon}_y(\omega)\tilde{\mu}(\omega) > 0$, it holds that $\tilde{\psi}(\omega)\tilde{\varepsilon}_y(\omega) \geq 0$.

A function $\psi(s)$ satisfying the above theorem always exists, for instance, $\psi(s) = \varepsilon_y(s)^{-1}$.

References

[1] J.-P. Berenger, *A perfectly matched layer for the absorption of electromagnetic waves*. J. Comput. Phys. 114 (1994), no. 2, 185–200

[2] J.-P. Berenger, *Three-dimensional perfectly matched layer for the absorption of electromagnetic waves*. J. Comput. Phys. 127 (1996), no. 2, 363–379

[3] E. Bécache, S. Fauqueux, P. Joly. *Stability of perfectly matched layers, group velocities and anisotropic waves*. Journal of Computational Physics, Elsevier, 2003, 188 (2), pp.399-433.

[4] E. Bécache, P. Joly, V. Vinoles. *On the analysis of perfectly matched layers for a class of dispersive media and application to negative index metamaterials*, submitted. Preprint available at https://hal.archives-ouvertes.fr/hal-01327315v2

[5] E. Bécache, M. Kachanovska, *Stable perfectly matched layers for a class of anisotropic dispersive models. Part I: necessary and sufficient conditions of stability*. Submitted. Preprint available at https://hal.archives-ouvertes.fr/hal-01356811v2

[6] M. Cassier, P. Joly, M. Kachanovska, *Mathematical models for dispersive electromagnetic waves: an overview*. Submitted. Preprint available at https://arxiv.org/pdf/1703.05178.pdf

[7] O. Brune, *Synthesis of a finite two-terminal network whose driving-point impedance is a prescribed function of frequency*, Journal of Mathematics and Physics 10 (1-4) (1931) 191–236.

[8] P. I. Richards, *A special class of functions with positive real part in a half-plane*, Duke Math. J. 14 (1947) 777–786.

Space-Time Discretisation and Solver Technology for Biot's Model of Poroelasticity

Uwe Köcher

The accurate, reliable and efficient numerical approximation of multi-physics processes in heterogeneous porous media with varying media coefficients that include fluid flow and structure interactions is of fundamental importance in energy, environmental, petroleum and biomedical engineering applications fields for instance. Important applications include lithium-ion polymer battery simulations, carbon sequestration, subsurface compaction drive, hydraulic and thermal fracturing and oil recovery. Biomedical applications include the simulation of vibration therapy for osteoporosis processes of trabeculae bones, estimating stress levels induced by tumour growth within the brain or next-generation spinal disc prostheses.

Variational space-time methods offer some appreciable advantages such as the flexibility of the triangulation for complex geometries in space and natural local time stepping, the straightforward construction of higher-order approximations and the application of efficient goal-oriented (duality-based) adaptivity concepts. In addition to that, uniform space-time variational methods appear to be advantageous for stability and a priori error analyses of the discrete schemes. Especially (high-order) discontinuous in time approaches appear to have favourable properties due to the weak application of the initial conditions.

The Biot poroelasticity equation system characterise a multi-physics problem of slightly compressible single-phase diffusive porous media flow coupled with quasi-static deformation as structure interaction. The fully-coupled partial differential equations system in strong form for the approximation of displacement $\boldsymbol{u}$, fluid flux $\boldsymbol{q}$ and fluid pressure p is given by

$$
\begin{aligned}
-\nabla\cdot(\boldsymbol{\sigma}_0+\boldsymbol{C}:\boldsymbol{\epsilon}(\boldsymbol{u}-\boldsymbol{u}_0)-b\,(p-p_0)\mathbf{1}) &= (\phi\rho_f+(1-\phi)\rho_s)\,\boldsymbol{g}\,,\\
\eta\boldsymbol{K}^{-1}\boldsymbol{q}+\nabla p &= \rho_f\,\boldsymbol{g}\,,\\
\tfrac{b}{K_{\mathrm{dr}}}\partial_t\sigma_v(\boldsymbol{u},p)+\big(\tfrac{1}{M}+\tfrac{b^2}{K_{\mathrm{dr}}}\big)\partial_t p+\operatorname{div}\boldsymbol{q} &= f\,,
\end{aligned}
$$

with $\boldsymbol{\epsilon}(\boldsymbol{u})=\frac{1}{2}(\nabla\boldsymbol{u}+\nabla\boldsymbol{u}^T)$, and denoting by $\boldsymbol{C}$ elasticity tensor, by ϕ the porosity, by ρ_s and ρ_f the solid and fluid densities, by η the fluid viscosity, by $\boldsymbol{K}$ the permeability tensor and using the volumetric mean stress

$$
\sigma_v(\boldsymbol{u},p)=\sigma_{v,0}+K_{\mathrm{dr}}\,\nabla\cdot(\boldsymbol{u}-\boldsymbol{u}_0)-b\,(p-p_0)\,,
$$

in $\Omega\times I$, $\Omega\subset\mathbb{R}^d$, $I=(0,T)$ and equipped with appropriate initial and boundary conditions. The coupling between the deformation and fluid flow is described by Biot using a coupling coefficient $b=1-K_{\mathrm{dr}}/K_{\mathrm{s}}$, $0<b<1$, and modulus $M>0$.

A discontinuous in time discretisation is applied in order to approximate the solution by employing Bochner spaces $\mathscr{V}$ with values in Hilbert spaces $\mathscr{H}$, e.g.

$$
\begin{aligned}
\mathscr{V}_\tau^r(I,\mathscr{H}) &= \Big\{v\in L^2(I,\mathscr{H})\;\Big|\;v|_{I_n}\in\mathbb{P}_r(I_n,\mathscr{H})\Big\},\\
\mathbb{P}_r(I_n,\mathscr{H}) &= \Big\{p:I_n\to\mathscr{H}\;\Big|\;p=\textstyle\sum_{j=0}^r p_n^j\,t^j,\;p_n^j\in\mathscr{H}\Big\},
\end{aligned}
$$

with $I_n=(t_{n-1},t_n)$ of a partition of the time domain. This construction allows to solve the discrete schemes in the sense of time marching schemes, due to the application of discontinuous Bochner spaces as test spaces. The discretisation in space yields a stable, high-order and locally mass conservative discrete scheme. Precisely, a Raviart-Thomas-Nédélec mixed finite element $\{\mathrm{Nc}^f(p)\text{-}\mathrm{dQ}(p\text{-}1)\}$ for the approximation of the flux and pressure combined with a continuous finite element method $\mathrm{cQ}(p)^d$, employing Gauß-Lobatto quadrature points for the construction of the piecewise polynomial tensor product basis functions, for the approximation of the displacement $\boldsymbol{u}$ is applied.

The development of monolithic multi-physics schemes, instead of iterative coupling methods between the physical problems, is a key component of the research to reduce the modeling error. Special emphasis is on the development of efficient multi-physics and multigrid preconditioning technologies and their implementation. State of the art monolithic schemes commonly deploy (low-order) distributional time integration. Arising block systems are solved with Schur-complement technologies using standard preconditioning strategies. Monolithic high-order $\mathrm{dG}(r)$ variational time discretisations allow and need the development of sophisticated solver and preconditioning technologies. An efficient preconditioning technology of the outer iterative solver GMRES for fully-coupled $\mathrm{dG}(0)$, or even $\mathrm{dG}(1)$, block systems is based on an optimised truncated fixed-stress solver

technology. The optimised fixed-stress iterative coupling method (as solver) for high-order continuous and discontinuous variational time discretisations is analysed in [1, 2].

The numerical simulation software DTM++ is a modularised framework written in C++11 and builds on top of deal.II toolchains; cf. [4, 6]. The implementation allows parallel simulations from notebooks up to cluster scale, cf. [1, 2, 3, 4, 5, 6].

References

[1] M. Bause, F. Radu, U. Köcher, *Space-time finite element approximation of the Biot poroelasticity system with iterative coupling*, Comput. Meth. Appl. Mech. Engrg. (2017), accepted, arXiv:1611.06335v1, 1–28.

[2] M. Bause, U. Köcher, *Iterative coupling of variational space-time methods for Biot's system of poroelasticity*, in B. Karasözen et. al. (eds.), Numer. Math. Adv. Appl. ENUMATH 2015, doi:10.1007/978-3-319-39929-4_15 (2016), Springer, Berlin, 143–151.

[3] M. Bause, U. Köcher, *Variational time discretization for mixed finite element approximations of nonstationary diffusion problems*, J. Comput. Appl. Math. **289** (2015), 208–224.

[4] U. Köcher, *Variational Space-Time Methods for the Elastic Wave Equation and the Diffusion Equation*, urn:nbn:de:gbv:705-opus-31129, Ph.D. thesis, Helmut-Schmidt-University Hamburg (2015), 1–188.

[5] U. Köcher, M. Bause, *Variational space-time discretisations for the wave equation*, J. Sci. Comput. **61(2)** (2014), 424–453.

[6] W. Bangerth, D. Davydov, T. Heister, L. Heltai, G. Kanschat, M. Kronbichler, M. Maier, B. Turcksin, and D. Wells *The deal.II Library, Version 8.4* doi:10.1515/jnma-2016-1045, J. Numer. Math. **24(3)** (2016), 135–141.

Aposteriori analysis of fully discretized wave equation via leap-frog type schemes

Omar Lakkis

(joint work with E.H. Georgoulis and C.G. Makridakis and J.M. Virtanen)

1. Set-up

Let Ω be an open domain in $\mathbb{R}^d$, $d = 1, 2, 3$, and $T > 0$, we are interested in the aposteriori error ananlysis of discretizations of the initial value problem of the wave equation for a space-time scalar function $u : \overline{\Omega} \times [0, T] \to \mathbb{R}$

$$\begin{aligned} \partial_{tt} u + \mathscr{A} u &= f \text{ on } \Omega \times (0, T] \\ u(0) = u_0 \text{ and } \partial_t u(0) &= v_0 \end{aligned} \tag{1}$$

($\phi(t) = \phi(t, \cdot)$ is the snapshot of a space-time function ϕ at time t) for a given space-time function $f : \Omega \times [0, T] \to \mathbb{R}$, and space functions $u_0, v_0 : \Omega \to \mathbb{R}$ and a *self-adjoint linear second-order elliptic operator* $\mathscr{A} : \mathscr{V} \to \mathscr{V}'$, where the domain of $\mathscr{A}$, $\mathscr{V}$, is a Hilbert subspace of a pivot space $\mathscr{H}$ forming the Gel'fand triple $\mathscr{V} \hookrightarrow \mathscr{H} \hookrightarrow \mathscr{V}'$, which is realized as a Sobolev space on the domain Ω, e.g., $\mathscr{V} := \mathrm{H}^1_0(\Omega)$, $\mathscr{H} = L^2(\Omega)$ and $\mathscr{V}' := \mathrm{H}^{-1}(\Omega)$. Analysis of the scalar linear wave equation IVP (1) in such a setting can be found in textbooks such as [Eva10] or [Bré11].

1.1. **The leap-frog scheme.** Consider a uniform time-grid

$$t_0 := 0 \text{ and } t_n := t_{n-1} + \tau \text{ where } \tau := {}^{T}/_{N}, \tag{2}$$

for some fixed $N \in \mathbb{N}$ and a family $\mathbb{V}_0, \dots, \mathbb{V}_N$, of finite dimensional subspaces, corresponding to the discrete time instants $t_0, \dots, t_N$. The *leap-frog scheme*

$$\begin{gathered} \partial^2 U^{n+1} + A_n U^n = f^n \\ U^0 = P^0_{\mathscr{H}} u_0 \text{ and } \partial U^0 = P^0_{\mathscr{H}} v_0 \end{gathered} \tag{3}$$

where $\partial_{\cdot}{}^{n+1}$ and $\partial^2{}_{\cdot}{}^{n+1}$ respectively denote the *first* and *second backward difference* operators with respect to the time-grid $(t_n)_{n=0,\dots,N}$, namely

$$\partial U^{n+1} = \frac{U^{n+1} - U^n}{\tau} \text{ and } \partial^2 U^{n+1} = \frac{\partial U^{n+1} - \partial U^n}{\tau}. \tag{4}$$

Also $P^n_{\mathscr{H}}\phi$ is the $\mathscr{H}$-orthogonal projection onto $\mathbb{V}_n$ for $n = 0, \dots, N$.

The IVP (1) and scheme (3) may be reformulated by introducing an auxilliary variable $v := \partial_t u$ in the continuous case and

$$V^{n+1/2} := \partial U^{n+1} \text{ and } t_{n+\frac{1}{2}} = (t_{n+1} + t_n)/2 \text{ for } n = 0, \dots, N-1 \tag{5}$$

in the discrete case where the half-index indicates a time-grid *staggered* with respect to $(t_n)_{n=0,\dots,N}$, we also define

$$V^{-1/2} := 2P^0_{\mathscr{H}} v_0 - V^{+1/2} \text{ and } \partial V^{n+\frac{1}{2}} := \frac{V^{n+1/2} - V^{n-1/2}}{k}, \tag{6}$$

which allows us to rewrite (3) as a system of two first order difference equations

$$\partial U^{n+1} - V^{n+1/2} = 0, \text{ and } \partial V^{n+\frac{1}{2}} - A_n U^n = f^n. \tag{7}$$

This method was known to Newton, and has been rediscovered many times, e.g., by Delambre, Cowell & Crommelin, Størmer, Newmark and Verlet [HLW03].

1.2. **Cosine schemes.** The analysis we present here is valid also for more general leap-frog type schemes, known by some authors as the *cosine* schemes. Details being provided in [GLMV16], we stick to the leap-frog scheme in this abstract for simplicity's sake.

1.3. **Time-discrete schemes.** For exposition's sake, we drop the spatial discretization in this report and replace all occurences of A_n by $\mathscr{A}$ and all the projectors $P^n_{\mathscr{H}}$ by the identity.

2. Aposteriori error analysis

2.1. **Continuous extension of the leap-frog scheme.** Given our main goal is aposteriori error analysis, our first step is to rewrite the leap-frog system (7) as an $\mathscr{V}'$-valued system of *ordinary differential equations* (ODEs). For this we need to extend the discrete functions U^n and $V^{n-1/2}$, for $n = 0, \dots, N$ to the whole interval $[-k, T]$. Let $\hat{u}_1 : [-k, N] \to \mathbb{R}$ be the *piecewise linear extension* of time-grid nodal points (t_n, U^n), for $n = -1, \dots, N$, and $\hat{v}_1 : [-{}^{k}/_{2}, N - {}^{k}/_{2}] \to \mathbb{R}$ the

piecewise linear extension of staggered time-grid nodal points $(t_{n-1/2}, V^{n-1/2})$ for $n = 0, \ldots, N$. Using the convention that

$$\phi^i = \phi(t_i) \text{ for } i \text{ integer or half-integer}, \tag{8}$$

we obtain

$$\hat{u}_1^{n+1/2} = (U^{n+1} + U^n)/2 \text{ and } \hat{v}_1^n = (V^{n+1/2} + V^{n-1/2})/2 \text{ for } n = 0, \ldots, N-1, \tag{9}$$

and thus we rewrite scheme (7) as

$$\begin{aligned} \partial U^{n+1} - (\hat{v}_1^{n+1} + \hat{v}_1^n)/2 &= -(V^{n+3/2} - 2V^{n+1/2} + V^{n-1/2})/4 =: {R_V}^{n+1/2}, \\ \partial V^{n+\frac{1}{2}} + \mathscr{A}(U^{n+1/2} + U^{n-1/2})/2 &= f^n + (U^{n+1} - 2U^n + U^{n-1})/4 =: {R_U}^n, \end{aligned} \tag{10}$$

where the newly introduced *aposteriori residuals* satisfy ${R_U}^n = \mathrm{O}(k^2) = {R_V}^{n+1/2}$, which makes (10) a second-order perturbation of (7). We compress notation further by introducing *second-level piecewise linear extension* $\hat{u}_2 : \left[t_{-1/2}, t_{N-1/2}\right] \to \mathbb{R}$ of staggered time-grid nodal points $(t_{n-1/2}, \hat{u}_1^{n-1/2})$, $n = 0, \ldots, N$, and $\hat{v}_2 : [0, t_{N-1}] \to \mathbb{R}$ piecewise-linear interpolation of time-grid nodal points $(t_n, \hat{v}_1^n)$, $n = 0, \ldots, N-1$. This finally allows us to write the following system of Hilbert-space-valued ODEs

$$\partial_t \hat{u}_1 - I\hat{v}_2 = R_V \text{ and } \partial_t \hat{v}_1 + \mathscr{A} I_{1/2} \hat{u}_2 = I_{1/2} f + R_U, \tag{11}$$

where I and $I_{1/2}$ are the piecewise constant mid-point interpolators, respectively, on the time-grid and the staggered time-grid.

2.2. **Time reconstructions.**

$$\begin{aligned} \tilde{v}(t) &:= V^{n-1/2} + \int_{t_{n-1/2}}^{t} [-\mathscr{A}\hat{u}_2 + I_1 f + R_U] \quad \text{for } t_{n-1/2} \le t \le t_{n+1/2}, \\ \tilde{u}(t) &:= U^{n-1} + \int_{t_{n-1}}^{t} [\hat{v}_2 + R_V] \qquad\qquad\quad \text{for } t_{n-1} \le t \le t_n, \end{aligned} \tag{12}$$

where I_1 is the piecewise linear interpolator with nodes on the staggered time-grid. The functions $\tilde{u}$ and $\tilde{v}$ are thus piecewise quadratic that coincide with U and V, respectively, on the time-grid and the staggered time-grid. Therefore the error $\tilde{u} - U$ and $\tilde{v} - V$ is just interpolation error, which is fully computable from U and V, of third order in k because of the quadratic. To estimate the remaining errors $\tilde{e}_u := \tilde{u} - u$ and $\tilde{e}_v := \tilde{v} - v$ we subtract memberwise system (10) from (7) as to obtain the *error-residual partial differential relation system*

$$\begin{aligned} \partial_t \tilde{e}_u - \tilde{e}_v = \tilde{v} - \hat{v}_2 - R_V &=: \mathscr{R}_2, \text{ and} \\ \partial_t \tilde{e}_v + \mathscr{A}\tilde{e}_u = F' - \mathscr{A}[\tilde{u} - \hat{u}_2] - R_U + F'f - I_1 f &=: \mathscr{R}_1 + \mathscr{R}_f, \end{aligned} \tag{13}$$

where the residuals defined on the right-hand side are piecewise quadratic combinations of computed quantities and therefore computable.

2.3. **Energy estimates.** Introducing the following *energy inner product*

$$\langle(\phi_0,\phi_1),(\psi_0,\psi_1)\rangle_e := \langle\phi_0,\mathscr{A}\psi_0\rangle + \langle\phi_1,\psi_1\rangle\,, \tag{14}$$

and the corresponding norm $\|(\phi_0,\phi_1)\|_e$, enables us to obtain an energy estimate for the error–residual relation (13) in the form

$$\frac{1}{2}\frac{\mathrm{d}}{\mathrm{d}\,t}\,\|(\tilde{e}_u,\tilde{e}_v)\|_e^2 \le \|(\mathscr{R},\mathscr{R}_1+\mathscr{R}_f)\|_e\,\|(\tilde{e}_u,\tilde{e}_v)\|_e\,. \tag{15}$$

Manipulations lead to the main result.

2.4. **Main result.** *Let u be the solution of (1), with the notation introduced hitherto the following aposteriori error result holds*

$$\sup_{[0,T]}\|(\tilde{e}_u,\tilde{e}_v)\|_e^2 \le 2\,\|(\tilde{e}_u(0),\tilde{e}_v(0))\|_e^2 + 4\Big(\int_0^T \|(\mathscr{R}_2,\mathscr{R}_1+\mathscr{R}_f)\|_e\Big)^2. \tag{16}$$

References

[Bré11] Ham Brézis, *Functional analysis, Sobolev spaces and partial differential equations*, Universitext, Springer, New York, 2011. MR 2759829 (2012a:35002)

[Eva10] Lawrence C. Evans, *Partial differential equations*, second ed., Graduate Studies in Mathematics, vol. 19, American Mathematical Society, Providence, RI, 2010. MR 2597943

[GLMV16] E. Georgoulis, O. Lakkis, C. Makridakis, and J. Virtanen, *A Posteriori Error Estimates for Leap-Frog and Cosine Methods for Second Order Evolution Problems*, SIAM Journal on Numerical Analysis **54** (2016), no. 1, 120–136.

[HLW03] Ernst Hairer, Christian Lubich, and Gerhard Wanner, *Geometric numerical integration illustrated by the Strmer-Verlet method*, Acta Numerica **12** (2003), 399–450.

Space-Time Isogeometric Analysis of Parabolic Diffusion Problems

Ulrich Langer

(joint work with S. Moore, M. Neumüller, I. Toulopoulos)

We present and analyze new stable single and multi-patch space-time Isogeometric Analysis (IgA) schemes of the form,

$$\text{find } u_h \in V_{0h} : a_h(u_h,v_h) = \ell_h(v_h) \quad \forall v_h \in V_{0h}, \tag{1}$$

for solving linear parabolic initial-boundary value problems like

$$\partial_t u - \Delta u = f \quad \text{in} \quad Q = \Omega\times(0,T) \tag{2}$$

with Dirichlet boundary conditions $u = u_D := 0$ on $\Sigma = \partial\Omega\times(0,T)$ and initial conditions $u = u_0 := 0$ on $\overline{\Sigma}_0 = \overline{\Omega}\times\{0\}$, and the spatial domain $\Omega\subset\mathbb{R}^d$.

The single-patch scheme was proposed and investigated in [3]. It was assumed that the space-time cylinder $Q = \mathbf{\Phi}(\widehat{Q})$ is the image of one single parameter domain $\widehat{Q} = (0,1)^{d+1}$ via some IgA map $\mathbf{\Phi}$, which has the form $\mathbf{\Phi}(\xi) = \sum_{i\in\overline{\mathscr{I}}}\mathbf{P}_i\widehat{\varphi}_i(\xi)$ with the control points $\{\mathbf{P}_i\}_{i\in\overline{\mathscr{I}}}$ and the B-spline or NURBS basis functions $\{\widehat{\varphi}_i\}_{i\in\overline{\mathscr{I}}}$. This approach allowed us to include moving spatial domains $\Omega(t)$ yielding a fixed

computational domain $Q = \{(x,t) \in \mathbb{R}^{d+1} : x \in \Omega(t),\, t \in (0,T)\} = \mathbf{\Phi}(\widehat{Q})$ in the space-time continuum $\mathbb{R}^{d+1}$ by means of a suitable IgA map $\mathbf{\Phi}$.

In this paper, we assume that the space-time cylinder Q has a multi-patch representation of the form $\overline{Q} = \cup_{n=1}^{N} \overline{Q}_n$ that consists of N subcylinders (patches or time slices) $Q_n = \Omega \times (t_{n-1}, t_n)$, $n = 1, \ldots, N$, where $0 = t_0 < t_1 < \ldots < t_N = T$ is some subdivision of the time interval $[0,T]$. The time faces between the time patches are denoted by $\overline{\Sigma}_n = \overline{Q}_{n+1} \cap \overline{Q}_n = \overline{\Omega} \times \{t_n\}$. We obviously have $\Sigma_N = \Sigma_T = \overline{\Omega} \times \{T\}$. Every time patch $Q_n = \mathbf{\Phi}_n(\widehat{Q})$ in the physical domain Q can be represented as the image of the parameter domain $\widehat{Q}$ by a sufficiently regular IgA map $\mathbf{\Phi}_n : \widehat{Q} \to Q_n$ that is defined in the same way as in the single-patch case. Now, we can construct the finite-dimensional IgA (B-Spline, NURBS etc.) space $V_{0h} = \{v_h : v_n = v_h|_{Q_n} \in V_{0n}, n = 1, \ldots, N\}$, the functions of which are smooth in each time patch Q_n in correspondence to the smoothness of the splines, but in general discontinuous across the time faces Σ_n, $n = 1, \ldots, N-1$. The smooth IgA spaces $V_{0n} = V_{0h_n} = \operatorname{span}\{\varphi_{n,i}\}_{i \in \mathscr{I}_n}$ are spanned by the IgA basis functions $\{\varphi_{n,i}\}_{i \in \mathscr{I}_n}$ that are nothing but the images of the basis functions $\{\widehat{\varphi}_{n,i}\}_{i \in \mathscr{I}_n}$, which were already used for defining the patch Q_n by the map $\mathbf{\Phi}_n$, i.e., $\varphi_{n,i} = \widehat{\varphi}_{n,i} \circ \mathbf{\Phi}_n^{-1}$. The basis functions $\varphi_{1,i}$ should vanish on Σ_0 for all $i \in \mathscr{I}_1$. Therefore, all functions v_h from V_{0h} fulfil homogeneous boundary and initial conditions. The discretization parameter h_n denotes the average mesh-size of the mesh induced by the corresponding mesh in the parameter domain $\widehat{Q}$ via the map $\mathbf{\Phi}_n$. The IgA technology of using the same basis functions for describing the patches of the compuational domain (geometry) and for defining the approximation spaces V_{0h} was introduced by Hughes, Cottrell and Bazilevs in 2005. In order to derive a consistent dG IgA scheme for defining an IgA solution $u_h \in V_{0h}$ of (2), we multiply the parabolic PDE (2) by a time-upwind test function of the form $v_n + \theta_n h_n \partial_t v_n$ with an arbitrary $v_n \in V_{0n}$ and a positive, sufficently small constant θ_n, and integrate over the space-time subcylinder Q_n. Integrating by parts with respect to (wrt) x, adding a consistent time-upwind term for stabilization, and summing over all time patches, we finally arrive at the multi-patch space-time IgA scheme (1) with the IgA bilinear form

$$a_h(u_h, v_h) = \sum_{n=1}^{N} a_n(u_h, v_h) = \sum_{n=1}^{N} \Bigg(\int_{Q_n} (\partial_t u_n (v_n + \theta_n h_n \partial_t v_n) + \nabla_x u_n \cdot \nabla_x v_n + \theta_n h_n \nabla_x u_n \cdot \nabla_x \partial_t v_n)\, dxdt + \int_{\Sigma_{n-1}} [|u_h|]\, v_n\, dx \Bigg)$$

and the linear form

$$l_h(v_h) = \sum_{n=1}^{N} l_n(v_h) = \sum_{n=1}^{N} \int_{Q_n} f(v_n + \theta_n h_n \partial_t v_n)\, dxdt.$$

where $[|u_h|] = u_n - u_{n-1}$ on Σ_{n-1} denotes the jump of u_h across Σ_{n-1}. Here we formally set $[|u_1|]$ on Σ_0 to zero since we assumed homogeneous initial conditions.

It is clear that this jump term can be used to include inhomogeneous initial conditions in a weak sense. The single-patch scheme, studied in [3], is obviously a special case of the multi-patch scheme setting N to 1.

It can be shown that the discrete bilinear form is elliptic on the IgA space V_{0h} wrt the mesh-dependent energy norm $\|v\|_h$ defined by the relation

$$\|v\|_h^2 = \sum_{n=1}^{N} \Big(\frac{1}{2} \|\nabla_x v\|_{L_2(Q_n)}^2 + \theta_n \, h_n \, \|\partial_t v\|_{L_2(Q_n)}^2 + \frac{1}{2} \| \, [|v|] \, \|_{L_2(\Sigma_{n-1})}^2 \Big) + \frac{1}{2} \|v\|_{L_2(\Sigma_N)}^2.$$

This property together with a corresponding boundedness property, consistency and approximation results for the IgA spaces yields the a priori discretization error estimates

$$\|u - u_h\|_h \leq (1 + \frac{\mu_b}{\mu_e}) \sum_{n=1}^{N} c_n h_n^{r_n - 1} \|u\|_{H^{r_n}(Q_n)} \tag{3}$$

provided that the θ_n are appropriately chosen, where μ_e is the V_{0h}-ellipticity constant that is here equal to 1, μ_b is the V_{0h}-boundedness constant, c_n denote generic constants, $r_n = \min\{s_n, p_n + 1\}$, p_n denotes the underlying polynomial degree of the B-splines or NURBS used in patch Q_n, and s_n is defined by the regularity of the solution u in the patch Q_n, with $n = 1, \ldots, N$. More precisely, we assume that $u|_{Q_n} \in H^{s_n}(Q_n)$. The proof of the discretization error estimate (3) can be found in [3] and [4] for the single- and multi-patch cases, respectively.

In practical computations, we have to generate and to solve one huge system of linear algebraic equations $\mathbf{L}_h \mathbf{u}_h = \mathbf{f}_h$ for determining all space-time degrees of freedoms all at once. Fast generation techniques, fast solvers, adaptivity, and parallelization are the tools for making the space-time IgA technology really efficient, in particular, if massively parallel computers with thousends of cores are available. If the IgA map $\mathbf{\Phi}_n : \widehat{Q} \to Q_n$ preserves the tensor product structure of the IgA basis functions $\varphi_{n,i} = \widehat{\varphi}_{n,i} \circ \mathbf{\Phi}_n^{-1}$, then the system matrix $\mathbf{L}_h$ can be generated very efficiently, and one can construct fast time and space parallel multigrid preconditioned GMRES solvers, cf. also [1], like the numerical results presented in Table 2 show. We solved the IBVP (2) in the unit hypercube $Q = (0,1)^{3+1}$ with a manufactured right-hand side f such that $u(x,t) = sin(\pi x_1) sin(\pi x_2) sin(\pi x_3) sin(\pi t)$ is the exact solution of (2). We here only used the lowest order splines of the degree $p = 1$ for discretization in space and time. The detailed description of the tensor product representation of the matrix and the solver as well as a more extensive discussion of the numerical results can be found in [4]. In more general cases of diffusion coefficients depending on x and t or moving spatial domains, low rank tensor methods proposed in [5] can be used to accelerate the generation and the solution of $\mathbf{L}_h \mathbf{u}_h = \mathbf{f}_h$. Functional a posteriori error estimates in connections with efficient methods for the global minimization of the majorant on significantly coarser, but higher-order IgA spaces of highest smoothness, and the use of THB splines lead to very efficient adaptive IgA procedures, see [2].

This research work has been supported by the Austrian Science Fund (FWF) under the grant NFN S117-03.

N	dofs/slice	dofs	L_2 error	eoc	iter	cx	ct	cores	time [s]
1	1125	1125	1.8815E-02	-	1	8	1	8	0.00
2	6561	13122	4.8619E-03	1.95	10	8	1	8	0.06
4	44217	176868	1.2294E-03	1.98	12	8	4	32	0.30
8	323433	2587464	3.0834E-04	2.00	14	8	8	64	3.40
16	2471625	39546000	7.7092E-05	2.00	15	8	16	128	47.38
32	19320201	618246432	1.9262E-05	2.00	16	32	32	1024	159.20

TABLE 2. Numerical results for $p_n = 1$: N - number of time slices (patches); dofs/slice $= (2^l + 1) \times (2^l + 1) \times (2^l + 1) \times 9$, $l = 2, 3, 4, 5, 6, 7$; dofs = total number of unknows $= N \times$ dofs/slice; eoc = experimental convergence rate wrt the $L_2(Q)$ norm; iter = number of iterations; cx / ct = number of cores for the parallelization in space / time; cores = total number of cores

REFERENCES

[1] M. Gander and M. Neumüller, *Analysis of a new space-time parallel multigrid algorithm for parabolic problems*, SIAM J. Sci. Comput., **38** (2016), A2173–A2208.

[2] U. Langer, S. Matculevich and S. Repin, *Functional type error control for stabilized space-time IgA approximations to parabolic problems*, Accepted for publication in the LSSC 2017 proceedings.

[3] U. Langer, S. Moore and M. Neumüller, *Space-time isogeometric analysis of parabolic evolution equations*, Comput. Methods Appl. Mech. Engrg., **306** (2016), 342–363.

[4] U. Langer, M. Neumüller and I. Toulopoulos, *Multipatch Space-Time Isogeometric Analysis of Parabolic Diffusion Problems*, 2017, in preparation.

[5] A. Mantzaflaris, B. Jüttler, B. Khoromskij and U. Langer, *Low rank tensor methods in Galerkin-based isogeometric analysis*, Comput. Methods Appl. Mech. Engrg., **316** (2017), 1062–1085.

Compressive space-time Galerkin discretizations of parabolic partial differential equations

STIG LARSSON

(joint work with Christoph Schwab)

We consider the parabolic initial-boundary value problem

$$\dot{u} + Au = f \quad \text{in} \quad \mathbb{R}_+ = (0, \infty) ,$$
$$u(0) = 0 .$$

The linear operator A, with corresponding bilinear form $a(\cdot, \cdot)$, is assumed to have the usual boundedness and coercivity properties with respect to a Gelfand triple $V \subset H \simeq H^* \subset V^*$.

A natural variational formulation of this problem, now on a finite time interval $(0,T)$, is: Find $u \in X := L^2((0,T);V) \cap H^1((0,T);V^*)$ such that

$$\int_0^T \Big({}_{V^*}\langle \dot{u}(t), y(t)\rangle_V + a(u(t),y(t)) \Big)\,\mathrm{d}t = \int_0^T {}_{V^*}\langle f(t), y(t)\rangle_V\,\mathrm{d}t.$$

for all $y \in Y := L^2((0,T);V)$. It is also possible to integrate by parts in time to get another variational formulation, where the roles of the trial and test spaces are interchanged. In either case, the Banach–Nečas–Babuska inf-sup theorem is applicable to obtain well-posedness with respect to the corresponding spaces. This was used in [7, 2] together with the adaptive wavelet methodology by Dahmen, Cohen, and Devore to obtain adaptive algorithms with optimal complexity. We remark that, in either formulation, this approach requires the normalization of Riesz bases in the dual space V^*, which is difficult.

In the present work we use a variational formulation based on time derivatives of order one half. This was developed by M. Fontes in [3, 4, 5], although it had been used earlier in [1]. We now use the spaces

$$X = H^{\frac12}_{00,\{0\}}(\mathbb{R}_+;H) \cap L^2(\mathbb{R}_+;V) \simeq \big(H^{\frac12}_{00,\{0\}}(\mathbb{R}_+)\otimes H\big) \cap \big(L^2(\mathbb{R}_+)\otimes V\big)\,,$$
$$Y = H^{\frac12}(\mathbb{R}_+;H) \cap L^2(\mathbb{R}_+;V) \simeq \big(H^{\frac12}(\mathbb{R}_+)\otimes H\big) \cap \big(L^2(\mathbb{R}_+)\otimes V\big)\,.$$

We also use the Riemann–Liouville fractional order derivatives $\mathrm{D}_+^{\frac12}$ and $\mathrm{D}_-^{\frac12}$. The variational problem is to find $u \in X$ such that

$$\int_{\mathbb{R}_+} \Big((\mathrm{D}_+^{\frac12}u, \mathrm{D}_-^{\frac12}v)_H + a(u,v) \Big)\,\mathrm{d}t = \int_{\mathbb{R}_+} {}_{V^*}\langle f, v\rangle_V\,\mathrm{d}t$$

for all $v \in Y$.

This problem satisfies the Banach–Nečas–Babuska inf-sup theorem. One advantage over the other formulations mentioned above is that the trial and test spaces are almost the same and, in particular, that the dual space V^* is not used. Hence, the adaptive wavelet approach is easier to apply. Another advantage is that the method of proof suggests a way to construct stable trial and test spaces based on tensorized wavlets or piecewise polynomials to be used in a non-adaptive Galerkin approximation. This is reported in [6].

References

[1] C. Baiocchi and F. Brezzi, *Optimal error estimates for linear parabolic problems under minimal regularity assumptions*, Calcolo, 20 (1983), pp. 143–176 (1984).

[2] N. Chegini and R. Stevenson, *Adaptive wavelet schemes for parabolic problems: sparse matrices and numerical results*, SIAM J. Numer. Anal., 49 (2011), pp. 182–212.

[3] M. Fontes, *Parabolic Equations with Low Regularity*, Doctoral Dissertation, Department of Mathematics, University of Lund, Sweden, 1996.

[4] ———, *A monotone operator method for elliptic-parabolic equations*, Comm. Partial Differential Equations, 25 (2000), pp. 681–702.

[5] ———, *Initial-boundary value problems for parabolic equations*, Ann. Acad. Sci. Fenn. Math., 34 (2009), pp. 583–605.

[6] S. Larsson and Ch. Schwab, *Compressive space-time Galerkin discretizations of parabolic partial differential equations*, http://arxiv.org/abs/1501.04514arXiv:1501.04514 [math.NA].

[7] Ch. Schwab and R. Stevenson, *Space-time adaptive wavelet methods for parabolic evolution problems*, Math. Comp., 78 (2009), pp. 1293–1318.

Discrete maximal parabolic regularity for Galerkin finite element methods and the fully discrete best approximation results

Dmitriy Leykekhman

(joint work with Boris Vexler)

Let Ω be a Lipschitz domain in $\mathbb{R}^d$, $d = 2, 3$ and $I = (0, T)$. As a model of a parabolic second order partial differential equation we consider the heat equation,

$$\begin{aligned} \partial_t u(t,x) - \Delta u(t,x) &= f(t,x), \quad (t,x) \in I \times \Omega, \\ u(t,x) &= 0, \qquad (t,x) \in I \times \partial\Omega, \\ u(0,x) &= u_0(x), \qquad x \in \Omega, \end{aligned} \tag{1}$$

with a right-hand side $f \in L^s(I; L^p(\Omega))$ for some $1 \le p, s \le \infty$ and $u_0 \in L^p(\Omega)$, $1 \le p \le \infty$.

The maximal parabolic regularity for $u_0 \equiv 0$ says that for $f \in L^s(I; L^p(\Omega))$ there exists a constant C such that,

$$\|\partial_t u\|_{L^s(I;L^p(\Omega))} + \|\Delta u\|_{L^s(I;L^p(\Omega))} \le C \|f\|_{L^s(I;L^p(\Omega))}, \quad 1 < p, s < \infty.$$

The maximal parabolic regularity is an important analytical tool and has a number of applications, especially to nonlinear problems and in general to problems when sharp regularity results are required.

We investigate maximal parabolic regularity for a family of time discontinuous Galerkin (dG) methods. To introduce the time discontinuous Galerkin discretization for the problem, we partition $I = (0, T)$ into subintervals $I_m = (t_{m-1}, t_m]$ of length $k_m = t_m - t_{m-1}$, where $0 = t_0 < t_1 < \cdots < t_{M-1} < t_M = T$. The maximal and minimal time steps are denoted by $k = \max_m k_m$ and $k_{\min} = \min_m k_m$, respectively. We impose the following conditions on the time mesh:

(1) There are constants $c, \beta > 0$ independent on k such that
$$k_{\min} \ge c k^{\beta}.$$

(2) There is a constant $\kappa > 0$ independent on k such that for all $m = 1, 2, \ldots, M-1$
$$\kappa^{-1} \le \frac{k_m}{k_{m+1}} \le \kappa.$$

(3) It holds $k \le \frac{1}{4} T$.

The semidiscrete space X_k^q of piecewise polynomial functions in time is defined by

$$X_k^q = \{u_k \in L^2(I; H_0^1(\Omega)) : \ u_k|_{I_m} \in \mathscr{P}_q(H_0^1(\Omega)), \ m = 1, 2, \ldots, M\},$$

where $\mathscr{P}_q(V)$ is the space of polynomial functions of degree q in time with values in a Banach space V. We will employ the following notation for functions in X_k^q

$$u_m^+ = \lim_{\varepsilon\to 0^+} u(t_m+\varepsilon), \quad u_m^- = \lim_{\varepsilon\to 0^+} u(t_m-\varepsilon), \quad [u]_m = u_m^+ - u_m^-. \tag{2}$$

Next we define the following bilinear form

(3)

$$B(u,\varphi) = \sum_{m=1}^{M} \langle \partial_t u, \varphi\rangle_{I_m\times\Omega} + (\nabla u, \nabla\varphi)_{I\times\Omega} + \sum_{m=2}^{M} ([u]_{m-1}, \varphi_{m-1}^+)_\Omega + (u_0^+, \varphi_0^+)_\Omega,$$

where $(\cdot,\cdot)_\Omega$ and $(\cdot,\cdot)_{I_m\times\Omega}$ are the usual L^2 space and space-time inner-products, $\langle\cdot,\cdot\rangle_{I_m\times\Omega}$ is the duality product between $L^2(I_m;H^{-1}(\Omega))$ and $L^2(I_m;H_0^1(\Omega))$. We note, that the first sum vanishes for $u\in X_k^0$. The dG(q) semidiscrete (in time) approximation $u_k\in X_k^q$ of (1) is defined as

$$B(u_k,\varphi_k) = (f,\varphi_k)_{I\times\Omega} + (u_0,\varphi_{k,0}^+)_\Omega \quad \text{for all } \varphi_k\in X_k^q. \tag{4}$$

There is a number of important properties making the dG schemes attractive for temporal discretization of parabolic equations. For example, such schemes allow for a priori error estimates of optimal order with respect to the regularity requirements for the solution, different systematic approaches for a posteriori error estimation and adaptivity developed for finite element discretizations can be adapted for dG temporal discretization of parabolic equations, an efficient and easy to implement approach that avoids complex coefficients, which arise in the equations obtained by a direct decoupling for high order dG schemes were developed recently, for the treatment of optimal control problems, Galerkin methods are particularly suitable since they have an important property that the two approaches optimize-then-discretize and discretize-then-optimize approaches lead to the same discretization scheme.

In [1], we established the corresponding discrete maximal parabolic regularity, i.e., when $u_0=0$,

$$\|\Delta u_k\|_{L^s(I;L^p(\Omega))} + \left(\sum_{m=1}^{M} k_m \left\| \frac{[u_k]_{m-1}}{k_m}\right\|_{L^p(\Omega)}^s\right)^{\frac{1}{s}} \le C\ln\frac{T}{k}\|f\|_{L^s(I;L^p(\Omega))}, \tag{5}$$

for $1\le s\le\infty$ and $1\le p\le\infty$, with obvious notation changes in the case of $s=\infty$. In the case of the lowest order piecewise constant method, i.e., $q=0$, the first terms on the left-hand sides of the above estimates vanish. We would like to point out that in the discrete setting the critical values of s and p, i.e. $s=1,\infty$ and $p=1,\infty$ are allowed, which explains the logarithm. The fully discrete analog of (5) also holds.

Similarly to the continuous case, the above discrete maximal parabolic regularity result has a number of applications. Thus, for the fully discrete approximation of the equation (1) assuming that the domain Ω is a polygonal/polyhedral convex domain we can establish best approximation property of the fully discrete solution in $L^\infty(\Omega\times I)$ norm.

Let $h \in (0, h_0]$; $h_0 > 0$, and $\mathscr{T}$ denote a quasi-uniform triangulation of Ω with mesh size h, i.e., $\mathscr{T} = \{\tau\}$ is a partition of Ω into cells (triangles or tetrahedrons) τ of diameter h_τ such that for $h = \max_\tau h_\tau$,

$$\operatorname{diam}(\tau) \le h \le C|\tau|^{\frac{1}{d}}, \quad \forall \tau \in \mathscr{T}, \quad d = 2, 3,$$

hold. Let V_h be the set of all functions in $H_0^1(\Omega)$ that are polynomials of degree r on each τ, i.e., V_h is the usual space of conforming finite elements. To obtain the fully discrete approximation we consider the space-time finite element space

$$X_{k,h}^{q,r} = \{v_{kh} : \ v_{kh}|_{I_m} \in \mathscr{P}_q(V_h), \ m = 1, 2, \ldots, M, \quad q \ge 0, \quad r \ge 1\}. \tag{6}$$

We define a fully discrete analog $u_{kh} \in X_{k,h}^{q,r}$ of u_k introduced in (4) by

$$B(u_{kh}, \varphi_{kh}) = (f, \varphi_{kh})_{I\times\Omega} + (u_0, \varphi_{kh}^+)_\Omega \quad \text{for all} \ \ \varphi_{kh} \in X_{k,h}^{q,r}. \tag{7}$$

The fully discrete maximal parabolic regularity results can be used to show best approximation property of $cG(\mathrm{r})dG(\mathrm{q})$ Galerkin solution in $L^\infty(I \times \Omega)$ norm [2].

Theorem (Global best approximation)
Let u and u_{kh} satisfy (1) and (7) respectively. Then, there exists a constant C independent of k and h such that

$$\|u - u_{kh}\|_{L^\infty(I\times\Omega)} \le C \ln \frac{T}{k} |\ln h| \inf_{\chi \in X_{k,h}^{q,r}} \|u - \chi\|_{L^\infty(I\times\Omega)}.$$

For the error at the point x_0 we can obtain a sharper result, that shows more localized behavior of the error at a fixed point. For elliptic problems similar results were obtained in the work of Schatz and Wahlbin. Let $B_d = B_d(x_0)$ be the ball of radius d centered at x_0.

Theorem (Interior best approximation)
Let u and u_{kh} satisfy (1) and (7), respectively and let $d > 4h$. Let $\tilde{t} \in I_m$ with some $m \in \{1, 2, \ldots, M\}$ and $\overline{B}_d \subset\subset \Omega$, then there exists a constant C independent of h, k, and d such that

$$|(u - u_{kh})(\tilde{t}, x_0)| \le C \ln \frac{T}{k} |\ln h| \inf_{\chi \in X_{k,h}^{q,r}} \Bigg\{ \|u - \chi\|_{L^\infty((0,t_m)\times B_d(x_0))}$$

$$+ d^{-\frac{N}{2}} \Big(\|u - \chi\|_{L^\infty((0,t_m);L^2(\Omega))} + h\|\nabla(u - \chi)\|_{L^\infty((0,t_m);L^2(\Omega))} \Big) \Bigg\}.$$

We would like to point out that the above results do not require any relationship between the space mesh size h and time steps k. This is important for example for problems on graded meshes.

Such error estimates in the form of the best approximation results for three dimensional problems are new are can be used for problems where regularity of the problem is low, for example for state contstained optimal control problems.

References

[1] D. Leykekhman and B. Vexler, *Discrete maximal parabolic regularity for Galerkin finite element methods*, Numer. Math. **135** (2017), 923–952.

[2] D. Leykekhman and B. Vexler, *Pointwise best approximation results for Galerkin finite element solutions of parabolic problems*, SIAM J. Numer. Anal. **54** (2016), 1365–1384.

Time or space adaptivity for exterior wave problems with gCQ

María López-Fernández

The application of Lubich's Convolution Quadrature (CQ) for the time discretization of exterior wave problems formulated as boundary integral equations is nowadays well understood [1, 2, 3]. The CQ method is however restricted by construction to use uniform time steps. More recently this limitation of the CQ method has been overcome and the so-called generalized Convolution Quadrature (gCQ) method has been developed [5, 6, 8], which allows to use a non uniform sequence of time steps. The gCQ method actually decouples time and space integration, allowing in principle to change the spatial grid from one time step to the next one [9] and also to use a quite general sequence of time points.

Once the use of nonuniform time grids is possible, the next step is the development of an adaptive scheme and thus of some mechanism to control the error. We address two possible strategies which are based on the *a priori* error estimates proven in [5] and [8]. We have tested the performance of the new methods with a scalar model problem arising from the resolution of the wave problem outside a sphere.

The class of problems under consideration can be very generally described as follows: Let B and D denote some normed vector spaces and let $\mathscr{L}(B,D)$ be the space of continuous, linear mappings. As a norm in $\mathscr{L}(B,D)$ we take the usual operator norm

$$\|\mathscr{F}\|_{D\leftarrow B} := \sup_{u\in B\setminus\{0\}} \frac{\|\mathscr{F}u\|_D}{\|u\|_B}.$$

For given $\phi : \mathbb{R}_{\geq 0} \to B$, we consider the evaluation of the time convolution

$$c(t) = \int_0^t k(t-\tau)\,\phi(\tau)\,d\tau \qquad \text{in } D \quad \text{for all } t\in[0,T], \tag{1}$$

where the kernel operator

$$k : [0,\infty) \to \mathscr{L}(B,D),$$

is defined as the inverse Laplace transform of a given *transfer operator* K. For $\sigma\in\mathbb{R}$ we introduce

$$\mathbb{C}_\sigma = \{z\in\mathbb{C} \mid \operatorname{Re} z > \sigma\}$$

and assume that $K : \mathbb{C}_{\sigma_K} \to \mathscr{L}(B,D)$, for some $\sigma_K\in\mathbb{R}$, and that K is analytic in $\mathbb{C}_{\sigma_K}$. We also assume that there exists $\mu\in\mathbb{R}$ such that, for any $\sigma > \sigma_K$, there is a constant $C(\sigma)$ satisfying

$$\|K(z)\|_{D\leftarrow B} \leq C(\sigma)\,(1+|z|)^\mu, \qquad \forall z\in\mathbb{C}_\sigma. \tag{2}$$

For $j \in \mathbb{Z}$, we define

$$K_j(z) := z^{-j} K(z) \tag{3}$$

and

$$C_0^j([0,T],B) := \left\{ \psi \in C^j([0,T],B) \mid \forall\, 0 \le r \le j-1 : \quad \psi^{(r)}(0) = 0 \right\}.$$

Then (1) is well-defined for any $\phi \in C_0^\nu([0,T],B)$, with $\nu = \lceil \mu + 1 \rceil$. Furthermore, by using the inverse Laplace transformation, the original problem (1) can be rewritten as

$$c(t) = \frac{1}{2\pi\,\mathrm{i}} \int_{\sigma + \mathrm{i}\,\mathbb{R}} K_\nu(z) u_\nu(z,t)\, dz \tag{4}$$

with u_ν the solution of the IVP

$$\partial_t u_\nu(z,t) = z u_\nu(z,t) + \partial_t^\nu \phi(t)\,; \qquad u_\nu(z,0) = 0. \tag{5}$$

The gCQ method is derived from (4). More precisely, given a sequence of time points $0 < t_1 < \cdots < t_N = T$, and a A-stable method for the approximation of the IVP (5), the gCQ approximates (1) at t_n, $n = 1, \ldots, N$, by

$$c(t_n) \approx \overline{c}(t_n) := \frac{1}{2\pi\,\mathrm{i}} \int_{\sigma + \mathrm{i}\,\mathbb{R}} K_\nu(z) u_{\nu,n}(z) \tag{6}$$

where $u_{\nu,n}(z) \approx u_\nu(z,t)$ is computed by the solver of choice for (5). Possible methods for the underlying ODEs are the implicit Euler method and the Runge–Kutta methods of the RadauIIA and Lobatto IIIC types. The line-contour $\sigma + \mathrm{i}\,\mathbb{R}$ in (6) is then deformed into a circle Γ in the right-half of the complex plane, enclosing the poles of $u_{\nu,n}(z)$, and a special quadrature formula following [7] is applied. This finally leads to the approximation

$$c(t_n) \approx c_n = \sum_{\ell=1}^{N_Q} w_\ell K_\nu(z_\ell) u_{\nu,n}(z_\ell)\,, \tag{7}$$

for certain quadrature nodes z_ℓ and weights w_ℓ.

The error analysis in [5] and [8] shows that if q is the *stage order* of the underlying Runge–Kutta method and $\phi \in C_0^{q+1}([0,T],B)$ then (6) is actually well-defined for the smaller regularization parameter $\nu = \lceil \mu - q \rceil$. In particular, for $\nu = 0$ the following *a priori* estimate of the *global error* holds

$$\|c(t_n) - c_n\|_D \le C e^{\sigma T} \|\phi\|_{C^{p+1}([0,T],B)} \Delta t_{\max}^{\min\{p, q-\mu\}}, \tag{8}$$

where p denotes the *classical order* of the Runge–Kutta solver.

Two observations now follow:

1. All ODE methods considered so far to define the gCQ are collocation methods. Thus they naturally provide a continuous approximation to the convolution, namely

$$c(t) \approx \overline{c}(t) := \frac{1}{2\pi\,\mathrm{i}} \int_\Gamma K(z) p_n(z,t)\, dz, \quad t \in [t_{n-1}, t_n), \tag{9}$$

where $p_n(z,t)$ denotes the collocation polynomial associated to the ODE method for the interval $[t_{n-1}, t_n)$.

2. In the applications to wave problems it is typically $\mu > 0$ in (2) and thus the convergence of the Runge–Kutta based gCQ is determined by the stage order q rather than the classical order p of the Runge–Kutta method.

The first observation leads naturally to an estimate of the error based on the comparison between $\overline{c}(t_{n-1} + \theta(\Delta t)_n)$ and $\widetilde{c}(t_{n-1} + \theta(\Delta t)_n)$, for some $\theta \in (0,1)$, with $\widetilde{c}$ defined as in (9) but with p_n replaced by a lower/higher order interpolant of the numerical solution $u_{n,\nu}(z)$. For the gCQ based on the implicit Euler method this leads to compare the piecewise constant interpolant with the piecewise linear interpolant of the numerical values c_n at some intermediate point $t_{n-1} + \theta(\Delta t)_n$, for instance the middle point $t_{n-\frac{1}{2}}$ of the n-th time-interval. Numerical results for the gCQ of the first order implemented with this approach were found satisfactory. For higher order versions of the gCQ this approach has not been properly tested yet but preliminary numerical results were not promising. Further analysis and testing is required.

The second observation suggests to use two different gCQ approximations to advance the solution from c_{n-1} to c_n, based on two different Runge–Kutta methods of stage order q and $q-1$, respectively. As an example, we choose the pair based on the RadauIIA methods of classical order 3 and 5, for which it is $q = 3$. The difference between the two approximations at t_n can be used to estimate the *local error*, which is assumed to behave like $O(\Delta_n^{q+1-\mu})$, according to the estimate (8). This procedure is very similar to what is typically done to control the steps in the approximation of ODEs [4], but it is expensive due to the lack of embedded formulas. Good numerical results are obtained by following this approach up to relatively short times T. As T increases the step controller *forces* to integrate with a quasi uniform (minimal) step. Further understanding of this phenomenon, which might be related with the dissipation introduced by the underlying A-stable method, is required and remedies need to be devised, analyzed and tested.

References

[1] L. Banjai. *Multistep and multistage convolution quadrature for the wave equation: Algorithms and experiments*, SIAM J. Sci. Comput., **32** (2010), 2964–2994.

[2] L. Banjai and C. Lubich. *An error analysis of Runge-Kutta convolution quadrature*, BIT, **51** (2011), 483–496.

[3] L. Banjai, C. Lubich, and J. M. Melenk. *Runge-Kutta convolution quadrature for operators arising in wave propagation*, Numer. Math., **119** (2011), 1–20.

[4] E. Hairer, S.P. Norsett, G. Wanner, *Solving Ordinary Differential Equations I.* Springer Series in Computational Mathematics. Springer-Verlag, Berlin, second edition, 1993.

[5] M. Lopez Fernandez, S. Sauter, *Generalized convolution quadrature with variable time stepping*, IMA J. Numer. Math. **33** (2013), 1156–1175.

[6] M. Lopez Fernandez, S. Sauter, *Generalized convolution quadrature with variable time stepping. Part II: Algorithm and numerical results*, App. Numer. Math. **94** (2015), 88–105.

[7] M. Lopez Fernandez, S. Sauter, *Fast and stable contour integration for high order divided differences via elliptic functions*, Math. Comput **84** (2015), 1291–1315.

[8] M. Lopez Fernandez, S. Sauter, *Generalized convolution quadrature based on Runge–Kutta methods*, Numer. Math **133** (2016), 743–779.
[9] R. Schnyder, *Time and Space Adaptive Solution to Retarded Potential Integral Equations*, Master Thesis, University of Zurich, 2013.

Space–time Trefftz discontinuous Galerkin methods for wave problems

Andrea Moiola
(joint work with Ilaria Perugia)

When solving a linear initial or boundary value problem with a standard finite element or discontinuous Galerkin method, one approximates the solution with a discrete function picked from a finite-dimensional linear space of piecewise polynomials. If the equation is homogeneous, i.e. no volume source term is present but the forcing is due to the initial and boundary conditions, then similar accuracy might be obtained using, on each mesh element, a much smaller discrete space formed by particular solutions of the PDE under consideration. This is the essential idea of Trefftz methods, named after the work [13] of Erich Trefftz in 1926.

For example, when approximating the homogeneous Laplace equation, one can use a discrete space of piecewise *harmonic* polynomials of a given maximal degree, as opposed to the full space of polynomials of the same degree [6]. Trefftz methods have been extensively studied in the case of linear (acoustic, electromagnetic and elastic) waves in time-harmonic regime; we refer to [5] for a survey of the scalar case modelled by the Helmholtz equation $-\Delta u - k^2 u = 0$, where $k > 0$ is the wavenumber. In time-harmonic problems, no polynomial Trefftz spaces are possible: typical basis functions are plane and circular waves.

Much less work has been devoted to Trefftz methods for time-domain partial differential equations. The first results on space–time Trefftz methods for wave problems are due to Maciąg and coworkers, e.g. [9], followed more recently by few works on the scalar wave equation [1, 12, 14] and on Maxwell equations [3, 4, 7, 8].

Following [10], we present the error analysis of a space–time Trefftz discontinuous Galerkin (DG) scheme for the first-order acoustic wave equation:

$$\begin{aligned}
&\nabla v + \partial_t \boldsymbol{\sigma} = \mathbf{0} && \text{in } \Omega \times (0,T),\\
&\nabla \cdot \boldsymbol{\sigma} + c^{-2}\partial_t v = 0 && \text{in } \Omega \times (0,T),\\
&v(\cdot,0) = v_0, \quad \boldsymbol{\sigma}(\cdot,0) = \boldsymbol{\sigma}_0 && \text{on } \Omega,\\
&v = g, && \text{on } \partial\Omega \times (0,T),
\end{aligned}$$

where Ω is a bounded, Lipschitz, open set in $\mathbb{R}^n$, $T > 0$, $n \in \mathbb{N}$, the wave speed c is positive, piecewise-constant and independent of time t, and $v_0, \boldsymbol{\sigma}_0$ and g are the problem data. Neumann and Robin boundary conditions can also be considered. Given a solution U of the second-order scalar wave equation $\Delta U - c^{-2}\partial_t^2 U = 0$, its derivatives $(v, \boldsymbol{\sigma}) = (\partial_t U, -\nabla U)$ satisfy the first-order system.

The proposed Trefftz-DG scheme is posed on an unstructured polytopic mesh partitioning the space–time cylinder $\Omega \times (0,T)$ and is determined by the choice

of upwind numerical fluxes on space-like mesh interfaces and penalised centred fluxes on the time-like ones. Since trial and test fields are taken to be elementwise solutions of the first-order wave equation, the variational formulation of the Trefftz-DG scheme is written in terms of integrals on the element faces only. The discrete solution can either be found by solving a linear system coupling all elements in the space–time cylinder, or as an implicit time-stepping method if the elements can be collected in time-slabs, or as an explicit method if the mesh constructed with the tent-pitching algorithm of e.g. [11].

We show that the scheme is well-posed, stable and quasi-optimal in a suitable mesh-dependent norm, for any choice of the discrete Trefftz space. Using a special duality technique we prove a priori error bounds in space–time mesh-independent Sobolev norms, under some further conditions on the problem and the mesh.

The simplest discrete Trefftz space can be defined as the space of fields that restricted to each mesh element are degree-p polynomial solutions of the first-order wave equation. Simple bases for this space can be constructed. For this discrete space we prove high orders of convergence in the meshwidth h. The Trefftz space has the same approximation properties of the full polynomial space of the same degree but much smaller dimension: this leads to faster convergence in the number of degrees of freedom. Convergence orders in p are proved in one space dimension.

The method can be extended to Maxwell equations [7] and to a class of symmetric hyperbolic first-order systems with piecewise-constant coefficients.

Formally, the Trefftz-DG scheme can be written similarly to the ultra weak variational formulation of [2] as the operator equation $(I - F^*\Pi)u = f$ on a suitable trace space, where I is the identity, F is an isometry defined in terms of local initial boundary value problems and Π is a trace-flipping operator.

For more details on the Trefftz-DG method and its analysis we refer to [10].

References

[1] L. Banjai, E. Georgoulis, O. Lijoka, *A Trefftz polynomial space-time discontinuous Galerkin method for the second order wave equation*, SIAM J. Numer. Anal., **55** (2017), 63–86.

[2] O. Cessenat, B. Després, *Application of an ultra weak variational formulation of elliptic PDEs to the two-dimensional Helmholtz equation*, SIAM J. Numer. Anal., **35** (1998), 255–299.

[3] H. Egger, F. Kretzschmar, S. M. Schnepp, I. Tsukerman, T. Weiland, *Transparent boundary conditions for a discontinuous Galerkin Trefftz method*, Appl. Math. Comput., **267** (2015), 42–55.

[4] H. Egger, F. Kretzschmar, S. M. Schnepp, T. Weiland, *A Space-Time Discontinuous Galerkin Trefftz Method for Time Dependent Maxwell's Equations*, SIAM J. Sci. Comput., **37** (2015), B689–B711.

[5] R. Hiptmair, A. Moiola, I. Perugia, *A Survey of Trefftz Methods for the Helmholtz Equation*, Lect. Notes Comput. Sci. Eng., Springer, 2016. 237–278.

[6] R. Hiptmair, A. Moiola, I. Perugia, C. Schwab, *Approximation by harmonic polynomials in star-shaped domains and exponential convergence of Trefftz hp-dGFEM*, ESAIM Math. Model. Numer. Anal., **48** (2014), 727–752.

[7] F. Kretzschmar, A. Moiola, I. Perugia, S. M. Schnepp, *A priori error analysis of space-time Trefftz discontinuous Galerkin methods for wave problems*, IMA J. Numer. Anal., **36** (2016), 1599–1635.

[8] F. Kretzschmar, S. M. Schnepp, I. Tsukerman, T. Weiland, *Discontinuous Galerkin methods with Trefftz approximations*, J. Comput. Appl. Math., **270** (2014), 211–222.
[9] A. Maciąg, J. Wauer, *Solution of the two-dimensional wave equation by using wave polynomials*, J. Engrg. Math., **51** (2005), 339–350.
[10] A. Moiola, I. Perugia, *A space–time Trefftz discontinuous Galerkin method for the first-order acoustic wave equation*, arXiv:1610.08002, (2016).
[11] P. Monk and G. R. Richter, *A discontinuous Galerkin method for linear symmetric hyperbolic systems in inhomogeneous media*, J. Sci. Comput., **22/23** (2005), 443–477.
[12] S. Petersen, C. Farhat, R. Tezaur, *A space-time discontinuous Galerkin method for the solution of the wave equation in the time domain*, Internat. J. Numer. Methods Engrg., **78** (2009), 275–295.
[13] E. Trefftz, *Ein Gegenstuck zum Ritzschen Verfahren*, Proc. 2nd Int. Cong. Appl. Mech., Zurich, 1926, (1926), 131–137.
[14] D. Wang, R. Tezaur, C. Farhat, *A hybrid discontinuous in space and time Galerkin method for wave propagation problems*, Internat. J. Numer. Methods Engrg., **99** (2014), 263–289.

Space-time multigrid methods for parabolic optimal control problems

Martin Neumüller

We present a new space-time multigrid method for solving an optimal control problem of the following form: We want to minimize the functional

$$\mathscr{J}(y,u) := \frac{1}{2}||y-\overline{y}||^2_{L_2(Q)} + \frac{\lambda}{2}||u||^2_{L_2(Q)} \tag{1}$$

under the constraint

$$\begin{aligned} \partial_t y(x,t) - \Delta y(x,t) &= u(x,t) && \text{for } (x,t) \in Q := \Omega \times (0,T), \\ y(x,t) &= 0 && \text{for } (x,t) \in \Sigma := \partial\Omega \times (0,T), \\ y(x,0) &= y_0(x) && \text{for } (x,t) \in \Sigma_0 := \overline{\Omega} \times \{0\}. \end{aligned} \tag{2}$$

Here $\Omega \subset \mathbb{R}^d, d = 1,2,3$ is a bounded domain with Lipschitz boundary $\partial\Omega$, $T > 0$ is some given simulation time and $y_0 \in L_2(\Omega)$ is some given initial datum. We want to reach some desired state $\overline{y} \in L_2(Q)$ by using a distributed control $u \in L_2(Q)$. The cost of the control u is scaled by some given cost coefficient $\lambda > 0$. For the problem (1)–(2) we obtain the following optimality system in strong form (see also [9]):

$$\begin{aligned} \partial_t y(x,t) - \Delta y(x,t) &= -\frac{1}{\lambda} p(x,t) && \text{for } (x,t) \in Q, \\ y(x,t) &= 0 && \text{for } (x,t) \in \Sigma, \\ y(x,0) &= y_0(x) && \text{for } (x,t) \in \Sigma_0, \\ -\partial_t p(x,t) - \Delta p(x,t) &= y(x,t) - \overline{y}(x,t) && \text{for } (x,t) \in Q, \\ p(x,t) &= 0 && \text{for } (x,t) \in \Sigma, \\ p(x,T) &= 0 && \text{for } (x,t) \in \Sigma_T := \overline{\Omega} \times \{T\}. \end{aligned} \tag{3}$$

Note that we eliminated the control $u \in L_2(Q)$ by using the optimality condition $p + \lambda u = 0$. Moreover we note that the optimality system (3) is a coupled system

of parabolic boundary value problems, where the adjoint problem is a backward problem. So we have to solve the problem (3) in the whole space-time domain Q. This motivates to use space-time methods, i.e. all at once methods in space and time, see for example [7, 8, 6]. Combining such methods with parallel solvers with respect to space and time result in very fast and efficient solvers for time dependent parabolic problems, see [3, 4] and their references therein. Here we will use space-time discretization schemes based on tensor product space-time finite elements. In detail we will combine a standard finite element approach in space with a dG-time stepping scheme with respect to time (forward and backward). For a scalar ODE like

$$\partial_t y(t) + y(t) = f(t), \quad \text{for } t \in (0,T) \quad \text{and} \quad y(0) = y_0,$$

the dG-time stepping scheme for one time interval $\tau_k := (t_{k-1}, t_k)$ reads: Find $y_k \in \mathbb{P}^{p_t}(t_{k-1}, t_k)$, such that

$$\begin{aligned} -\int_{t_{k-1}}^{t_k} y_k\, \partial_t v_k \mathrm{d}t + y_k(t_k) v_k(t_k) + \int_{t_{k-1}}^{t_k} y_k\, v_k \mathrm{d}t \\ = \int_{t_{k-1}}^{t_k} f\, v_k \mathrm{d}t + y_{k-1}(t_{k-1}) v_k(t_{k-1}), \end{aligned} \tag{4}$$

for all $v_k \in \mathbb{P}^{p_t}(t_{k-1}, t_k)$. Using a basis representation for the space $\mathbb{P}^{p_t}(t_{k-1}, t_k)$ results in the equivalent linear system

$$[K_\tau + M_{\tau_k}]\, \underline{y}_k = \underline{f}_k + N_\tau \underline{y}_{k-1}. \tag{5}$$

Note that the matrices K_τ and N_τ do not depend on the time step size $|\tau_k| := t_{k-1} - t_k$, which we indicate with the index τ only. Similar we obtain for the backward problem

$$-\partial_t p(t) + p(t) = f(t), \quad \text{for } t \in (0,T) \quad \text{and} \quad p(T) = p_N,$$

the dG-time stepping scheme: Find $p_k \in \mathbb{P}^{p_t}(t_{k-1}, t_k)$, such that

$$\begin{aligned} \int_{t_{k-1}}^{t_k} p_k\, \partial_t v_k \mathrm{d}t + p_k(t_{k-1}) v_k(t_{k-1}) + \int_{t_{k-1}}^{t_k} p_k\, v_k \mathrm{d}t \\ = \int_{t_{k-1}}^{t_k} f\, v_k \mathrm{d}t + p_{k+1}(t_k) v_k(t_k), \end{aligned} \tag{6}$$

for all $v_k \in \mathbb{P}^{p_t}(t_{k-1}, t_k)$. Using the same basis representation as for the forward problem (4) the variational problem (6) results in the linear system

$$\left[K_\tau^\top + M_{\tau_k}\right] \underline{p}_k = \underline{f}_k + N_\tau^\top \underline{p}_{k+1}. \tag{7}$$

Using a standard finite element approach in space and the above dG-time stepping schemes for the forward and backward problem results for the time interval $\tau_k = (t_{k-1}, t_k)$ in the following linear system

$$\begin{pmatrix} \frac{1}{\lambda} M_h \otimes M_{\tau_k} & M_h \otimes K_\tau + K_h \otimes M_{\tau_k} \\ M_h \otimes K_\tau^\top + K_h \otimes M_{\tau_k} & -M_h \otimes M_{\tau_k} \end{pmatrix} \begin{pmatrix} \underline{p}_k \\ \underline{y}_k \end{pmatrix} = \begin{pmatrix} M_h \otimes N_\tau \underline{y}_{k-1} \\ M_h \otimes N_\tau^\top \underline{p}_{k+1} + \underline{g}_k \end{pmatrix}, \tag{8}$$

where the vector $\underline{g}_k$ corresponds to the functional induced by the negative value of the desired state $\overline{y} \in L_2(Q)$. Moreover K_h is the usual stiffness matrix and M_h is the standard mass matrix with respect to the computational domain Ω. The linear system (8) is coupled via the right hand side with the unknown value $\underline{y}_{k-1}$ coming from the past and the value $\underline{p}_{k+1}$ coming from the future. Hence we have to combine all equations for each time steps together into one big linear system and we obtain

$$\begin{pmatrix} A_{\tau_1,h} & B_{\tau,h}^\top & & & \\ B_{\tau,h} & A_{\tau_2,h} & B_{\tau,h}^\top & & \\ & B_{\tau,h} & A_{\tau_3,h} & \ddots & \\ & & \ddots & \ddots & B_{\tau,h}^\top \\ & & & B_{\tau,h} & A_{\tau_N,h} \end{pmatrix} \begin{pmatrix} \underline{x}_1 \\ \underline{x}_2 \\ \underline{x}_3 \\ \vdots \\ \underline{x}_N \end{pmatrix} = \begin{pmatrix} \underline{f}_1 \\ \underline{f}_2 \\ \underline{f}_3 \\ \vdots \\ \underline{f}_N \end{pmatrix}, \tag{9}$$

with the matrices and vectors

$$\begin{aligned} A_{\tau_k,h} &:= \begin{pmatrix} \frac{1}{\lambda} M_h \otimes M_{\tau_k} & M_h \otimes K_\tau + K_h \otimes M_{\tau_k} \\ M_h \otimes K_\tau^\top + K_h \otimes M_{\tau_k} & -M_h \otimes M_{\tau_k} \end{pmatrix}, \\ B_{\tau,h} &:= \begin{pmatrix} 0 & -M_h \otimes N_\tau \\ 0 & 0 \end{pmatrix}, \\ \underline{x}_k &:= \begin{pmatrix} \underline{p}_k \\ \underline{y}_k \end{pmatrix}, \qquad \underline{f}_k := \begin{pmatrix} 0 \\ \underline{g}_k \end{pmatrix}. \end{aligned}$$

We will solve the linear system (9), in short $L_{t,h}\underline{x} = \underline{f}$, by applying the multigrid method in time and space. Which will result in a method which is fully parallel in space and time. Other multigrid methods for such optimality systems can be found for example in [5, 2, 1]. To obtain a parallel method with respect to time we will use an additive smoothing procedure, i.e. an (inexact) damped block Jacobi scheme given by

$$\underline{x}^{(n+1)} = \underline{x}^{(n)} + \omega_t D_{\tau,h}^{-1} \left[\underline{f} - L_{t,h} \underline{x}^{(n)} \right] \quad \text{for } n = 0, 1, \ldots, \tag{10}$$

where $D_{\tau,h} := \operatorname{diag}\{A_{\tau_k,h}\}_{k=1}^N$ is the block diagonal matrix of $L_{\tau,h}$. Since the exact inversion of $D_{\tau,h}$ is in general costly we approximate the exact inverse by one multigrid V-cycle with respect to space, where we use a geometric tensor product multigrid method or an algebraic multigrid method, which can be also be applied in parallel. For the coarsening in space and time we consider the two following strategies:

- Coarsening in time only, i.e. we combine two time steps together into one time step.
- Coarsening in space and time, i.e. standard coarsening in space combined with the above coarsening in time.

Applying the local Fourier mode analysis to the two-grid operators obtained by the smoothing iteration (10) in combination with the two coarsening strategies

space levels	cost coefficient $\log(\lambda)$												
	-6	-5	-4	-3	-2	-1	0	1	2	3	4	5	6
0	10	10	9	9	9	9	9	9	9	9	9	9	9
1	10	10	10	10	10	9	9	9	9	9	9	9	9
2	10	10	10	10	10	10	10	10	10	10	10	10	10
3	10	10	10	10	10	10	10	10	10	10	10	10	10
4	10	10	10	10	10	10	10	10	10	10	10	10	10
5	11	11	11	10	10	10	10	10	10	10	10	10	10
6	11	11	10	10	10	10	10	10	10	10	10	10	10
7	11	11	10	10	10	10	10	10	10	10	10	10	10
8	11	10	10	10	10	10	10	10	10	10	10	10	10

TABLE 3. Space-time multigrid iterations for Example 1.

above with respect to the discretization parameter $\mu := \frac{\tau}{h^2}$ and the cost coefficient λ results in small two-grid contraction numbers ($\ll 1$) in the following cases:

- Coarsening in time only: for any $\mu > 0$, any $\lambda > 0$ and any $p_t \in \mathbb{N}_0$.
- Coarsening in space and time: for $\mu \geq \mu^* \approx 1$, any $\lambda > 0$ and any $p_t \in \mathbb{N}_0$.

With this knowledge we define the space-time coarsening in the multilevel setting based on the discretization parameter $\mu = \frac{\tau}{h^2}$ similar as in the work [4]. Hence we have all ingredients to test this method in the following examples.

Example 1. In this example we test the robustness of the proposed method with respect to the cost coefficient and the discretization with respect to space. To do so we consider the domain $\Omega = (0,1)^2$ discretized with piecewise linear elements based on a triangular subdivision. Moreover we set $T = 1$ and use a time discretization with $N = 256$ uniform time steps and set $p_t = 1$. For the geometric tensor product multigrid method with respect to space we use a damped Jacobi scheme with a damping $\omega_x = \frac{2}{3}$ and two pre- and post-smoothing steps. For the time multigrid settings we use also two pre- and post-smoothing steps with $\omega_t = \frac{1}{2}$. For a zero right hand side $\underline{f} = \underline{0}$ and a random initial guess $\underline{x}^{(0)}$ with values between zero and one we apply the proposed space-time multigrid method until we reach a relative residual error reduction of $\varepsilon = 10^{-8}$. In Table 3 we show the used iteration numbers for different refinement levels in space and different cost coefficients λ from 10^{-6} to 10^6. We observe that the proposed method results in small and robust iteration numbers.

Example 2. In this example we test the parallel performance of the proposed method with respect to space and time. For the space solver we use a parallel algebraic multigrid method coming from the *hypre*-package. For the problem in space we consider the three-dimensional domain $\Omega = (0,1)^3$ decomposed into 262 144 tetrahedra which are equipped with piecewise linear functions for the approximation. For the discretization with respect to time we use 512 time steps with a uniform time step size of $\tau = 10^{-2}$ and use $p_t = 0$. We use a fixed cost coefficient

		processors space							
		4	8	16	32	64	128	256	512
processors time	4	–	20 057.5	12 666.6	6 490.8	3 633.4	2 010.4	1 569.1	1 083.3
	8	18 834.6	10 030.7	6 519.3	3 354.0	1 828.4	1 011.4	796.3	553.9
	16	9 439.4	5 037.7	3 216.7	1 719.3	921.6	510.4	410.4	291.0
	32	4 740.3	2 529.4	1 601.4	868.6	466.2	261.0	217.7	160.8
	64	2 388.7	1 279.3	828.6	442.7	239.5	136.3	122.6	90.7
	128	1 213.2	653.3	425.5	228.2	117.9	68.2	71.4	62.4
	256	627.1	341.5	219.2	121.9	69.6	40.4	50.3	48.9
	512	327.9	183.8	119.8	70.5	41.7	27.5	41.4	-

TABLE 4. Solving times in [s] for Example 2.

of $\lambda = 10^{-2}$ and for the time multigrid we use the same settings as in Example 1. This results in a problem with 549 250 unknowns in space and 281 216 000 unknowns overall. In Table 4 we solved always the same problem with different numbers of processors in space and time. We observe that in the most cases it is better to use all the processors available for the time parallelization. The reason for this can be explained by the fact that the communication with respect to time is much simpler than the communication with respect to space, since we only have to communicate forward and backward in time. Moreover we see excellent strong scalings with respect to the time parallelization and also with respect to space when the problem size per core is large enough. At the end we can solve the huge linear system in 27.5 seconds by using 128 processors in space and 512 processors in time, i.e. overall we use 65 536 cores.

REFERENCES

[1] D. Abbeloos, M. Diehl, M. Hinze, and S. Vandewalle. Nested multigrid methods for time-periodic, parabolic optimal control problems. *Comput. Vis. Sci.*, 14(1):27–38, 2011.

[2] A. Borzì. Multigrid methods for parabolic distributed optimal control problems. *J. Comput. Appl. Math.*, 157(2):365–382, 2003.

[3] M. Gander. 50 years of time parallel time integration. In T. Carraro, M. Geiger, S. Körkel, and R. Rannacher, editors, *Multiple Shooting and Time Domain Decomposition*, pages 69–114. Springer-Verlag, 2015.

[4] M. Gander and M. Neumüller. Analysis of a new space-time parallel multigrid algorithm for parabolic problems. *SIAM J. Sci. Comput.*, 38(4):A2173–A2208, 2016.

[5] W. Hackbusch. On the fast solving of parabolic boundary control problems. *SIAM J. Control Optim.*, 17(2):231–244, 1979.

[6] U. Langer, S. Moore, and M. Neumüller. Space-time isogeometric analysis of parabolic evolution equations. *Comput. Methods Appl. Mech. Engrg.*, 306:342–363, 2016.

[7] M. Neumüller and O. Steinbach. Refinement of flexible space-time finite element meshes and discontinuous Galerkin methods. *Comput. Vis. Sci.*, 14(5):189–205, 2011.

[8] M. Neumüller and O. Steinbach. A DG space-time domain decomposition method. In *Domain decomposition methods in science and engineering XX*, volume 91 of *Lect. Notes Comput. Sci. Eng.*, pages 623–630. Springer, Heidelberg, 2013.

[9] F. Tröltzsch. *Optimal control of partial differential equations*, volume 112 of *Graduate Studies in Mathematics*. American Mathematical Society, Providence, RI, 2010. Theory, methods and applications, Translated from the 2005 German original by Jürgen Sprekels.

A PDE approach to space–time fractional parabolic problems

Enrique Otárola

We consider the numerical approximation of an initial boundary value problem for a space–time fractional parabolic equation. Let $\Omega \subset \mathbb{R}^d$ be a bounded domain with Lipschitz boundary. Given $s \in (0,1)$, $\gamma \in (0,1]$, a forcing function f, and an initial datum u_0, the parabolic problem reads as follows: find u such that

$$\partial_t^\gamma u + \mathscr{L}^s u = f \ \text{ in } \Omega \times (0,T), \quad u(0) = u_0 \ \text{ in } \Omega, \quad u = 0 \text{ on } \partial\Omega \times (0,T). \tag{1}$$

The second order elliptic operator $\mathscr{L}$ is defined by

$$\mathscr{L} w = -\mathrm{div}_{x'}(A \nabla_{x'} w) + cw,$$

where $0 \leq c \in L^\infty(\Omega)$ and $A \in C^{0,1}(\Omega, \mathsf{GL}(d,\mathbb{R}))$ is symmetric and positive definite; $\mathscr{L}$ is supplemented with homogeneous Dirichlet boundary conditions. The fractional powers of the operator $\mathscr{L}$ are defined on the basis of spectral theory. The latter yields the existence of a countable collection of eigenpairs $\{\varphi_k, \lambda_k\}_{k\in\mathbb{N}}$ such that $\mathscr{L}\varphi_k = \lambda_k \varphi_k$ in Ω and $\varphi_k = 0$ on $\partial\Omega$. The eigenfunctions $\{\varphi_k\}_{k\in\mathbb{N}}$ form an orthonormal basis in $L^2(\Omega)$. We thus define the fractional powers of $\mathscr{L}$ by

$$\mathscr{L}^s w := \sum_{k=1}^{\infty} \lambda_k^s w_k \varphi_k, \quad w \in C_0^\infty(\Omega), \quad w_k = \int_\Omega w \varphi_k dx', \quad s \in (0,1).$$

By density this definition can be extended to $\mathbb{H}^s(\Omega) = [L^2(\Omega), H_0^1(\Omega)]_s$ [NOS15]. For $s \in (0,1)$ we denote by $\mathbb{H}^{-s}(\Omega)$ the dual space of $\mathbb{H}^s(\Omega)$.

The fractional derivative ∂_t^γ for $\gamma \in (0,1)$ is understood as *the left-sided Caputo fractional derivative of order* γ with respect to t, which is defined by [SKM93]

$$\partial_t^\gamma u(x',t) := \frac{1}{\Gamma(1-\gamma)} \int_0^t \frac{1}{(t-r)^\gamma} \frac{\partial u(x',r)}{\partial r} \, \mathrm{d}r, \tag{2}$$

where Γ is the Gamma function. For $\gamma = 1$, we consider the usual derivative ∂_t.

One of the main difficulties in the study of problem (1) is the nonlocality of the fractional time derivative and the fractional space operator [CS07, SKM93]. A possible approach to overcome the nonlocality in space is given by the seminal result of Caffarelli and Silvestre in $\mathbb{R}^d$ [CS07] and its extensions to bounded domains. Set $\alpha = 1 - 2s$, $\mathscr{C} = \Omega \times (0,\infty)$ and consider the elliptic equation:

$$\mathscr{L}\mathscr{U} - \frac{\alpha}{y}\partial_y \mathscr{U} - \partial_{yy}\mathscr{U} = 0 \text{ in } \mathscr{C}, \ \mathscr{U} = 0 \text{ on } \partial_L \mathscr{C}, \ \partial_\nu^\alpha \mathscr{U} = d_s f \text{ on } \Omega \times \{0\}, \tag{3}$$

where $\partial_L \mathscr{C} = \partial\Omega \times (0,\infty)$, $\partial_{\nu^\alpha}\mathscr{U} = -\lim_{y\downarrow 0} y^\alpha \partial_y \mathscr{U}$, and $d_s = 2^\alpha \Gamma(1-s)/\Gamma(s)$. The localization result of [CS07] yields that $u = \mathrm{tr}_\Omega \mathscr{U} = \mathscr{U}(\cdot, 0)$ solves

$$\mathscr{L}^s u = f \text{ in } \Omega. \tag{4}$$

On the basis of this localization technique, we have proposed in [NOS15] a simple strategy to find the solution of problem (4) in general polytopal domains Ω in $\mathbb{R}^d$ ($d \geq 1$). Moreover, we have derived a quasi-optimal a priori error analysis, in the context of weighted Sobolev spaces, valid for tensor product elements which may be graded in Ω and exhibit a large aspect ratio in y (anisotropy) to fit the

behavior of $\mathscr{U}(x', y)$ with $x' \in \Omega$, $y > 0$. The a priori error analysis combines asymptotic properties of Bessel functions, a polynomial interpolation theory on weighted Sobolev spaces [NOS16b] and weighted regularity estimates for the solution to (3). Since the scheme of [NOS15] is based on local techniques, the ensuing linear systems can be efficiently solved using multilevel techniques [CNOS16].

The result of [NOS15] can be applied to analyze and propose numerical techniques for the parabolic problem (1). We rewrite (1) as a quasi-stationary elliptic problem with dynamic boundary condition:

(5)
$$\begin{cases} -\operatorname{div}(y^\alpha \mathbf{A}\nabla\mathscr{U}) + y^\alpha c\,\mathscr{U} = 0 \text{ in } \mathscr{C}\times(0,T), & \mathscr{U} = 0 \text{ on } \partial_L\mathscr{C}\times(0,T), \\ d_s\partial_t^\gamma \mathscr{U} + \partial_\nu^\alpha \mathscr{U} = d_s f \text{ on } (\Omega\times\{0\})\times(0,T), & \mathscr{U} = u_0, \text{ on } \Omega\times\{0\}, t = 0, \end{cases}$$

where for all $(x', y) \in \mathscr{C}$, $\mathbf{A}(x', y) := \operatorname{diag}\{A(x'), 1\}$; $A \in C^{0,1}(\mathscr{C}, \mathsf{GL}(d+1, \mathbb{R}))$.

1. Time discretization

Let $\mathscr{K} \in \mathbb{N}$ denote the number of time steps. We define the uniform time step as $\tau = T/\mathscr{K} > 0$, and set $t_k = k\tau$ for $0 \le k \le \mathscr{K}$. We also define $I_k = (t_k, t_{k+1}]$ for $0 \le k \le \mathscr{K}-1$. If $\mathscr{X}$ is a normed space with norm $\|\cdot\|_{\mathscr{X}}$, then for $\phi \in C([0,T], \mathscr{X})$ we denote $\phi^k = \phi(t_k)$ and $\phi^\tau = \{\phi^k\}_{k=0}^{\mathscr{K}}$.

1.1. **Case $\gamma = 1$.** For $\gamma = 1$ the time discretization is based on the backward Euler scheme.

1.2. **Case $\gamma \in (0,1)$.** We discretize ∂_t^γ using the finite difference scheme proposed in [LX07]: Taylor's formula with integral remainder yields, for $0 \le k \le \mathscr{K}-1$,

$$\partial_t^\gamma u(\cdot, t_{k+1}) = \frac{1}{\Gamma(2-\gamma)} \sum_{j=0}^{k} a_j \frac{u(\cdot, t_{k+1-j}) - u(\cdot, t_{k-j})}{\tau^\gamma} + r_\gamma^{k+1}(\cdot), \tag{6}$$

where

$$a_j = (j+1)^{1-\gamma} - j^{1-\gamma}, \qquad r_\gamma^{k+1} = \frac{1}{\Gamma(1-\gamma)} \sum_{j=0}^{k} \int_{I_j} \frac{1}{(t_{k+1}-t)^\gamma} R(\cdot, t)\,\mathrm{d}t \tag{7}$$

denotes the remainder and R is defined by

$$R(\cdot, t) = \partial_t u(\cdot, t) - \frac{1}{\tau}\big(u(\cdot, t_{j+1}) - u(\cdot, t_j)\big) \qquad \forall t \in I_j. \tag{8}$$

On the basis of (6) we consider an implicit semi–discrete scheme for problem (5). The proposed scheme is unconditionally stable and satisfies

$$I^{1-\gamma}\|\operatorname{tr}_\Omega V^\tau\|^2_{L^2(\Omega)}(T) + \|V^\tau\|^2_{\ell^2 \mathring{H}^1_L(y^\alpha, \mathscr{C}))} \lesssim I^{1-\gamma}\|u_0\|^2_{L^2(\Omega)}(T) + \|f^\tau\|^2_{\ell^2(\mathbb{H}^{-s}(\Omega))}.$$

Deducing an energy estimate for problem (5) is nontrivial due to the nonlocality of the fractional time derivative. In this sense, the previous discrete energy estimate has an important consequence at the continuous level:

$$I^{1-\gamma}\|\operatorname{tr}_\Omega \mathscr{U}\|^2_{L^2(\Omega)}(T) + \|\mathscr{U}\|^2_{\ell^2 \mathring{H}^1_L(y^\alpha, \mathscr{C}))} \lesssim I^{1-\gamma}\|u_0\|^2_{L^2(\Omega)}(T) + \|f^\tau\|^2_{\ell^2(\mathbb{H}^{-s}(\Omega))}.$$

The regularity assumptions usually made in the literature to analyze the consistency error of the discretization (6) are unrealistic [LX07]. For $\gamma < 1$ the behavior of $\partial_{tt} u$ is very singular as $t \to 0^+$. In fact, in [NOS16], we showed that

$$\partial_t u \in L \log L(0,T;\mathbb{H}^{-s}(\Omega)), \qquad \partial_{tt}^2 u \in L^2(t^\sigma;0,T;\mathbb{H}^{-s}(\Omega)),\ \sigma > 3-2\gamma.$$

Using these refined results we analyzed the consistency error: The fractional residual $r_\gamma^\tau = \{r_\gamma^k\}_{k=0}^{\mathscr{K}}$ satisfies

$$\|r_\gamma^\tau\|_{L^2(0,T;\mathbb{H}^{-s}(\Omega))} \lesssim \tau^\theta, \quad 0 < \theta = 2 - \gamma - \frac{\sigma}{2} < \frac{1}{2}. \tag{9}$$

2. A fully discrete scheme for $\gamma \in (0,1)$

The space discretization hinges on the finite element method on a truncated cylinder discussed in [NOS15]. The discretization in time uses an implicit finite difference scheme based on (6) for $\gamma \in (0,1)$; the backward Euler scheme is used when $\gamma = 1$. We proved that the proposed scheme is unconditionally stable, obtaining an estimate similar to (1.2) and obtained the following error estimates.

Let $\gamma \in (0,1)$, u be the solution to (1) and $\operatorname{tr}_\Omega V_{\mathscr{T}_\gamma}^\tau$ be its fully discrete approximation [NOS15]. Then

$$[I^{1-\gamma}\|u^\tau - \operatorname{tr}_\Omega V_{\mathscr{T}_\gamma}^\tau\|_{L^2(\Omega)}^2(T)]^{\frac{1}{2}} \lesssim \tau^\theta + |\log N|^{2s} N^{-\frac{1+s}{d+1}},$$

and

$$\|u^\tau - \operatorname{tr}_\Omega V_{\mathscr{T}_\gamma}^\tau\|_{\ell^2(\mathbb{H}^s(\Omega)))} \lesssim \tau^\theta + |\log N|^s N^{\frac{-1}{d+1}},$$

where N denotes the number the degrees of freedom of the graded mesh in space, $0 < \theta < \frac{1}{2}$ and the hidden constants blow up as $\theta \uparrow \frac{1}{2}$.

References

[CNOS16] L. Chen, R. H. Nochetto, E. Otárola, and A. J. Salgado. Multilevel methods for nonuniformly elliptic operators and fractional diffusion. *Math. Comp.*, 85(302):2583–2607, 2016.

[CS07] L. Caffarelli and L. Silvestre. An extension problem related to the fractional Laplacian. *Comm. Partial Differential Equations*, 32(7-9):1245–1260, 2007.

[LX07] Y. Lin and C. Xu. Finite difference/spectral approximations for the time-fractional diffusion equation. *J. Comput. Phys.*, 225(2):1533–1552, 2007.

[NOS15] R. H. Nochetto, E. Otárola, and A. J. Salgado. A PDE approach to fractional diffusion in general domains: a priori error analysis. *Found. Comput. Math.*, 15(3):733–791, 2015.

[NOS16a] R. H. Nochetto, E. Otárola, and A. J. Salgado. A PDE approach to space-time fractional parabolic problems. *SIAM J. Numer. Anal.*, 54(2):848–873, 2016.

[NOS16b] R. H. Nochetto, E. Otárola, and Abner J. Salgado. Piecewise polynomial interpolation in Muckenhoupt weighted Sobolev spaces and applications. *Numer. Math.*, 132(1):85–130, 2016.

[SKM93] S. G. Samko, A. A. Kilbas, and O. I. Marichev. *Fractional integrals and derivatives*. Gordon and Breach Science Publishers, Yverdon, 1993. Theory and applications, Edited and with a foreword by S. M. Nikol′skiĭ, Translated from the 1987 Russian original, Revised by the authors.

Space-time Trace Finite Element Methods

Arnold Reusken
(joint work with Jörg Grande, Sven Groß, Christoph Lehrenfeld, Maxim Olshanskii, Igor Voulis)

We present different recent applications of *trace* and *unfitted* space-time finite element methods to classes of problems that are motivated by the simulation of two-phase incompressible flow problems. More precisely, we address the following topics:

a. Space-time trace finite element methods for parabolic PDEs on evolving surfaces. These methods are applicable to the so-called surfactant transport equation that occurs in two-phase flow models with surfactants.
b. CutFEM for the discretization of mass transport equations in two-phase flows.
c. CutFEM for the discretization of a time dependent Stokes interface model problem.

ad. a. Recently, several numerical approaches for the discretization of partial differential equations on (evolving) surfaces have been introduced. We refer to [2] for a recent overview of such methods. In this presentation we outline an Eulerian surface finite element method studied in [4, 5, 6]. The key idea of this method is to use restrictions of (usual) space-time volumetric finite element functions to the space-time manifold. This trace finite element technique was introduced for stationary surfaces in [7]. We address the key ideas of this space-time trace-FEM and some main results of the error analysis, in particular a result on second order accuracy of the method in space and time. These results are derived in [4, 5]. Results of numerical experiments show that the method is extremely robust and that even for the case with a topological singularity (droplet collision) accurate results can be obtained on a fixed Eulerian (space-time) grid with a large time step.

ad b. In the mass transport equations in two-phase flow, which model the transport of a solute between the two-phases, a so-called Henry condition is used. Due to this condition, the solution has a discontinuity across the evolving interface. Furthermore, due to the use of a level set technique for interface capturing, the grids that are applied for the discretization of this transport equation are not fitted to the interface. In this setting a particular class of unfitted FEM, namely the so-called CutFEM [1], turns out to be a very efficient approach. We present a space-time variant of this CutFEM approach which has a second order accuracy (with linears both in space and time) for this class of time dependent convection-diffusion equations with moving discontinuities. The results of the error analysis that we present are derived in [3].

ad c. In the sharp interface models for two-phase incompressible flows the fluid dynamics is modeled by a Navier-Stokes equation which has discontinuous density and viscosity coefficients across the interface. Furthermore, the pressure and the derivative of the velocity are in general discontinuous across the evolving interface.

Due to the use of a level set technique for interface capturing, the grids are not fitted to the interface. In such a setting, due to the moving discontinuities, it is very difficult to obtain a finite element method that has optimal discretization accuracy. In current research we try to extend the approach developed for the scalar mass transport equation, cf. topic b. above, to such a flow system. For this we consider a model problem of a time-dependent Stokes equation with a given smoothly evolving interface. Both the density and viscosity coeffient are allowed to jump across this interface and the effect of (surface tension) forces localized at the interface is included. For such a problem a new space-time weak formulation is presented. In recent work we proved well-posedness of this weak formulation. We briefly introduce the space-time CutFEM that we currently develop for this Stokes interface problem.

References

[1] Erik Burman, Susanne Claus, Peter Hansbo, Mats Larson, André Massing, *CutFEM: Discretizing geometry and partial differential equations*, International Journal for Numerical Methods in Engineering 104 (7), 472–501 (2015).

[2] G. Dziuk, C.M Elliott, *Finite element methods for surface PDEs*, Acta Numerica **22** (2013), 289–396.

[3] C. Lehrenfeld. A. Reusken, *Analysis of a Nitsche-XFEM-DG discretization for a class of two-phase mass transport problems*, SIAM J. Numer. Anal. 51, (2), 958-983 (2013).

[4] M. Olshanskii, A. Reusken, X. Xu, *An Eulerian space-time finite element method for diffusion problems on evolving surfaces*, SIAM J. Numer. Anal. 52 (3), 1354-1377 (2014).

[5] M. Olshanskii, A. Reusken, *Error analysis of a space-time finite element method for solving PDEs on evolving surfaces*, SIAM J. Numer. Anal. 52 (4), 2092-2120 (2014).

[6] J. Grande, *Finite element methods for parabolic equations on moving surfaces*, SIAM J. Sci. Comput. 36, B248-B271 (2014).

[7] M. Olshanskii, A. Reusken, J. Grande, *A finite element method for elliptic equations on surfaces*, SIAM J. Numer. Anal. **47** (2009), 3339–3358.

Nonlinear evolution problems involving fractional operators

Abner J. Salgado

We discuss two nonlinear evolution problems governed by nonlocal models. The nonlocality in space will be given by the spectral fractional Laplacian $(-\Delta)^s$: Let $\Omega \subset \mathbb{R}^d$ be a bounded domain with Lipschitz boundary. The Laplacian $-\Delta$, supplemented with homogeneous Dirichlet boundary conditions, has a countable collection of eigenpairs $\{\varphi_k, \lambda_k\}_{k=1}^{\infty}$: $-\Delta\varphi_k = \lambda_k\varphi_k$ in Ω and $\varphi_k = 0$ on $\partial\Omega$. The eigenfunctions form an orthonormal basis in $L^2(\Omega)$. In this basis, we have

$$u = \sum_{k=1}^{\infty} u_k\varphi_k \overset{(-\Delta)^s}{\longmapsto} (-\Delta)^s u = \sum_{k=1}^{\infty} \lambda_k^s u_k\varphi_k, \tag{1}$$

which is well defined for every $u \in \mathbb{H}^s(\Omega) = [H_0^1(\Omega), L^2(\Omega)]_{1-s}$.

$(-\Delta)^s$ is a nonlocal operator. To localize it, we employ the Caffarelli-Silvestre extension [CS07]: Set $\alpha = 1 - 2s$, $\mathscr{C} = \Omega \times (0, \infty)$ and let $\mathfrak{u} \in \mathring{H}_L^1(y^\alpha, \mathscr{C})$ solve

$$-\operatorname{div}(y^\alpha \nabla \mathfrak{u}) = 0 \ \text{ in } \mathscr{C}, \quad \mathfrak{u} = 0 \text{ on } \partial_L\mathscr{C}, \quad \partial_{\nu^\alpha}\mathfrak{u} = d_s f \text{ on } \Omega \times \{0\}, \tag{2}$$

where $\partial_L \mathscr{C} = \partial\Omega \times (0,\infty)$, $\partial_{\nu^\alpha} \mathfrak{u} = -\lim_{y\downarrow 0} y^\alpha \partial_y \mathfrak{u}$, and $d_s = 2^\alpha \Gamma(1-s)/\Gamma(s)$. Then, as shown in [CS07] the function $u = \operatorname{tr}_\Omega \mathfrak{u} = \mathfrak{u}(\cdot, 0)$ solves

$$(-\Delta)^s u = f \text{ in } \Omega. \tag{3}$$

Based on (2) we developed, in [NOS15b], a finite element method on tensor product meshes. We showed that the method is nearly optimal provided the meshes are suitably graded. In addition, since this is now a local problem, the ensuing linear systems can be efficiently solved using multilevel techniques [CNOS16].

A space-time fractional optimal control problem. The first problem is a PDE constrained optimization problem where the state is governed by a space-time fractional evolution equation. We must find the minimum of

$$J(u,z) = \frac{1}{2}\int_0^T \left(\|u - u_d\|^2_{L^2(\Omega)} + \mu \|z\|^2_{L^2(\Omega)} \right) \mathrm{d}t, \tag{4}$$

subject to

$$\partial_t^\gamma u + (-\Delta)^s u = f + z, \qquad u_{|t=0} = u_0 \tag{5}$$

and, for $a, b \in \mathbb{R}$ with $a < b$:

$$z \in \mathsf{Z}_{\mathrm{ad}} = \left\{ \mathfrak{z} \in L^2(0,T; L^2(\Omega)) : a \le \mathfrak{z} \le b \right\}. \tag{6}$$

In (5) ∂_t^γ denotes the Caputo derivative of order $\gamma \in (0,1)$, defined by

$$\partial_t^\gamma u(x,t) = \frac{1}{\Gamma(1-\gamma)} \int_0^t \frac{\partial_r u(x,r)}{(t-r)^\gamma} \,\mathrm{d}r = I^{1-\gamma}[\partial_t u(x,\cdot)](t).$$

Based on definition (1) of $(-\Delta)^s$ one can show that the solution to (5) reads

$$u(x,t) = \sum_{k=1}^\infty u_k(t)\varphi_k(x),$$

$$u_k(t) = E_{\gamma,1}(-\lambda_k^s t^\gamma) u_{0,k} + \int_0^t r^{\gamma-1} E_{\gamma,\gamma}(-\lambda_k^s r^\gamma)(f_k + z_k)(t-r)\,\mathrm{d}r,$$

provided $f + z \in L^\infty(0,T; \mathbb{H}^{-s}(\Omega))$ and $u_0 \in L^2(\Omega)$. Here $E_{\gamma,\delta}$ denotes the Mittag-Leffler function. In addition to existence and uniqueness, we can use this representation formula to study the regularity of the solution to (5). In particular, in [NOS16], we showed that

$$\partial_t u \in L\log L(0,T; \mathbb{H}^{-s}(\Omega)), \qquad \partial_{tt}^2 u \in L^2(t^\sigma; 0, T; \mathbb{H}^{-s}(\Omega)),\ \sigma > 3 - 2\gamma, \tag{7}$$

provided $f + z \in H^2(0,T; \mathbb{H}^{-s}(\Omega))$ and $u_0 \in \mathbb{H}^s(\Omega)$. With these properties at hand we can propose an analysis of the discretization of the state equation. To discretize the Caputo derivative we consider the L1 scheme. In [NOS16] we showed stability of this scheme, which combined with the regularity results given in (7) allows us to provide error estimates for the state equation (5).

However, when dealing with the optimal control problem (4)–(6), the most natural way to discretize the cost is via space-time piecewise constant functions, i.e., we introduce a simplicial triangulation $\mathscr{T} = \{K\}$ of Ω and a uniform time

partition $\mathscr{T} = \{I_k = [t_k, t_{k+1})\}_{k=0}^{\mathscr{K}}$ with $t_k = k\tau$ for a time-step $\tau > 0$. The space of discrete controls is then given by

$$\mathbb{Z} = \left\{\mathfrak{Z} \in L^2(0,T;L^2(\Omega)) : \mathfrak{Z}_{|K\times I_k} \in \mathbb{P}_0\right\}, \qquad \mathbb{Z}_{ad} = \mathbb{Z} \cap \mathsf{Z}_{\mathrm{ad}}.$$

This, in particular, implies that the data regularity required for (7) to hold is not valid. In addition, due to time discretization and the localization of the fractional Laplacian as in (2), the cost functional must be replaced by

$$J_{\mathscr{T}}^{\mathscr{T}}(V_{\mathscr{T}}^{\tau}, Z^{\tau}) = \frac{1}{2}\tau \sum_{k=1}^{\mathscr{K}} \left(\| \operatorname{tr}_{\Omega} V_{\mathscr{T}}^{\tau} - u_d^{\tau}\|_{L^2(\Omega)}^2 + \frac{\mu}{2}\|Z^{\tau}\|_{L^2(\Omega)}^2 \right),$$

where $V_{\mathscr{T}}^{\tau}$ is a discrete state obtained with a finite element discretization in space as in [NOS15b] and the L1 scheme in time. In summary, the cost is being modified and the data of the state does not possess enough smoothness to assert rates of convergence.

Instead of the standard approach, we showed in [AOS16] that $J_{\mathscr{T}}^{\mathscr{T}} \xrightarrow{\Gamma} J$, i.e. the discrete cost Γ-converges to the continuous one. This in particular required to show the adjoint consistency of the L1 scheme. As a consequence, we obtain that $Z^{\tau} \rightharpoonup z$ in $L^2(\Omega)$ and a similar result for the state.

The fractional obstacle problem. Our second problem is

$$\min\{\partial_t u + (-\Delta)^s u - f, u - \psi\} = 0, \quad u_{|t=0} = u_0, \tag{8}$$

which can also be rewritten as the complementarity conditions

$$\partial_t u + (-\Delta)^s u \geq f, \quad u \geq \psi, \quad (\partial_t u + (-\Delta)^s u - f)(u - \psi) = 0$$

or the evolution variational inequality

$$\partial_t u - f \in \partial\Psi(u),\ (\partial_t u, u - v)_{L^2(\Omega)} + \langle u, u - v\rangle_{\mathbb{H}^{-s}(\Omega),\mathbb{H}^s(\Omega)} \leq (f, u - v)_{L^2(\Omega)},\ \forall v \in \mathscr{K},$$

where $\Psi(v) = \frac{1}{2}\|v\|_{\mathbb{H}^s(\Omega)}^2 + \mathbf{1}_{\mathscr{K}}(v)$ with $\mathscr{K} = \{v \in \mathbb{H}^s(\Omega) : v \geq \psi\}$. With (2), problem (8) can be recast as an evolutionary *thin* obstacle problem, i.e.

$$\int_{\Omega} \partial_t \operatorname{tr}_{\Omega} \mathfrak{u} \operatorname{tr}_{\Omega}(\mathfrak{u} - w) + \int_{\mathscr{C}} y^{\alpha} \nabla\mathfrak{u}\nabla(\mathfrak{u} - w) \leq \int_{\Omega} f \operatorname{tr}_{\Omega}(\mathfrak{u} - w),\ \forall w \in \mathfrak{K} \tag{9}$$

where $\mathfrak{K} = \left\{ w \in \mathring{H}_L^1(y^{\alpha}, \mathscr{C}) : \operatorname{tr}_{\Omega} w \geq \psi \right\}$.

In [NOS15a] we considered the stationary version of this problem. We extended the ideas of [NOS15b] and proposed a finite element method to discretize the stationary analogue of (9). We showed that the proposed method is near optimal. The analysis of this method required a fine interplay between Sobolev regularity of the solution, as shown in [NOS15b], and the Hölder regularity for the solution and extension shown in [CSS08] and [ALP15], respectively.

The available regularity results for the time dependent problem are rather limited. In fact, the only reference that deals with it is [CF13] where Hölder regularity for the solutions is shown, under rather restrictive compatibility assumptions between the initial condition, obstacle and forcing term. Nevertheless, in [OS16] we considered the discretization of this problem. We showed convergence with

minimal regularity assumptions and, in the setting of [CF13], optimal rates of convergence.

References

[ALP15] M. Allen, E. Lindgren, and A. Petrosyan. The two-phase fractional obstacle problem. *SIAM J. Math. Anal.*, 47(3):1879–1905, 2015.

[AOS16] H. Antil, E. Otárola, and A. J. Salgado. A space-time fractional optimal control problem: analysis and discretization. *SIAM J. Control Optim.*, 54(3):1295–1328, 2016.

[CF13] L. Caffarelli and A. Figalli. Regularity of solutions to the parabolic fractional obstacle problem. *J. Reine Angew. Math.*, 680:191–233, 2013.

[CNOS16] L. Chen, R. H. Nochetto, E. Otárola, and A. J. Salgado. Multilevel methods for nonuniformly elliptic operators and fractional diffusion. *Math. Comp.*, 85(302):2583–2607, 2016.

[CS07] L. Caffarelli and L. Silvestre. An extension problem related to the fractional Laplacian. *Comm. Partial Differential Equations*, 32(7-9):1245–1260, 2007.

[CSS08] L. A. Caffarelli, S. Salsa, and L. Silvestre. Regularity estimates for the solution and the free boundary of the obstacle problem for the fractional Laplacian. *Invent. Math.*, 171(2):425–461, 2008.

[NOS15a] R. H. Nochetto, E. Otárola, and A. J. Salgado. Convergence rates for the classical, thin and fractional elliptic obstacle problems. *Philos. Trans. Roy. Soc. A*, 373(2050):20140449, 14, 2015.

[NOS15b] R. H. Nochetto, E. Otárola, and A. J. Salgado. A PDE approach to fractional diffusion in general domains: a priori error analysis. *Found. Comput. Math.*, 15(3):733–791, 2015.

[NOS16] R. H. Nochetto, E. Otárola, and A. J. Salgado. A PDE approach to space-time fractional parabolic problems. *SIAM J. Numer. Anal.*, 54(2):848–873, 2016.

[OS16] E. Otárola and A. J. Salgado. Finite element approximation of the parabolic fractional obstacle problem. *SIAM J. Numer. Anal.*, 54(4):2619–2639, 2016.

Discrete waves in viscoelastic media

Francisco-Javier Sayas

(joint work with Thomas S Brown, Shukai Du, Hasan Eruslu)

We are addressing the numerical analysis and simulation aspects of several viscoelastic models. In the simplest case, with homogeneous Dirichlet boundary conditions on the boundary of the viscoelastic domain at all times, we are studying the model equations

$$\begin{aligned} \rho\,\ddot{\mathbf{u}} = \operatorname{div}\boldsymbol{\sigma} + \mathbf{f}, &\qquad \text{in } \Omega\times(0,\infty),\\ \gamma\mathbf{u} = 0, &\qquad \text{on } \partial\Omega\times(0,\infty), \end{aligned}$$

with vanishing initial conditions $\mathbf{u}(0) = \dot{\mathbf{u}}(0) = 0$. Here $\Omega \subset \mathbb{R}^d$ is a Lipschitz bounded domain, $\rho \in L^\infty(\Omega)$ is a strictly positive mass density, the upper dots denote time differentiation, and γ is the trace operator. The stress $\boldsymbol{\sigma}$ will be defined in terms of the strain with a *distributional* convolutional law

$$\boldsymbol{\sigma} = \mathscr{D} * \dot{\boldsymbol{\varepsilon}}, \qquad \boldsymbol{\varepsilon} = \tfrac{1}{2}(\nabla\mathbf{u} + \nabla\mathbf{u}^\top).$$

The convolutional kernel is better described through the Laplace transform

$$\mathrm{C}(s) := s\,\mathscr{L}\{\mathscr{D}\},$$

as a fourth order tensor with components in $L^\infty(\Omega)$, well defined for $s \in \mathbb{C}_+ := \{s \in \mathbb{C} : \operatorname{Re} s > 0\}$ and with the following properties: for all $s \in \mathbb{C}_+$,

$$\begin{aligned} \mathrm{C}(\overline{s}) &= \overline{\mathrm{C}(s)}, \\ (\mathrm{C}(s)\mathrm{M}) : \mathrm{N} &= (\mathrm{C}(s)\mathrm{N}) : \mathrm{M} && \forall \mathrm{M}, \mathrm{N} \in \mathbb{C}^{d\times d}, \\ \mathrm{C}(s)\mathrm{M} &\in \mathbb{C}^{d\times d}_{\mathrm{sym}} && \forall \mathrm{M} \in \mathbb{C}^{d\times d}, \\ \operatorname{Re}(\overline{s}\mathrm{C}(s)\mathrm{M} : \overline{\mathrm{M}}) &\geq c_0 \operatorname{Re} s \|\mathrm{M}\|^2 && \forall \mathrm{M} \in \mathbb{C}^{d\times d}_{\mathrm{sym}}. \end{aligned}$$

The above equalities and inequalities hold almost everywhere in Ω, $\mathbb{C}^{d\times d}_{\mathrm{sym}}$ is the space of symmetric (not Hermitian) complex matrices, the colon represents the Frobenius real inner product of matrices, and $c_0 > 0$. Our work studies the following aspects:

- Solvability of the transient model and mapping properties showing dependence of $\mathbf{u}$ with respect to the source function $\mathbf{f}$.
- Semidiscretization in space using general Finite Element schemes, including stability (dependence of the discrete solution with respect to the data), and semidiscrete convergence estimates (comparison of the exact and semidiscrete solutions, depending on approximation properties).
- Extension of the above to non-homogeneous Dirichlet (given displacement) or Neumann (given normal traction) boundary conditions, possibly mixing them in different parts of $\partial\Omega$.

The full discretization is achieved with Convolution Quadrature techniques [5], which, in practice, means that we end up solving a collection of problems in the Laplace domain (frequency domain problems with complex frequencies) and combine them to produce a transient solution.

Among the models that are covered by the general hypotheses above is the generalized Zener's model [6, 7]. Let C_0 and C_1 are constant-in-time well defined elastic tensors with the usual hypotheses in linear elasticity theory [1]: for $\circ \in \{0, 1\}$

$$\begin{aligned} &C_{ijkl,\circ} \in L^\infty(\Omega) && i,j,k,l = 1,\dots,d, \\ &C_{ijkl,\circ} = C_{jikl,\circ} = C_{klij,\circ} && i,j,k,l = 1,\dots,d, \\ &\sum_{ijkl} C_{ijkl,\circ}\xi_{ij}\xi_{kl} \geq c_\circ \sum_{ij} \xi_{ij}^2 && \forall \xi_{ij} = \xi_{ji}. \end{aligned}$$

If $a \in L^\infty(\Omega)$ is a strictly positive function and

$$\mathrm{C}_{\mathrm{diff}} := \mathrm{C}_1 - a\mathrm{C}_0,$$

satisfies

$$\sum_{ijkl} C_{ijkl,\mathrm{diff}}\xi_{ij}\xi_{kl} \geq 0 \qquad \forall \xi_{ij},$$

then the transfer function

$$\mathrm{C}(s) := (1 + a\,s)^{-1}(\mathrm{C}_0 + s\,\mathrm{C}_1) = \mathrm{C}_0 + s(1 + a\,s)^{-1}\mathrm{C}_{\mathrm{diff}}$$

satisfies all the above hypotheses. The elastic model C_0 acts as the basic or ground elastic model, while $\mathrm{C}_{\mathrm{diff}}$ can be understood as the diffusive part of the model. It can happen that $\mathrm{C}_{\mathrm{diff}} = 0$ in parts of the domain, which allows for the combination of pure elastic and viscoelastic behavior in different parts of the domain. In the time domain, this model corresponds to the differential equation

$$\boldsymbol{\sigma} + a\,\dot{\boldsymbol{\sigma}} = \mathrm{C}_0\boldsymbol{\varepsilon} + \mathrm{C}_1\dot{\boldsymbol{\varepsilon}},$$

to relate strain and stress. Another model that is covered by our framework is the fractional Zener model [7, 8, 3, 11]

$$\mathrm{C}_\nu(s) := \mathrm{C}(s^\nu) = (1 + a\,s^\nu)^{-1}(\mathrm{C}_0 + s^\nu\,\mathrm{C}_1), \qquad \nu \in (0, 1),$$

where C satisfies the hypotheses of Zener's model, so that viscoelastic and purely elastic behavior can coexist in different part of the domain. In fact, one of the nice features of the Laplace domain analysis [10], is that it allows us to show that the fractional Zener's model (corresponding to a fractional differential implicit law to relate strain and stress) has the same properties as Zener's model in all aspects we are discussing: mapping properties, behavior under Finite Element semidiscretization in space, and behavior under full discretization using Convolution Quadrature.

A direct-in-time-domain analysis for Zener's model is also viable, using a nontrivial first order formulation involving displacement, strain, and diffusive stress, and adapting the equations so that the classical theory of C_0-semigroups of operators can be used [9, 2].

References

[1] P. Ciarlet, *Mathematical elasticity, Vol. 1: Three-dimensional elasticity*, Studies in Mathematics and its Applications 29, North-Holland, 1988.

[2] M. E. Hassell, T. Qiu, T. Sánchez-Vizuet, and F.-J. Sayas, *A new and improved analysis of the time domain integral operators for the acoustic wave equation*, Journal of Integral Equations and Applications **29** (2017), 107–136.

[3] S. Larsson, M. Racheva, and F. Saedpanah, *Discontinuous Galerkin method for an integro-differential equation modeling dynamic fractional order viscoelasticity*, Computer Methods in Applied Mechanics and Engineering **283** (2015),196–209.

[4] H. Li, Z. Zhao, and Z. Luo, *A space-time continuous finite element methods for 2D viscoelastic wave equation*, Boundary Value Problems 53, (2016), 17 pp.

[5] C. Lubich, *On the multistep time discretization of linear initial-boundary value porblems and their boundary integral equations*, Numerische Mathematik **3** (1994), 365–389.

[6] F. Mainardi, *Wave Propagation in Viscoelastic Media*, Pitman Research Notes in Mathematics 52, Pitman, 1982.

[7] F. Mainardi, *Fractional calculus and waves in linear viscoelasticity*, Imperial College Press, 2010.

[8] S. Näsholm and S. Holm, *On a fractional Zener wave equation*, Fractional Calculus and Applied Analysis **16** (2013), 26–50.

[9] A. Pazy, *Semigroups of linear operators and applications to partial differential equations*, Applied Mathematical Sciences 44, Springer, 1983.

[10] F.-J. Sayas, *Retarded Potentials and time domain boundary integral equations: a roadmap*, Springer Series in Computational Mathematics 50, Springer, 2016.
[11] Y. Yu, P. Perdikaris, and G. Karniadakis, *Fractional modeling of viscoelasticity in 3D cerebral arteries and aneurysms*, Journal of Computational Physics **323** (2016), 219–242.

Boundary Element formulation with variable time steps in Acoustics and Thermoelasticity

Martin Schanz
(joint work with Stefan A. Sauter)

In the context of Boundary Element Methods (BEM) mostly constant time step sizes are used. For non-smooth timely behaviour of the solution an adjustable step size could preserve the convergence rates. Further, in technical applications solutions are sought for where often in the beginning the time behavior changes rapidly and, afterwards, the solution becomes more or less steady. Also in this case, an adaption of the time step size is promising.

A variable time step size for BEM has been proposed by Sauter and Veit [3] using a global shape function in time and by Lopez-Fernandez and Sauter [1, 2] with a generalized convolution quadrature method (gCQ). The latter approach shares all benefits of the original convolution quadrature method but allows a variable time step size. This approach is used here and can be summarised using an generic convolution integral $y(t) = (f * g)(t) = \int_0^t f(t-\tau)g(\tau)\,\mathrm{d}\,\tau$ and the BDF 1 as underlying time stepping.

- First Euler step
$$y\left(t_1\right) = \hat{f}\left(\frac{1}{\Delta t_1}\right) g_1$$
with implicit assumption of zero initial condition
- For all steps $n = 2, \ldots, N$ two steps are performed
  (1) Update the solution vector x_{n-1} at all integration points s_ℓ with an implicit Euler step
$$x_{n-1}\left(s_\ell\right) = \frac{x_{n-2}\left(s_\ell\right)}{1 - \Delta t_{n-1} s_\ell} + \frac{\Delta t_{n-1}}{1 - \Delta t_{n-1} s_\ell} g_{n-1}$$
for $\ell = 1, \ldots, N_Q$ with the number of integration points N_Q.
  (2) Compute the solution of the integral at the actual time step t_n
$$y\left(t_n\right) = \hat{f}\left(\frac{1}{\Delta t_n}\right) g_n + \sum_{\ell=1}^{N_Q} \omega_\ell \frac{\hat{f}\left(s_\ell\right)}{1 - \Delta t_n s_\ell} x_{n-1}\left(s_\ell\right)$$

Within this algorithm several parameters must be set as given in [2], where s_ℓ can be seen as the complex frequencies to be used. An essential parameter is the number of integration points $N_Q = N \log\left(N\right)$, which shows the almost linear complexity in time. Further, it must be remarked that the algorithm depend on the relation $\frac{\Delta t_{max}}{\Delta t_{min}}$ and not on all time step sizes Δt_n.

Acoustics with absorbing boundary conditions

The homogeneous wave equation with constant sound speed c models the sound pressure in some domain with boundary Γ. Suitable boundary conditions have to be prescribed. For so-called absorbing boundary conditions a Robin-type boundary condition can be formulated. The solution for this setting can be found employing layer potentials to express the solution in terms of retarded potentials. The absorbing boundary condition leads to the boundary integral equation for the single layer ansatz

$$-\left(\frac{\varphi}{2} - \mathscr{K}' * \varphi\right) - \frac{\alpha}{c}\left(\mathscr{V} * \dot{\varphi}\right) = f \quad \text{a.e. in } \Gamma \times \mathbb{R}_{>0}\ , \tag{1}$$

using the notation $\mathscr{V}$ for the single layer potential and $\mathscr{K}'$ for the adjoint double layer potential. The density is denoted with φ. The sound pressure is finally determined by the single layer potential (for details see [4]). In (1), α denotes the non-negative admittance, which is the inverse of the specific impedance of the surface Γ. This specific impedance is scaled by the density and the wave velocity. The mathematical analysis allows any non-negative finite value for α, however, realistic values are in the range $0 \leq \alpha \leq 1$. The lower limit models a sound hard wall and the upper limit is a totally absorbing surface.

The geometrical discretization is done with linear triangles and the data are approximated by piecewise linear shape functions. The temporal discretisation uses the gCQ algorithm as stated above. This allows an easy realisation of the time derivative in (1) as a simple multiplication by the Laplace variable. For a scattering sphere with absorbing boundary conditions an analytical solution can be found [4]. Assuming a non-smooth function $f(t) = t^{1/2}e^{-ct}$, a graded time step should keep the expected convergence order of 1. In Fig 1, the convergence behaviour is shown for three different spatial discretisation and the semi-analytical solution. The time steps are computed with $t_n = T\left(\frac{n}{N}\right)^2$. For a constant time step size the convergence order would be only 1/2.

Uncoupled thermoelasticity

In uncoupled thermoelasticity only the influence of the temperature on the displacements and stresses is taken into account and not vice versa. The direct boundary integral formulation for the temperature $\theta(x,t)$ and the displacement $u(x,t)$ is given with

$$c(y)\,\theta(y,t) = \int_\Gamma \{[\Theta * q](x,y,t) - [Q * \theta](x,y,t)\}\,\mathrm{d}\,\Gamma \tag{2}$$

$$\begin{aligned} c_{ij}(y)\,u_j(y,t) = \int_\Gamma \{&U_{ij}(x,y)t_j(x,t) - T_{ij}(x,y)\ u_j(x,t) \\ &+ [G_i * q](x,y,t) - [F_i * \theta](x,y,t)\}\,\mathrm{d}\,\Gamma \end{aligned} \tag{3}$$

with the kernel functions $\Theta(x,y,t)$ and $Q(x,y,t)$ of the heat equation, $U_{ij}(x,y)$ and $T_{ij}(x,y)$ from elastostatics, and $G_i(x,y,t)$, $F_i(x,y,t)$ for the one sided coupling. As before, the convolution integrals in time are discretised with gCQ and the spatial

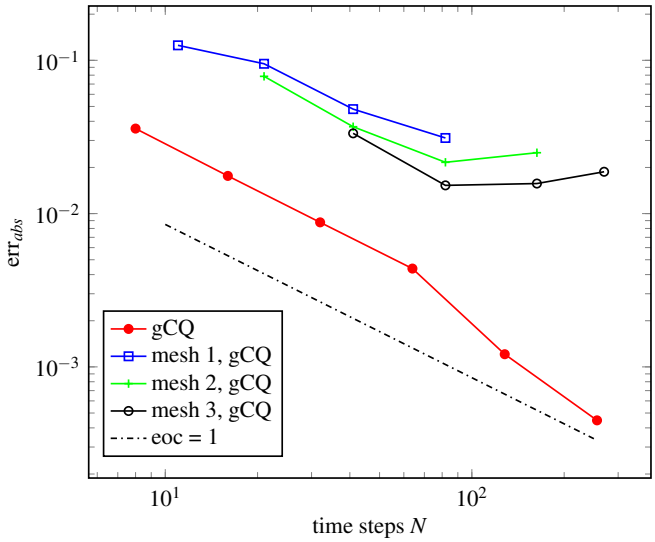

FIGURE 1. Acoustics: Maximum error in time versus time steps

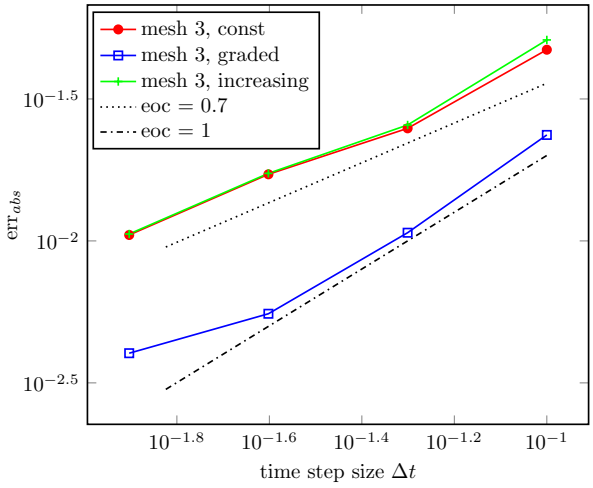

FIGURE 2. Thermoelasticity: Maximum error in time versus time steps

discretisation is done with continuous linear shape functions for the temperature and displacements and discontinuous constant shape functions for the flux and tractions. The point wise error compared to an analytical solution is given in Fig. 2 for different time gradings. The label const denotes a computation with constant time step size and increasing denotes a slightly increased step size. Graded denotes the time steps computed as above in the acoustic example.

References

[1] M. Lopez-Fernandez and S. Sauter. Generalized convolution quadrature with variable time stepping. *IMA J. of Numer. Anal.*, 33(4):1156–1175, 2013.
[2] M. Lopez-Fernandez and S. Sauter. Generalized convolution quadrature with variable time stepping. part II: Algorithm and numerical results. *Appl. Num. Math.*, 94:88–105, 2015.
[3] S. Sauter and A. Veit. A Galerkin method for retarded boundary integral equations with smooth and compactly supported temporal basis functions. *Numer. Math.*, 123(1):145–176, 2013.
[4] S.A. Sauter and M. Schanz. Convolution quadrature for the wave equation with impedance boundary conditions. *J. Comput. Phys.*, 334:442–459, 2017.

Guaranteed energy norm a posteriori error estimates for high-order discretizations of parabolic problems

Iain Smears

(joint work with Alexandre Ern and Martin Vohralík)

We present a posteriori error estimates in parabolic energy norms for space-time discretisations based on arbitrary-order conforming FEM in space and discontinuous Galerkin methods in time. Using the heat equation as a model problem, we show a posteriori error estimates in a norm of $L^2(H^1)\cap H^1(H^{-1})$-type that is suitably extended to functions of the nonconforming discrete space. The estimators give guaranteed upper bounds on the error, and locally space-time efficient lower bounds. Furthermore, the efficiency constants are robust with respect to the discretisation parameters, including the polynomial degrees in both space and time, and also with respect to refinement and coarsening between time-steps, thereby removing the need for the transition conditions required in earlier works.

References

[1] A. Ern, I. Smears, and M. Vohralík, *Guaranteed, locally space-time efficient, and polynomial-degree robust a posteriori error estimates for high-order discretizations of parabolic problems*, submitted for publication (2016). Preprint available at `https://hal.archives-ouvertes.fr/hal-01377086`.
[2] A. Ern, I. Smears and M. Vohralík, *Equilibrated flux a posteriori error estimates in $L^2(H^1)$-norms for high-order discretizations of parabolic problems*, submitted for publication (2017). Preprint available at `https://hal.archives-ouvertes.fr/hal-01489721`.
[3] ———, *Discrete p-robust discrete p-robust $\boldsymbol{H}$(div)-liftings and a posteriori error analysis of elliptic problems with H^{-1} source terms*, Calcolo (2017). doi:10.1007/s10092-017-0217-4.

Quasi-optimality in parabolic spatial semidiscretizations

Andreas Veeser

(joint work with Francesca Tantardini and, partially, Christian Kreuzer and Rüdiger Verfürth)

We shall assess the interplay of the time derivative ∂_t and the space discretization for parabolic initial-boundary value problems.

Elliptic discretizations as benchmark. To present our approach and viewpoint, let us first consider the homogeneous Dirichlet problem for the Poisson equation

$$-\Delta u = f \text{ in } \Omega \subset \mathbb{R}^d, \quad u = 0 \text{ on } \partial\Omega$$

and write $V := H^1_0(\Omega)$ and $\|\cdot\|_V := |\cdot|_{1;\Omega} := (\int_\Omega |\nabla\cdot|^2)^{1/2}$. In order to approximate the weak solution $u \in V$, let $\mathscr{M}$ be a simplicial and conforming mesh of Ω, let $\mathbb{P}_k(\mathscr{M})$ the space of piecewise polynomials of degree at most $k \in \mathbb{N}$ over $\mathscr{M}$, and let U be the Galerkin approximation to u in $S := \mathbb{P}_k(\mathscr{M}) \cap V$. Then

$$\|u-U\|_V = \inf_{v\in S} \|u-v\|_V \approx \left(\sum_{K\in\mathscr{M}} \inf_{p\in\mathbb{P}_k} |u-p|^2_{1;K}\right)^{\frac{1}{2}} \lesssim \left(\sum_{K\in\mathscr{M}} h_K^{2k}|u|^2_{k+1;K}\right)^{\frac{1}{2}}$$

thanks to Céa's Lemma, to best error localization from [6, Corollary 1], and to the Bramble-Hilbert lemma applied on elements. The hidden constants depend on the shape regularity of $\mathscr{M}$. Consequently, the Galerkin approximation U is here an optimal choice in the discrete trial space S, is quasi-optimal with respect to the shape functions $\mathbb{P}_k(\mathscr{M})$ (or the continuity constraint in S does not downgrade the approximation power) and its error can be bounded with minimal regularity within elements.

In what follows, we investigate to what extent these nice features of the elliptic Galerkin error carry over to parabolic spatial semidiscretizations.

Inf-sup theory for parabolic problems. We recall a variational formulation casting parabolic equations in the framework of the inf-sup theory. This is convenient to handle the non-symmetry of the time derivative ∂_t and allows one to use the following abstract result about Petrov-Galerkin approximation from [2, 3]. Let H_i, $i = 1, 2$, be Hilbert spaces with norms $\|\cdot\|_1$, $\|\cdot\|_2$ and let

$$\text{find } u \in H_1 \quad \text{s.th.} \quad \forall \varphi \in H_2 \; b(u,\varphi) = \ell(\varphi) \tag{1}$$

be well-posed for all $\ell \in H_2^*$. Choosing subspaces $M_i \subset H_i$, $i = 1, 2$, such that the Petrov-Galerkin approximations

$$U \in M_1 \quad \text{s.th.} \quad \forall \varphi \in M_2 \; b(U,\varphi) = \ell(\varphi) \tag{2}$$

are well defined, we have

$$\|u-U\|_1 \le C_{\text{qopt}} \inf_{v\in M_1} \|u-v\|_1$$

with the *best* constant

$$C_{\text{qopt}} = \sup_{\varphi\in M_2} \frac{\sup_{u\in H_1:\|u\|_1=1} b(u,\varphi)}{\sup_{U\in M_1:\|U\|_1=1} b(U,\varphi)}.$$

To illustrate the application of this result for parabolic problems, consider the initial-boundary value problem for the heat equation

$$\partial_t u - \Delta u = f \text{ in } \Omega \times (0,T), \quad u = 0 \text{ on } \partial\Omega \times (0,T) \quad u(\cdot,0) = w \text{ on } \Omega. \tag{4}$$

In view of $\int_0^T \partial_t u\, \varphi = [u\varphi]_0^T - \int_0^T u\, \partial_t \varphi$, there are (at least) two ways of dealing with ∂_t in a weak formulation. This talk addresses the more common way associated with the left-hand side, while similar results hold for the way associated with the right-hand side; see [2, 3, 4]. Clearly, the two ways are linked by duality.

We let $V^* = H_0^1(\Omega)^*$ with dual norm $\|\ell\|_{V^*} = \sup_{\varphi\in V} \langle \ell, \varphi\rangle / \|\varphi\|_V$, $W = L^2(\Omega)$ with norm $\|w\|_W = (\int_\Omega |w|^2)^{1/2}$ so that $V \subset W \simeq W^* \subset V^*$ is a Hilbert triple and write $\langle\cdot,\cdot\rangle$ for the scalar product in W and the duality pairing $V^* \times V$. Moreover, we choose the Hilbert spaces $H_1 := L^2(V) \cap H^1(V^*)$ and $H_2 := W \times L^2(V)$ with respective norms

$$\|u\|_1^2 = \|u(T)\|_W^2 + \int_0^T \|\partial_t u\|_{V^*}^2 + \|u\|_V^2, \quad \|\varphi\|_2^2 = \|\varphi_0\|_W^2 + \int_0^T \|\varphi_1\|_V^2$$

and the continuous forms

$$b(u,\varphi) = \langle u(0), \varphi_0\rangle + \int_0^T \langle \partial_t u, \varphi_1\rangle + \langle \nabla u, \nabla \varphi_1\rangle, \quad \ell(\varphi) = \langle v, \varphi_0\rangle + \int_0^T \langle f, \varphi_1\rangle. \tag{5}$$

Thus (1) gets a weak formulation of (4) and choosing $\varphi = (u(0), u + (-\Delta)^{-1}\partial_t u)$ shows that the inf-sup constant of b is 1, as its continuity constant.

Time-independent parabolic semidiscretizations. Let us now investigate the following time-independent spatial semidiscretization of (4):

$$U(0) = P_S w, \quad \partial_t U - \Delta_S U = P_S f \text{ in } (0,T)$$

where P_S denotes the W-orthogonal projection onto $S = \mathbb{P}_k(\mathscr{M}) \cap V$ and is defined also on V^* thanks to $S \subset V$ as well as $\Delta_S = P_S \circ \Delta$ denotes the discrete Laplacian. Then U is the Petrov-Galerkin approximation (2) corresponding to $M_1 = H^1(S)$ and $M_2 = S \times L^2(S)$ and satisfies

$$\begin{aligned} \|u - U\|_1 &\le \|P_S\|_{L(V)} \inf_{v\in M_1} \|u - v\|_1 \\ &\approx \left(\sum_{z\in\mathscr{N}} \inf_{v\in S_{|\omega_z}} \left[\|u(0) - v\|_{0;\omega_z}^2 + \int_0^T |\partial_t u - v|_{-1;\omega_z}^2 + |u - v|_{1;\omega_z}^2 \right] \right)^{\frac12} \\ &\lesssim \left(\sum_{K\in\mathscr{M}} h_K^{2k} \left[|u(0)|_{k;K}^2 + \int_0^T |\partial_t u|_{k-1;K}^2 + |u|_{k+1;K}^2 \right] \right)^{\frac12} \end{aligned} \tag{6}$$

where $\lesssim$ hides also $\|P_S\|_{L(V)}$, $\mathscr{N}$ denotes the set of vertices of $\mathscr{M}$ and $S_{|\omega_z}$ the restriction of S to the star ω_z around a vertex z. The first inequality with best constant $\|P_S\|_{L(V)}$ follows from (3) by deriving a discrete inf-sup condition with $\varphi = (U(0), U + (-\Delta_S)^{-1}\partial_t U)$ and by

$$\langle \ell, (-\Delta_S)^{-1}\ell\rangle^{\frac12} = \sup_{s\in S} \frac{\langle \ell, s\rangle}{\|s\|_V} \le \langle \ell, (-\Delta)^{-1}\ell\rangle^{\frac12} = \sup_{v\in V} \frac{\langle \ell, v\rangle}{\|v\|_V} \le C_S \langle \ell, (-\Delta_S)^{-1}\ell\rangle^{\frac12}$$

for any discrete functional $\ell \in S^* \simeq S$, where the best constant is

$$C_S = \|P_S\|_{L(V)} = \|P_S\|_{L(V^*)}.$$

The best error localization, where the inf could be applied also on the single terms between the brackets, is in collaboration with Rüdiger Verfürth; see also [5].

Time-dependent parabolic semidiscretizations. Next, we allow for discontinuous changes of the spatial discretization at certain instants: given $0 = t_0 < t_1 < \cdots < t_N = T$, assign to each interval $I_n = (t_{n-1}, t_n)$ a mesh $\mathscr{M}_n$ and set $S_n := \mathbb{P}_k(\mathscr{M}_n) \cap V$. Writing P_n, Δ_n etc. for the quantities associated with S_n, we define $U : [0,T] \to V$ by

$$U(0) = P_0 w, \quad \partial_t U - \Delta_n U = P_n f \text{ in } I_n, \quad U(t_n^+) = P_{n+1} U(t_n^-),$$

which corresponds to

$$M_1 = \{v = (v_0, v_1) \mid v_0 \in S_0,\ v_1|_{I_n} \in H^1(I_n; S_n),\ v_1(t_n^+) = P_{n+1} v_1(t_n^-)\},$$
$$M_2 = \{\varphi = (\varphi_0, \varphi_1) \mid \varphi_0 \in S_0,\ \varphi_{1|I_n} \in H^1(I_n; S_n)\}$$

and broken variants of (5). Notice that, while M_1 is nonconforming, M_2 is still conforming. We therefore can proceed as before in a piecewise manner and obtain a broken variant of (6) with the following important difference, see [2]: After the second inequality, i.e. when localizing in time the best error, there arises

$$\left(\|P_1(I - P_0)u(0)\|_W^2 + \sum_{n=0}^{N-1} \|P_n^+(I - P_n)u(t_n)\|_W^2 \right)^{\frac{1}{2}} \lesssim \left(\sum_{n=0}^{N-1} \sum_{K \in \mathscr{M}_n} h_K^{2(k+m)} |u(t_n)|_{k+m;K}^2 \right)^{\frac{1}{2}},$$

where P_n^+ is the W-orthogonal projection onto $S_n + S_{n+1}$ and $m \in \{0, 1\}$. This additional term, whose derivation relies on a novel interpolation operator, is sharp in certain cases, overestimates in others, and is consistent with Dupont's example of (non-)convergence in [1].

The results of this paragraph are in collaboration with Christian Kreuzer.

References

[1] T. Dupont, *Mesh modification for evolution equations*, Math. Comp. **39**, (1982), 85–107.

[2] F. Tantardini, *Quasi-optimality in the backward Euler-Galerkin method for linear parabolic problems*, PhD thesis, Università degli Studi di Milano, 2014.

[3] F. Tantardini, A. Veeser, *The L^2-projection and quasi-optimality of Galerkin methods for parabolic equations*, SIAM J. Numer. Anal. **54** (2016), 317–340.

[4] F. Tantardini, A. Veeser, *Quasi-optimality constants for parabolic Galerkin approximation in space*, In: Karasözen B. et al. (eds), Numerical Mathematics and Advanced Applications. ENUMATH 2015. Lecture Notes in Computational Science and Engineering 112, Springer.

[5] F. Tantardini, A. Veeser, R. Verfürth, *Robust localization of the best error with finite elements in the reaction-diffusion norm*, Constructive Approximation **42** (2015), 313–347.

[6] A. Veeser, *Approximating gradients with continuous piecewise polynomial functions*, Found. Comput. Math. **16** (2016), 723–750.

A posteriori error estimates for linear and nonlinear evolution problems using space-time dual norms

Martin Vohralík
(joint work with Vít Dolejší, Alexandre Ern)

We derive a framework for a posteriori error estimates in unsteady, nonlinear, possibly degenerate, advection-diffusion problems. Our estimators are based on a space-time equilibrated flux reconstruction and are locally computable. They are derived for the error measured in a space-time mesh-dependent dual norm stemming from the problem and meshes at hand, augmented by a jump seminorm measuring possible nonconformities in space. Owing to this choice, a guaranteed and globally efficient upper bound is achieved, as well as robustness with respect to nonlinearities, advection dominance, domain size, final time, and absolute and relative size of space and time steps. Local-in-time and in-space efficiency is also shown. In order to apply the framework to a given numerical method, two simple conditions, local space-time mass conservation and an approximation property of the reconstructed fluxes, need to be verified. We show how to do this for the interior-penalty discontinuous Galerkin method in space and the Crank–Nicolson scheme in time. Numerical experiments illustrate the theory. In particular, effectivity indices quite close to the optimal value of 1 are observed for a variety of problems with various sizes of advection, nonlinearity, and possibly degenerate diffusion, for varying ratio of the space step to the time step, and for spatial approximation polynomial degrees between 1 and 3. Similar effectivity indices are in fact also observed for a weighted $L^2(L^2)$ error in both the scalar and flux approximations, which is a localized upper bound on the error measured in the selected space-time mesh-dependent dual norm. The details can be found in [1].

References

[1] V. Dolejší, A. Ern, and M. Vohralík, *A framework for robust a posteriori error control in unsteady nonlinear advection-diffusion problems*, SIAM J. Numer. Anal. **51** (2013), 773–793.

Iterative Galerkin Methods for Semilinear Parabolic PDE

Thomas P. Wihler
(joint work with Mario Amrein)

We consider the numerical approximation of semilinear parabolic partial differential equations by the so-called *iterative Galerkin approach*. Specifically, in the present work [2], we study initial/boundary value problems of the form

$$\begin{aligned} \partial_t u(\boldsymbol{x},t) - \varepsilon\Delta u(\boldsymbol{x},t) &= f(u(\boldsymbol{x},t),\boldsymbol{x},t), && (\boldsymbol{x},t)\in\Omega\times(0,T], \\ u(\boldsymbol{x},t) &= 0, && (\boldsymbol{x},t)\in\partial\Omega\times(0,T], \\ u(\boldsymbol{x},0) &= g(\boldsymbol{x}), && \boldsymbol{x}\in\Omega. \end{aligned} \tag{1}$$

Here $\Omega \subset \mathbb{R}^d$, with $d \in \{1, 2\}$, is an open and bounded 1d interval or a 2d Lipschitz polygon, respectively. Moreover, $\varepsilon > 0$ is a (possibly small) diffusion coefficient, and $T > 0$ is a final time. Furthermore, $f : \mathbb{R} \times \Omega \times (0, T] \to \mathbb{R}$ is a given continuously differentiable nonlinearity, and $g \in L^2(\Omega)$ is a prescribed initial function.

In the framework of a posteriori error estimates, the iterative Galerkin methodology has been introduced and studied recently in a series of papers; see e.g., [1, 3, 4, 5, 6, 7]. The main idea is to replace the underlying nonlinear partial differential equation by a sequence of linearized problems, each of which is approximated by means of a suitable Galerkin discretization. Then, an iterative solution algorithm is based on a carefully derived residual-type a posteriori analysis which allows to identify individual sources of error (including discretization as well as linearization errors) in terms of computable quantities. This approach is attractive from both a computational as well as from an analytical view point: Indeed, working with a sequence of linear problems allows the application of linear solvers as well as the use of a linear numerical analysis framework (e.g., in deriving error bounds).

In the context of the semilinear parabolic problem (1), we apply the Newton method to locally linearize the nonlinearity f arising in (1). The resulting linearized problem is then discretized by applying the backward Euler scheme in time and a standard conforming finite element method in space [2]. The (ε-robust) a posteriori error analysis reveals three error indicators accounting for the temporal error, the spatial error, and the linearization error. Based on these theoretical results, we present a computational algorithm which implements a simultaneous interplay between the Newton iteration (linearization) and the full discretization (in space and time); more precisely, in each step of the iterative procedure the main source of error is identified, and a corresponding refinement is performed. Numerical tests for both a smooth as well as a problem with finite time blow-up singularity are presented.

References

[1] M. Amrein, and T. P. Wihler, *Fully Adaptive Newton–Galerkin Methods for Semilinear Elliptic Partial Differential Equations*, SIAM J. Sci. Comput. **37** (2015), A1637–A1657.

[2] M. Amrein, and T. P. Wihler, *An adaptive space-time Newton–Galerkin approach for semilinear singularly perturbed parabolic evolution equations*, IMA J. Numer. Anal. (2016), in press.

[3] M. Amrein, J. M. Melenk, and T. P. Wihler, *An hp-adaptive Newton-Galerkin finite element procedure for semilinear boundary value problems*, Math. Meth. Appl. Sci. **40(6)** (2017), 1973–1985.

[4] A. Chaillou, M. Suri, *Computable error estimators for the approximation of nonlinear problems by linearized models*, Comput. Meth. Appl. Mech. Eng. **196(1-3)** (2006), 210–224.

[5] A. Chaillou, and M. Suri, *A posteriori estimation of the linearization error for strongly monotone nonlinear operators*, J. Comput. Appl. Math. **205(1)** (2007), 72–87.

[6] S. Congreve, and T. P. Wihler, *Iterative Galerkin discretizations for strongly monotone problems*, J. Comput. Appl. Math. **311** (2017), 457–472.

[7] L. El Alaoui, A. Ern, and M. Vohralík, *Guaranteed and robust a posteriori error estimates and balancing discretization and linearization errors for monotone nonlinear problems*, Comput. Meth. Appl. Mech. Eng. **200** (2011), 2782–2795.

Analysis of Space-Time Discontinuous Galerkin Methods for Hyperbolic Conservation Laws

Mohammad Zakerzadeh
(joint work with Georg May)

1. Introduction

We consider space-time discontinuous Galerkin (DG) schemes for general m-system of conservation law

$$\boldsymbol{u}_t + \nabla \cdot \boldsymbol{f}(\boldsymbol{u}) = 0, \qquad \text{in } (0,\infty) \times \mathbb{R}^d =: \mathbb{R}^{d+1}_+ \tag{1a}$$

$$\boldsymbol{u}(0,\cdot) = \boldsymbol{u}_0, \qquad \text{in } \mathbb{R}^d, \tag{1b}$$

where $\boldsymbol{f} = (f_1, \ldots, f_d)$ is a smooth flux function and $\boldsymbol{u}_0 \in [L^\infty(\mathbb{R}^d)]^m$ has compact support in $\Omega \subset \mathbb{R}^d$.

Due to the presence of shocks and discontinuities, the traditional notion of solution of (1) is the entropy weak solution; i.e., a weak solution which satisfies the entropy inequality in the distributional sense, for any convex entropy U and its associated entropy flux $F = (F_1, \ldots, F_d)$.

The well-posedness of the entropy weak solutions for scalar conservation laws is a classical result. However, for multidimensional hyperbolic systems, there is no global well-posedness theory and the scope of the analysis often restricted to stability estimates and stronger proofs of convergence are difficult to come by. On the other hand, some numerical evidence (cf. [8]) casts doubt on that entropy solutions constitute the appropriate solution paradigm for general systems of conservation laws, and alternatively, entropy-measure-valued (EMV) solutions [1] are conjectured to be the appropriate notion of solution for general systems.

In case of scalar problems, one can prove the reduction of EMV solutions to entropy weak solutions. In fact, using DiPerna's results [1], one can assert strong convergence to the entropy weak solution, provided that the sequence of solutions are, uniformly bounded in $L^\infty(\mathbb{R}^{d+1}_+)$, weakly consistent with all entropy inequalities, and strongly consistent with the initial data.

Building on previous results (cf. [2]), we prove in [4] that bounded solutions of a certain class of space-time DG schemes converge to an EMV solution. For scalar problems this result can be strengthened as in [5]; one can rigorously prove the $L^\infty(\mathbb{R}^{d+1}_+)$-boundedness of the solutions, without using a finer auxiliary triangulation like the one in [3]. Hence, the convergence to the unique entropy weak solution can be obtained.

The main novelty in our work is that no streamline-diffusion (SD) terms are used for stabilization unlike the previous literature such as [2]. This is the way DG schemes were originally proposed, and are most often used in practice. We show that a properly chosen nonlinear shock-capturing (SC) operator suffices to provide the necessary estimates.

2. Space-Time Discontinuous Galerkin Method

We define the space-time coordinates $x = (x_0, x_1, \ldots, x_d)$ with $x_0 \equiv t$. For arbitrary $T > 0$, consider a sequence of time instances $0 \equiv t_0 < t_1 < \cdots < t_N \equiv T$, and define corresponding time intervals $I_n = (t_n, t_{n+1})$. Let $\mathscr{T}_h^n = \{\kappa\}$ be a subdivision of the space-time slab $I_n \times \mathbb{R}^d$ into disjoint simplices. Define $\mathscr{T}_h := \bigcup_{n=0}^{N-1} \mathscr{T}_h^n$, and let $h := \sup_{\kappa \in \mathscr{T}_h} h_\kappa$, where $h_\kappa := diam(\kappa)$. Convergence analysis will be carried out for shape-regular families of triangulation $\{\mathscr{T}_h\}$. Also we set the technical assumption $t_{n+1} - t_n = \mathscr{O}(h)$.

We define the following approximation space

$$V_{h,q}^n = \{\boldsymbol{v} : \boldsymbol{v}|_\kappa \in [\mathscr{P}^q(\kappa)]^m, \forall \kappa \in \mathscr{T}_h^n\}, \qquad V_{h,q} = \prod_{n=0}^{N-1} V_{h,q}^n, \tag{2}$$

where $\mathscr{P}^q$ is the space of $(d+1)$-variate polynomials of total degree q. Here we set $q \geq 1$. The space-time SC-DG scheme then is defined as the following; find $\boldsymbol{v}^h \in V_{h,q}$ such that

$$\mathscr{B}^{DG}(\boldsymbol{v}^h, \boldsymbol{w}) + \mathscr{B}^{SC}(\boldsymbol{v}^h, \boldsymbol{w}) = 0, \qquad \forall \boldsymbol{w} \in V_{h,q}. \tag{3}$$

Note that we realize the functions in terms of entropy variables $\boldsymbol{v}^h = \partial_{\boldsymbol{u}} U$ as the basic unknowns. The dependent conservative variables are derived via $\boldsymbol{u}(\boldsymbol{v}^h)$.

The semi-linear form of space-time DG discretization is

$$\mathscr{B}^{DG}(\boldsymbol{v}^h, \boldsymbol{w}) := \sum_{n=0}^{N-1} \sum_{\kappa \in \mathscr{T}_h^n} \left\{ \int_\kappa \nabla \cdot \widetilde{\boldsymbol{f}}(\boldsymbol{v}^h) \boldsymbol{w} \, \mathrm{d}x + \int_{\partial\kappa} \left(\hat{\boldsymbol{f}} - \widetilde{\boldsymbol{f}}(\boldsymbol{v}_h^{(\kappa)}) \cdot \nu \right) \boldsymbol{w} \, \mathrm{d}s \right\}, \tag{4}$$

where $\widetilde{\boldsymbol{f}} = (\boldsymbol{u}, f(\boldsymbol{u}))$ is the space-time flux, and on $\partial\kappa$ we define the interior trace values as $\boldsymbol{v}_h^{(\kappa)}(x) = \lim_{\epsilon \to 0^-} \boldsymbol{v}^h(x + \epsilon\nu)$, where $\nu = (\nu_t, \nu_{x_1}, \ldots, \nu_{x_d})$ is the outward pointing normal. We denote as $\kappa_e \in \mathscr{T}_h$ the element separated from κ on $e \subset \partial\kappa$, and introduce the numerical flux function $\hat{\boldsymbol{f}} \equiv \hat{\boldsymbol{f}}(\boldsymbol{v}_h^{(\kappa)}, \boldsymbol{v}_h^{(\kappa_e)}; \nu)$, defined to be Lipschitz-continuous, entropy stable (cf. [6]), and consistent with $\widetilde{\boldsymbol{f}}$. On interfaces where $\nu = (\pm 1, 0, \ldots, 0)^T$, the numerical flux reduces to pure upwinding in time.

Furthermore, we augment the semi-linear form (4) with an SC operator

$$\mathscr{B}^{SC}(\boldsymbol{v}^h, \boldsymbol{w}) := \sum_{n=0}^{N-1} \sum_{\kappa \in \mathscr{T}_h^n} \int_\kappa \varepsilon(\boldsymbol{v}^h) \nabla \boldsymbol{v}^h \cdot \nabla \boldsymbol{w} \, \mathrm{d}x, \tag{5}$$

with the viscosity parameter ε dependent on the residual of the PDE at each element and the jumps over inter-element interfaces. We omit the explicit form here and refer to [4] and [5] for such details. Also one might confer with [2, 3, 7].

3. Theoretical Results

For a general hyperbolic system, we provide the following entropy stability result:

Theorem 1. *Assume that* (1) *is equipped with an entropy pair* (U, F)*, and the exact and approximate solutions have compact support in* Ω*. Then, the SC-DG scheme* (3) *is entropy stable, i.e.,* $\boldsymbol{u}^h$ *admits the following:*

$$\int_\Omega U(\boldsymbol{u}^*(t_-^0))\,\mathrm{d}x \le \int_\Omega U(\boldsymbol{u}(\boldsymbol{v}^h(t_-^N,x)))\,\mathrm{d}x \le \int_\Omega U(\boldsymbol{u}(\boldsymbol{v}^h(t_-^0,x)))\,\mathrm{d}x,$$

where $\boldsymbol{u}^*(t_-^0)$ *is the entropy state of the projected initial data, defined as*

$$\boldsymbol{u}^*(t_-^0) = \frac{1}{|\Omega|}\int_\Omega \boldsymbol{u}(\boldsymbol{v}^h(t_-^0,x))\,\mathrm{d}x.$$

Moreover, the convergence to EMV solution can be established as the following:

Theorem 2. *Let* $\boldsymbol{v}^h$ *be the approximate solution of* (3) *produced by scheme* (3)*. If* $\boldsymbol{u}_{\boldsymbol{v}}$ *has spectral bound and* $\boldsymbol{f}_{\boldsymbol{v}}$ *has upper bound on its eigenvalues (cf.* [4]*) and*

$$\|\boldsymbol{v}^h\|_{L^\infty([0,T]\times\Omega)} \le C,$$

then there exists a sequence of measures, $\{\boldsymbol{\mu}^h_{(x,t)}\}_{h>0}$*, parameterized by the mesh size* h*, where the following holds: for all test functions* $\boldsymbol{\varphi} \in [\mathbb{R}^d \times \mathbb{R}_+]^m$ *one has*

$$\liminf_{h\to 0}\left\{\int_{\mathbb{R}^d}\int_{\mathbb{R}_+}\langle\langle\boldsymbol{\sigma},\boldsymbol{\mu}^h_{(x,t)}\rangle_E,\boldsymbol{\varphi}_t\rangle + \sum_{k=1}^d\langle\langle\boldsymbol{f}^k(\boldsymbol{\sigma}),\boldsymbol{\mu}^h_{(x,t)}\rangle_E,\boldsymbol{\varphi}_{x_k}\rangle\,\mathrm{d}x\,\mathrm{d}t\right\} = 0.$$

Furthermore, the entropy admissibility is satisfied, i.e,

$$\liminf_{h\to 0}\left\{\int_{\mathbb{R}^d}\int_{\mathbb{R}_+}\langle U(\boldsymbol{\sigma}),\boldsymbol{\mu}^h_{(x,t)}\rangle_E\varphi_t + \sum_{k=1}^d\langle F^k(\boldsymbol{\sigma}),\boldsymbol{\mu}^h_{(x,t)}\rangle_E\varphi_{x_k}\,\mathrm{d}x\,\mathrm{d}t\right\} \ge 0,$$

for all $0 \le \varphi \in \mathscr{C}_c^\infty(\mathbb{R}^d \times \mathbb{R}_+)$*.*

Here $\boldsymbol{\mu}_{(x,t)}$ is a measurable map from $\mathbb{R}^d \times \mathbb{R}_+$ to the space of non-negative measures on $\mathbb{R}^m$ with unit mass. Also $\langle\cdot,\cdot\rangle$ and $\langle\cdot,\cdot\rangle_E$ denotes the inner product and the expectation integral with respect to the measure $\boldsymbol{\mu}$ on $\mathbb{R}^m$, respectively.

3.1. **Scalar Problems.** For scalar settings, the formulation is realized in terms of conservative variables, i.e. entropy variables associated with $U(\boldsymbol{u}) = \boldsymbol{u}^2/2$. Thanks to far richer family of entropy functions, Theorem 1 can be generalized for all entropy functions u^p/p for $p = 2m$ and $m \ge 1$. Consequently, $L^\infty(\mathbb{R}_+^{d+1})$ boundedness can be established as:

Lemma 1. *Let* $\boldsymbol{u}^h$ *be the solution produced by scheme* (3)*. There exists a constant* C *such that*

$$\|\boldsymbol{u}^h\|_{L^\infty([0,T]\times\Omega)} \le C, \qquad \forall h > 0.$$

This result has already been introduced in [3] with some subtrinagulation and linear projected values inside each subelement. This technical issue can be avoided by using H^1-projection and some polynomial inequalities, see [4]. Moreover, there is a counterpart of Theorem 2 as

Lemma 2. *Let $\boldsymbol{u}^h$ be the solution produced by scheme* (3)*. Then, for all entropy pairs (U, F) with convex U, there holds*

$$\liminf_{h\to 0}\left\{\int_{\mathbb{R}^d}\int_{\mathbb{R}_+} U(\boldsymbol{u}^h)\varphi_t + \sum_{k=1}^{d} F^k(\boldsymbol{u}^h)\varphi_{x_k}\,\mathrm{d}x\,\mathrm{d}t\right\} \geq 0,$$

for all $0 \leq \varphi \in \mathscr{C}_c^\infty(\mathbb{R}^d \times \mathbb{R}_+)$.

Application to DiPerna's conditions [1], Lemmas 1 and 2, and consistency with the initial data, one can establish the convergence to entropy weak solution for the solutions of (3).

References

[1] R. J. DiPerna, *Measure-valued solutions to conservation laws*, Arch. Ration. Mech. Anal., **88**(3), 223–270, (1985).

[2] A. Hiltebrand and S. Mishra, *Entropy stable shock capturing space-time discontinuous Galerkin schemes for systems of conservation laws*, Numer. Math., **24**(3), 103–151 (2014).

[3] C. Johnson, A. Szepessy and P. Hansbo, *On the convergence of shock-capturing streamline diffusion finite element methods for hyperbolic conservation laws*, Math. Comp., **54**(189), 107–129 (1990).

[4] M. Zakerzadeh and G. May, *On the convergence of a shock capturing discontinuous Galerkin method for nonlinear hyperbolic systems of conservation laws*, SIAM J. Num. Anal., **54**(2), 874–898 (2016).

[5] G. May and M. Zakerzadeh, *On the convergence of space-time discontinuous Galerkin schemes for scalar conservation laws*, SIAM J. Num. Anal., **54**(4), 2452–2465 (2016).

[6] E. Tadmor, *Entropy stability theory for difference approximations of nonlinear conservation laws and related time-dependent problems*, Acta Numerica, **12**, 451–512 (2003).

[7] J. Jaffre, C. Johnson and A. Szepessy, *Convergence of the discontinuous Galerkin finite element method for hyperbolic conservation laws*, Math. Mod. Meth. App. Sci., **5**(3), 367–386 (1995).

[8] U.S. Fjordholm, R. Kappeli, S. Mishra and E. Tadmor, *Construction of approximate entropy measure-valued solutions for hyperbolic systems of conservation laws*, Found. Comp. Math., pp.1-65 (2015).

Reporter: Christian Wieners

Participants

Prof. Dr. Georgios Akrivis
Department of Computer Science
University of Ioannina
Ioannina 45100
GREECE

Dr. Lehel Banjai
School of Mathematics and Computer Science
Heriot-Watt University
Colin Maclaurin Building
Riccarton
Edinburgh EH14 4AS
UNITED KINGDOM

Prof. Ph.D. Marek Behr
Chair of Computational Analysis of Technical Systems (CATS)
Center for Computational Engineering Science
Aachen University (RWTH)
52056 Aachen
GERMANY

Prof. Dr. Andrea Bonito
Department of Mathematics
Texas A & M University
College Station, TX 77843-3368
UNITED STATES

Prof. Dr. Carsten Carstensen
Institut für Mathematik
Humboldt-Universität zu Berlin
Unter den Linden 6
10099 Berlin
GERMANY

Hanzhi Diao
Institut für Mathematik
Universität Zürich
Winterthurerstrasse 190
8057 Zürich
SWITZERLAND

Prof. Dr. Willy Dörfler
Institut für Angewandte und Numerische Mathematik II
Karlsruher Institut für Technologie (KIT)
76128 Karlsruhe
GERMANY

Johannes Ernesti
Institut für Angewandte und Numerische Mathematik
Universität Karlsruhe
Englerstrasse 2
76131 Karlsruhe
GERMANY

Prof. Dr. Silvia Falletta
Dipartimento di Matematica
Politecnico di Torino
Corso Duca degli Abruzzi, 24
10129 Torino
ITALY

Prof. Dr. Martin Gander
Département de Mathématiques
Université de Geneve
Case Postale 64
2-4, rue du Lievre
1211 Genève 4
SWITZERLAND

Prof. Dr. Jay Gopalakrishnan
Department of Mathematical Sciences
Portland State University
P.O. Box 751
Portland, OR 97207-0751
UNITED STATES

Prof. Dr. Marcus Grote
Departement Mathematik und Informatik
Universität Basel
Fachbereich Mathematik
Spiegelgasse 1
4051 Basel
SWITZERLAND

Prof. Dr. Ralf Hiptmair
Seminar für Angewandte Mathematik
ETH-Zentrum
Rämistrasse 101
8092 Zürich
SWITZERLAND

Prof. Dr. Marlis Hochbruck
Karlsruher Institut für Technologie (KIT)
Institut für Angewandte und Numerische Mathematik
Englerstrasse 2
76131 Karlsruhe
GERMANY

Prof. Dr. Patrick Joly
Departement de Mathematiques
ENSTA/UMA
828, Boulevard des Maréchaux
91762 Palaiseau Cédex
FRANCE

Dr. Maryna Kachanovska
Département de Mathématiques
ENSTA / UMA
828, Boulevard des Maréchaux
91762 Palaiseau Cédex
FRANCE

Prof. Dr. Guido Kanschat
I W R
Universität Heidelberg
Im Neuenheimer Feld 205
69120 Heidelberg
GERMANY

Dr. Uwe Köcher
Fakultät für Maschinenbau
- Numerische Mathematik -
Universität der Bundeswehr Hamburg
22039 Hamburg
GERMANY

Prof. Dr. Rolf Krause
Facolta di Scienze Informatiche
Universita della Svizzera Italiana
Via Giuseppe Buffi 13
6904 Lugano
SWITZERLAND

Dr. Omar Lakkis
Computer Science and Technology
Free University of Bozen / Bolzano
Room 1.16
Dominikanerplatz 3
39100 Bolzano
ITALY

Prof. Dr. Ulrich Langer
Institut für Numerische Mathematik
Johannes Kepler Universität Linz
Altenbergerstraße 69
4040 Linz
AUSTRIA

Prof. Dr. Mats G. Larson
Department of Mathematics
University of Umea
901 87 Umeå
SWEDEN

Prof. Dr. Stig Larsson
Department of Mathematical Sciences
Chalmers University of Technology and the
University of Gothenburg
412 96 Göteborg
SWEDEN

Prof. Dr. Dmitriy Leykekhman
Department of Mathematics
University of Connecticut
1084 Shennecossett Road
Groton, CT 06340-6097
UNITED STATES

Dr. Maria Lopez-Fernandez
Mathematics Department
Universita degli Studi di Roma I
"La Sapienza"
Piazzale Aldo Moro, 5
00185 Roma
ITALY

Prof. Dr. Charalambos Makridakis
Department of Mathematics
University of Sussex
Falmer
Brighton BN1 9QH
UNITED KINGDOM

Prof. Dr. Jens M. Melenk
Institut für Analysis und
Scientific Computing
Technische Universität Wien
Wiedner Hauptstrasse 8 - 10
1040 Wien
AUSTRIA

Dr. Andrea Moiola
Department of Mathematics
University of Reading
Whiteknights
Reading RG6 6AX
UNITED KINGDOM

Prof. Dr. Peter Monk
Department of Mathematical Sciences
University of Delaware
Newark, DE 19716-2553
UNITED STATES

Martin Neumüller
Institut für Numerische Mathematik
Johannes Kepler Universität Linz
Altenberger Straße 69
4040 Linz
AUSTRIA

Prof. Dr. Ricardo H. Nochetto
Institute for Physical Science and
Technology
Department of Mathematics
University of Maryland
College Park, MD 20742-2431
UNITED STATES

Dr. Enrique Otárola
Departamento de Matemática
Universidad Técnica Federico Santa
Maria
Avenida Espana 1680
Valparaiso
CHILE

Prof. Dr. Arnold Reusken
Institut für Geometrie
und Praktische Mathematik
RWTH Aachen
Templergraben 55
52061 Aachen
GERMANY

Prof. Dr. Abner J. Salgado
Department of Mathematics
University of Tennessee
Knoxville, TN 37996-1300
UNITED STATES

Prof. Dr. Stefan A. Sauter
Institut für Mathematik
Universität Zürich
Winterthurerstrasse 190
8057 Zürich
SWITZERLAND

Prof. Dr. Francisco J. Sayas
Department of Mathematical Sciences
University of Delaware
501 Ewing Hall
Newark, DE 19716-2553
UNITED STATES

Prof. Dr. Martin Schanz
Institut für Baumechanik
Technische Universität Graz
Technikerstraße 4/II
8010 Graz
AUSTRIA

Prof. Dr. Joachim Schöberl
Institut für Analysis und
Scientific Computing
Technische Universität Wien
Wiedner Hauptstrasse 8 - 10
1040 Wien
AUSTRIA

Prof. Dr. Christoph Schwab
Seminar für Angewandte Mathematik
ETH Zentrum, HG G 57.1
Rämistrasse 101
8092 Zürich
SWITZERLAND

Dr. Iain Smears
INRIA de Paris
2, Rue Simone Iff
75589 Paris 12
FRANCE

Prof. Dr. Olaf Steinbach
Institut für Numerische Mathematik
Technische Universität Graz
Steyrergasse 30
8010 Graz
AUSTRIA

Prof. Dr. Rob P. Stevenson
Korteweg-de Vries Instituut
Universiteit van Amsterdam
Postbus 94248
1090 GE Amsterdam
NETHERLANDS

Céline Torres
Institut für Mathematik
Universität Zürich
Winterthurerstrasse 190
8057 Zürich
SWITZERLAND

Prof. Dr. Andreas Veeser
Dipartimento di Matematica
Universita di Milano
Via C. Saldini, 50
20133 Milano
ITALY

Prof. Dr. Martin Vohralik
Equipe SERENA
INRIA de Paris
2, rue Simone Iff
75589 Paris 12
FRANCE

Prof. Dr. Christian Wieners
Karlsruher Institut für Technologie
(KIT)
Institut für Angewandte und
Numerische Mathematik
Englerstrasse 2
76131 Karlsruhe
GERMANY

Prof. Dr. Thomas P. Wihler
Mathematisches Institut
Universität Bern
Sidlerstrasse 5
3012 Bern
SWITZERLAND

Christoph Wintersteiger
Institut für Analysis und Scientific Computing
Technische Universität Wien
Wiedner Hauptstrasse 8 - 10
1040 Wien
AUSTRIA

Mohammad Zakerzadeh
Graduiertenschule AICES
RWTH Aachen
Schinkelstrasse 2
52062 Aachen
GERMANY